EXPERIMENTAL INVESTIGATION INTO THE ENERGY SAVINGS FOR AN AIR-TO-AIR RESIDENTIAL HEAT PUMP UTILIZING INDIRECT EVAPORATIVE COOLING

By

D. CHRISTOPHER CHENG

A THESIS PRESENTED TO THE GRADUATE SCHOOL
OF THE UNIVERSITY OF FLORIDA IN PARTIAL FULFILLMENT
OF THE REQUIREMENTS FOR THE DEGREE OF
MASTER OF SCIENCE

UNIVERSITY OF FLORIDA

2006

This document is dedicated to my beloved grandmother Mary A. Ducharme.

ACKNOWLEDGMENTS

First I would like to thank Dr. D.Y. Goswami for the opportunity to work with his team of engineers contributing towards a sustainable society. I would also like to thank Dr. Skip Ingley and Dr. S. A. Sherif for their participation on my committee. I must express my great appreciation for Dr. Sanjay Vijayaraghavan's mentorship during my research. I thank Chuck Garretson for his time and effort in preparing the test facility. I thank all my colleagues at the Solar Energy and Energy Conversion Laboratory for their advice and help during my experience at the University of Florida. Thanks go to Florida Power and Light for its funding and research opportunity.

I would like to express my gratitude for my family and their support while I achieved this goal. My greatest appreciation is for my girlfriend Davin whose sacrifice and support allowed me to be successful in this accomplishment.

TABLE OF CONTENTS

page

LIST OF TABLES

LIST OF FIGURES

NOMENCLATURE

CE	cooling efficiency (%)
COP	coefficient of performance
c_p	specific heat (Btu/lbmR)
DBT	dry-bulb temperature
EER	energy efficiency ratio (Btu/Whr)
fpm	feet per minute
gpm	gallons per minute
h	enthalpy (Btu/lbm)
i_{fg}	latent heat of vaporization (J/kg)
$\dot{m}$	mass flow rate (lbm/hr)
p_g	saturated pressure at dry-bulb temperature (psia)
p_v	partial pressure of water vapor (psia)
P	power (kW)
PF	performance factor (%)
$\dot{Q}$	rate of heat transfer (Btu/hr)
R	gas constant
RH	relative humidity (%)
SCFM	standard airflow rate (ft^3/min)

SEER	Seasonal energy efficiency ratio (Btu/Whr)
T	temperature (^{o}F)
v	specific volume (ft^3/lbm)
w	humidity ratio (lbm of water/lbm of dry air)
$\dot{W}$	rate of work (Btu/hr)

Greek

ϕ	relative humidity (%)

Subscripts

air	properties associated with air
c	compressor
db	dry-bulb
in	inlet
out	outlet
L	heat removal
latent	latent heat
net	net
water	properties associated with water
sensible	sensible heat
wb	wet-bulb

Abstract of Thesis Presented to the Graduate School
of the University of Florida in Partial Fulfillment of the
Requirements for the Degree of Master of Science

EXPERIMENTAL INVESTIGATION INTO THE ENERGY SAVINGS FOR AN AIR-TO-AIR RESIDENTIAL HEAT PUMP UTILIZING INDIRECT EVAPORATIVE COOLING

By

D. Christopher Cheng

May 2006

Chair: D. Y. Goswami
Major Department: Mechanical and Aerospace Engineering

Air-conditioners are one of the major energy consuming devices in a home. Even with use being primarily in the summer months, the U.S. Energy Information Administration attributed 16% of the total yearly electricity consumption to them in 2001. These systems typically use air-cooled condensers. Therefore ambient temperature directly affects performance of such systems. The simple concept of evaporative cooling has proven to be an effective method for improving the performance of an air-cooled condenser in the past. This work shows the potential of the energy savings for five cities in Florida using this concept.

Experiments were run on a typical residential air-conditioner at the University of Florida heat pump test facility. The experiments showed that the performance of the system varied as the outdoor conditions, specifically the dry-bulb temperature and relative humidity, changed. The evaporative cooling device improved the energy

efficiency ratio (EER) by humidifying the air, thus lowering the dry-bulb temperature seen by the condenser. The data were then applied to the weather data of the five Florida cities and potential energy savings were predicted from a comparison with the baseline case without evaporative cooling. It was confirmed that the net energy consumption was reduced despite the additional energy used to achieve evaporative cooling.

CHAPTER 1
INTRODUCTION

Air-conditioning has become a standard feature in many U.S. homes today. Correspondingly, a large portion of U.S. residential electricity consumption goes towards air-conditioning. The U.S. Energy Information Administration [1] reported that as of 2001, of the 107 million homes in the United States, 80.8 million used some form of air-conditioning. Figure 1-1 shows that 16% of residential electricity use is consumed by air-conditioning equipment leading to an annual electric consumption of 183 billion kilowatt-hours [1].

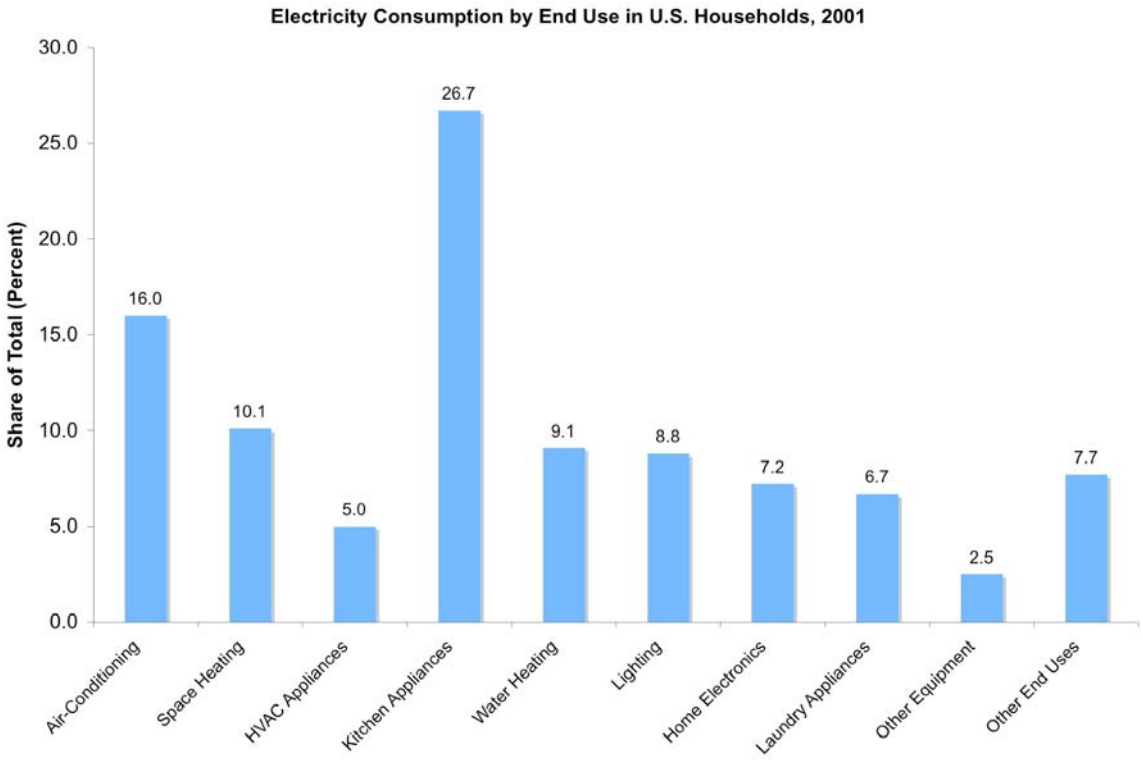

Figure 1-1. The breakdown of annual electricity consumption by end use for homes EIA [2].

A reduction in this magnitude will have a considerable effect on household energy consumption. Utility companies have a particular interest in reducing the peak loads from the residential sector. Decreasing the peak demand leads to a larger decrease of production because of the efficiencies associated with the conversion and distribution processes. Most lower tonnage residential air-conditioning systems use air-cooled condensers. A simple and effective way to improve the efficiency (COP or EER) is to cool the ambient air before it enters the condenser coils. Using evaporative cooling can do this by adding humidity to the air entering the condenser coils, thus lowering the corresponding refrigerant temperature and pressure.

Vapor-Compression Cycle

The vapor-compression cycle is the fundamental thermodynamic cycle that is used in the common electric driven heat pumps and air-conditioners. A description can be found in any thermodynamics text [3]; however a brief description is provided. The cycle takes the working fluid through four processes as shown in Figure 1-2. The refrigerant enters the compressor where its pressure is increased to make it a superheated vapor entering the condenser. While in the condenser the refrigerant rejects heat to the ambient air and condenses to form a liquid. The high temperature liquid is then throttled through an expansion valve to a low pressure where the refrigerant is a two-phase mixture at a low temperature. Finally, the refrigerant passes through the evaporator where the liquid absorbs heat from the air blown over the evaporator and evaporates. The vapor is then compressed to start the cycle over again.

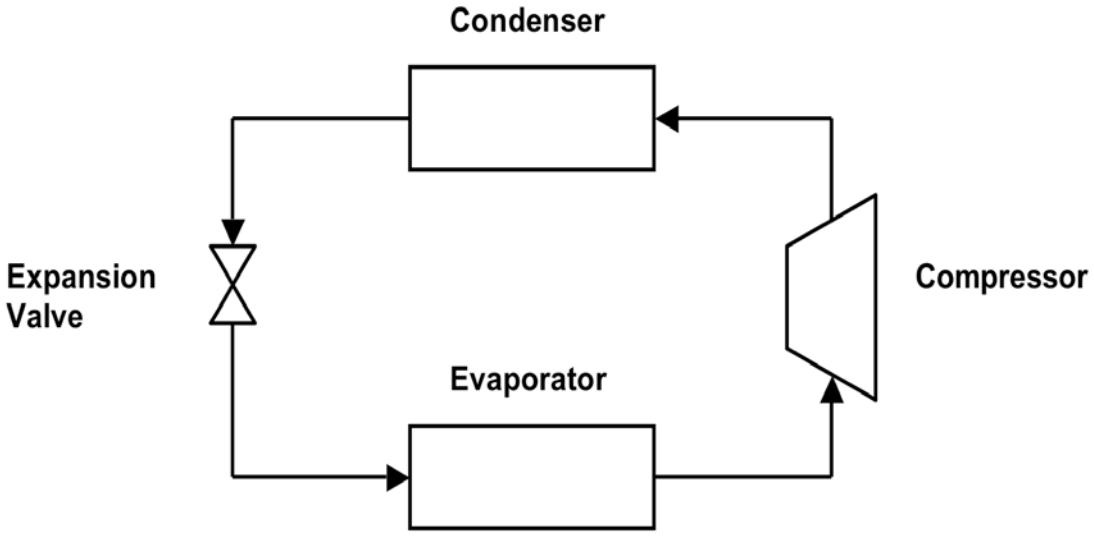

Figure 1-2. Schematic diagram of the vapor compression cycle.

The thermodynamic performance of the vapor-compression cycle is measured by its coefficient of performance (COP). The COP is expressed as the ratio of rate of heat removal to rate of work done by the compressor as in Equation 1-1:

$$COP = \frac{\dot{Q}_L}{\dot{W}_{net,in}} \tag{1-1}$$

Residential Air-Conditioning System

Air-conditioning systems are commonly used in the summer to provide comfortable conditions inside buildings and homes. A typical residential system is called a unitary air-conditioner. It consists of an evaporator and air handler which is situated indoors and a compressor condenser combination which is located outdoors [4]. A blower forces return air from the conditioned space across the evaporator coils providing cooling and dehumidification. Outdoor air is drawn over the condenser coils to remove heat from the refrigerant. The environment thus acts as the heat sink for the cycle. An air-cooled condenser is used because of its low maintenance requirements as opposed to water or evaporative cooled condensers. An air-conditioner's performance is rated by its

energy efficiency ratio (EER), which is defined as the amount of heat removed from a cooled space in Btu's for every Watt-hour of electricity consumed [3]. EER is related to COP by the following equation:

$$EER = 3.412COP \tag{1-2}$$

The two heat exchange processes in the evaporator and condenser coils primarily affect the COP of a given system. The most practical way for a user to increase the COP is through the thermostat setting. The higher it is set, the more energy that will be saved.

The focus of this study is on saving energy by improving the performance of the air-cooled condenser. Since it is outside, it experiences a wide range of temperatures throughout the day. It is completely dependent upon the dry-bulb temperature of the ambient air. The higher it is, the more work the compressor has to do. Evaporative cooling can lower the dry-bulb temperature of the air before it enters the condenser coils.

Evaporative Cooling

Consider a stream of warm air flowing in contact with water. Humidity is added to the flowing air stream, which will eventually become saturated, given sufficient time of contact. This process is shown in Figure 1-3. Under adiabatic conditions (no external heat addition), the heat from the air is used to evaporate the water. This leads to lowering of the dry-bulb temperature of the air while the evaporation leads to a rise in relative humidity and humidity ratio. The lowest temperature that can be reached is that of saturated air, which is referred to as the wet-bulb temperature of the air. The performance of an evaporative cooling device is defined using its cooling efficiency or performance factor [5].

$$CE \text{ or } PF = \frac{T_{db,in} - T_{db,out}}{T_{db} - T_{wb}} \tag{1-3}$$

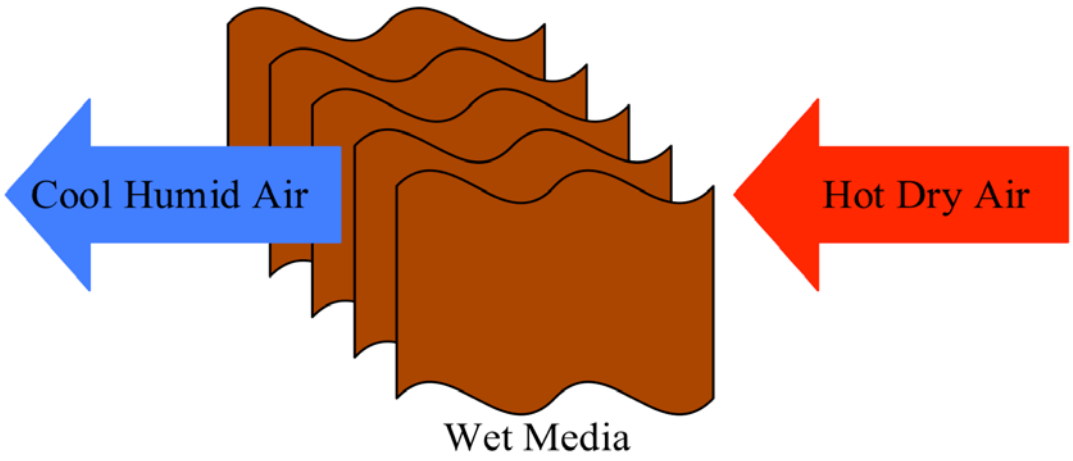

Figure 1-3. Picture of the evaporative cooling process.

Evaporative cooling has a number of applications because of its characteristics of lowering the dry-bulb temperature, humidification, and high heat transfer. It is predominantly used in cooling towers for large tonnage air-conditioning systems for commercial and industrial buildings as well as in power plants. In cooling towers, warm water comes into contact with air, and evaporative cooling is used to cool the water instead of the air. Another application is pre-cooling of the return air before it enters the cooling coils. In hot arid climates swamp coolers are used as air-conditioners. They take advantage of the low humidity in the air and can lower the temperature of the air by more than twenty degrees Fahrenheit. The ideal candidates for direct evaporative cooling are places where both a constant supply of fresh air and cooling is needed, especially in warm, arid climates. Some examples include greenhouses, farm animal shelters and mines [5].

The particular method of indirect evaporative cooling utilized in this research was cooling the ambient air before it enters the condenser. A retrofit was constructed to house a wetted media pad surrounding an air-cooled condenser. The ambient air was forced into the media pad where it was humidified and dry-bulb temperature lowered.

The outdoor air was essentially pre-cooled, so the condenser experiences a lower temperature than the ambient conditions. Further details of this system and setup are detailed in the subsequent chapters.

Using evaporative cooling to pre-cool the ambient air is parasitic in nature. There has to be a source of water, which adds to the cost of operation. It requires additional power to circulate the water. The wetted media reduces the airflow because of the pressure drop through it. The design has to be such that the advantage gained by cooling the air is not negated by the airflow reduction as well as the parasitic power requirements for circulating water.

CHAPTER 2
LITERATURE REVIEW AND OBJECTIVES

There are two approaches in which evaporative cooling is applied to air-conditioning. In direct evaporative cooling, the process is either used to meet the entire cooling load or to pre-cool the return air going to the evaporator coils. In indirect evaporative cooling, the ambient air is cooled before it enters the condenser coils or evaporative condensers are used. The indirect approach is predominately used because it reduces the electricity consumption of the compressor in vapor compression cycles.

Previous Work

There have been several studies on improving the performance of an air-cooled condenser taking advantage of evaporative cooling. The studies reviewed in this chapter concluded that the methods are effective in increasing the performance of an air-conditioner. The advantage that can be gained depends to a large extent on the climatic conditions. Evaporative cooling is more effective in a warm, dry place. There has been a particular interest in this subject in the Middle East and India. Many of the studies examine the improvement in efficiency at peak weather conditions (highest outdoor temperature with the lowest relative humidity) for their geographical area.

Pre-Cooling the Ambient Air for Air-Cooled Condensers

As stated before, air-cooled condensers are commonly used in residential air conditioners. By evaporatively cooling the ambient air entering the condenser, the heat transfer from the refrigerant to the air in the condenser can be improved. This will

require a retrofit such that air is passed through some wetted media prior to entering the condenser coils.

The hot refrigerant entering the condenser loses sensible heat to the air blowing on the condenser coils. The rate of heat transfer is found by the following equation:

$$\dot{Q}_{sensible} = \dot{m}_{air} c_{p,air} \left(T_{air,out} - T_{air,in} \right) \tag{2-1}$$

Cooler air temperatures result in lower refrigerant pressures in the cycle, which leads to less compressor work. The compressor uses a majority of the electric power consumed by the air-conditioning unit. The lower pressures also leads to a reduction in refrigerant temperature in the evaporator. This causes an increase in cooling capacity, which further enhances the performance of the system.

Pre-cooling the ambient air has proven to improve the efficiency (COP or EER) of the vapor compression cycle in air-conditioning. Goswami et al. [6] experimentally studied the efficiency improvement of a small tonnage air-conditioner. A wetted media pad surrounded the condenser to pre-cool the ambient air lowering the refrigerant condensing temperature. Data was collected for three weeks for both the baseline case without indirect evaporative cooling and with the media pads installed. The data were compiled from the actual use of a building and daily weather conditions. There was a 20% EER improvement with the evaporative cooling system installed because of the lower compressor power consumption and the gain in cooling capacity. Grant et al. [7] also experimented with indirect evaporative cooling where a wetted media pad was used to pre-cool the ambient air. This study was done with a window-mounted air-conditioner. A further step was also investigated by using a desiccant to lower the relative humidity of the ambient air before entering the evaporative cooling zone. This

extra step in turn, would lower the wet-bulb temperature of the ambient air to achieve additional evaporative cooling. An 18% increase in COP was obtained by the experiment for peak weather conditions in upstate New York. Mathur and Kaushik [8] took a theoretical approach to the potential energy savings of evaporative cooling. The analysis of weather data and the air-conditioner manufacturer's data yielded a 28% efficiency improvement at peak weather conditions in New Delhi, India. It was a result of reducing the power consumption and increasing the cooling capacity.

A simulation was done on a geothermal power plant using indirect evaporative cooling for the air-cooled condenser [9]. The goal was to increase the output of the plant by pre-cooling the ambient air. Four different methods were considered and then economically analyzed. All of the methods increased the capacity of the plant, but one failed to pay back because the minimal increase of plant performance and high cost. This was using the same media pad as in the Goswami et al. [6] study.

Energy can be saved over the cooling season because of the gain in efficiency. Goswami et al. [6] reported 317 kilowatt-hours of energy savings for the entire year in Jacksonville, Florida. Mathur and Kaushik [8] estimated 114 kWh for two months in New Delhi, India. The climate of each city had a direct effect on the amount of energy saved. New Delhi can experience temperature depressions of 20^{o}C while Jacksonville rarely has temperature depressions of 14^{o}C [6,8]. Two months in New Delhi account for a third of the energy saved in Jacksonville for the entire year. Hot arid climates have potential to save more energy because the ambient temperature can be reduced more than in humid climates.

Evaporative Condenser

The evaporative condensers described in this section differs from the condenser mentioned in the previous section by their design. The evaporative condensers are made for air and water to contact the condenser tubes, whereas no water touches the cooled coils of the indirect evaporatively cooled condenser. A typical evaporative condenser can be seen in Figure 2-1.

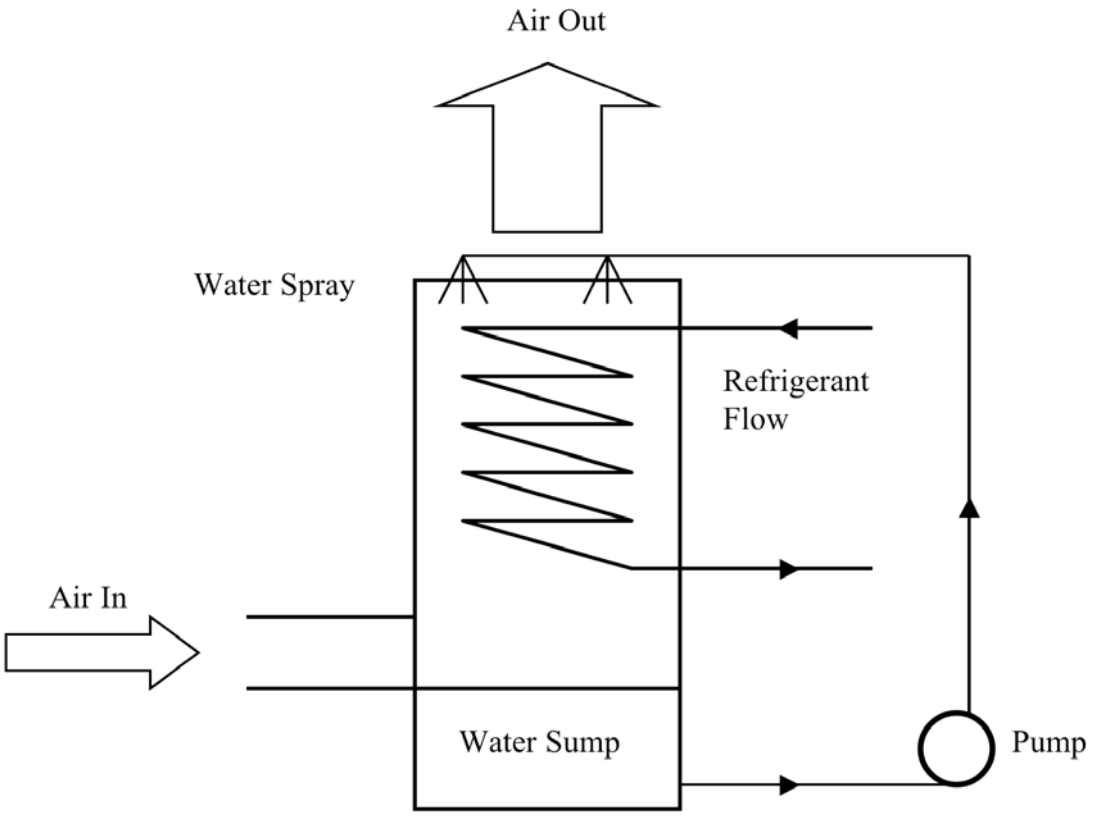

Figure 2-1. Schematic drawing of a typical evaporative condenser.

Water is pumped from the bottom of the condenser to the top where it is released onto the condenser tubes. The water evaporatively cools the tubes and the ambient air that passes through. The heat transfer is greatly increased because the water evaporates on the coils and in the air, dropping its temperature. It uses both sensible and latent heat

transfer, however, the latent heat transfer dominates. The rate of latent heat transfer is defined by the following equation [10]:

$$\dot{Q}_{latent} = \dot{m}_{air} i_{fg,water} \left(w_{air,out} - w_{air,in} \right) \tag{2-2}$$

Evaporatively cooled condensers can have a smaller heat transfer area and lower air flow rate for the same overall heat transfer coefficient as its air-cooled counterpart [11].

Evaporative condensers have shown greater efficiency than air-cooled condensers due to the lower power requirements of the compressor and more cooling capacity. This is a result of reduced pressures and temperatures to condense the refrigerant. Ettouney et al. [11] used the same condenser for both air-cooled and evaporatively cooled configurations. The set up was of an evaporative condenser in Figure 2-1, but when it was to act as an air-cooled condenser the water pump did not run. The experiments were run with the condenser experiencing actual weather conditions throughout the day. A system efficiency increase of 10% was reported with the evaporative condenser. Hwang et al. [10] introduced an entirely new setup for an evaporative condenser shown in Figure 2-2.

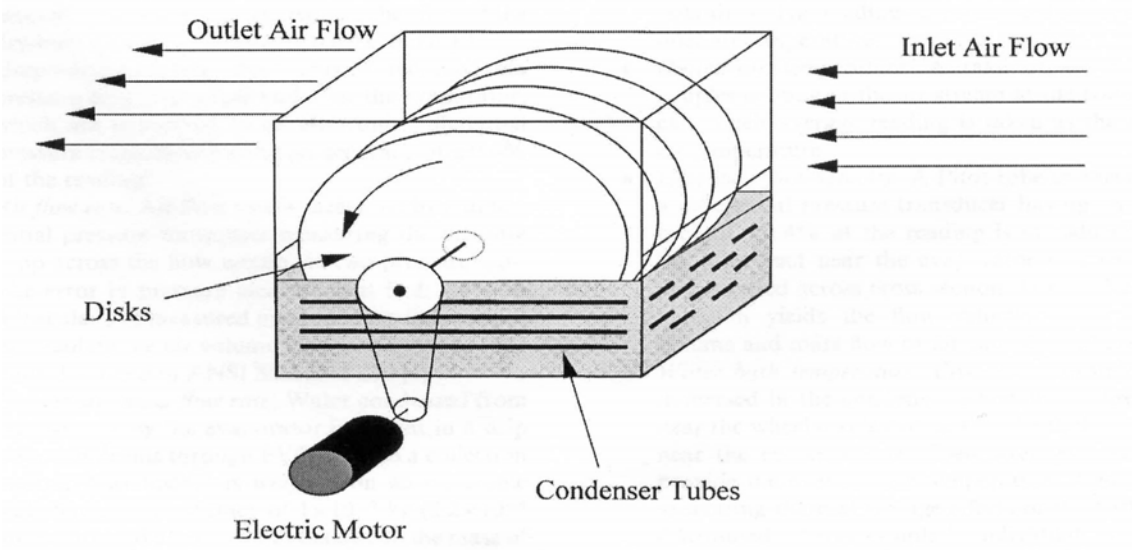

Figure 2-2. Picture of a prototype evaporative condenser, Hwang et al. [10].

Here the condenser tubes are submersed in water with no air able to contact them. The disks pull water into the airflow where the evaporation takes place. The water that does not evaporate re-enters and cools the pool. A conventional heat pump was tested with its air-cooled condenser and with the evaporative condenser in its place. The experiments were run at ASHRAE Standard 116 and results showed a 14.5% improvement in SEER and 8.1% increase in cooling capacity. Goswami et al. [12] modified a standard air-cooled condenser of a three-ton heat pump system to act as an evaporative condenser. This was accomplished with a product that placed a spray nozzle directly in front of the condensing coils. Water was sprayed on the coils to give the evaporative cooling effect. Using ASHRAE standard testing conditions, the EER was increased 27% with water spray on the condenser coils. A reduction in compressor power again enhanced the efficiency. Hosoz and Kilicarlsan [13] also studied the direct comparison of an air-cooled condenser and evaporative condenser using the same refrigeration system. The system showed a 14.3% gain in COP with the evaporative condenser over the air-cooled condenser while operating at the same evaporating temperature. Contrary to convention, compressor power increased 10.1% for the evaporative condenser. The system's improvement was due to a 31% increase in refrigeration capacity.

Air-cooled condensers use a finned tube design to increase the heat transfer area to achieve higher heat transfer. Evaporative condensers normally use plain tube design to exchange heat. Less heat transfer area is needed because the water's latent heat transfer can make up the difference. An investigation was carried out by Hasan [14] to observe the heat transfer of plain and finned tube evaporatively cooled heat exchangers. Under

the same operating conditions a maximum increase of 140% was found for the finned tube evaporatively cooled heat exchanger. The extra surface area is the main reason for the improvement even though the fin performance declined compared to dry conditions.

Evaporative Cooling Media Materials

If pre-cooling the ambient air is the objective then a wet media pad should be used to cool the outside air before it reaches the condenser coils. In this case the type of media used is of greatest importance. The important characteristics when choosing a material are the pressure drop through it, how well it humidifies the air or cooling efficiency, and how it holds up to water damage. Water damage will deteriorate the material's performance because of salts deposits and mold formation. This will lower the cooling efficiency and increase the pressure drop. Another consideration that should not be neglected when selecting the material is the cost. This is very important when analyzing a system's economic advantage.

All the criteria mentioned have been taken into account when testing potential media used for evaporative cooling applications. Al-Sulaiman [15] contrasted three natural fibers to commercial product Aspen-wood excelsior, for a baseline. The three materials were date palm fibers, jute, and luffa, which are inexpensive and indigenous to the Middle East. The cooling efficiency and the effect of water were examined. To perform an equal test for cooling efficiency the materials were arranged to have the same pressure drop. Jute showed the highest cooling efficiency of 62.1%, but the worst in resisting water damage. Combining all factors the luffa was the best performer. The commercial product was one of the worst performers in all categories. Liao [16] conducted experiments with PVC (polyvinyl chloride) sponge mesh with fine and coarse fibers. The materials were tested in a controlled environment inside a wind tunnel to vary

the face velocity. The effects of thickness were also observed. The higher face velocities resulted in higher-pressure drops and lower cooling efficiencies. The lower face velocities produced low-pressure drops and high cooling efficiencies of up to 84% and 92% for coarse and fine fabric PVC sponge respectively. The effect of water was not considered in this study.

Munters Corporation [17] makes a commercially available product for evaporative cooling called CELdek. It is made of cellulose paper that is chemically treated to reduce the degradation from water, but also maintain a high absorbency. It has a self-cleaning design to prevent clogging and provides even airflow with cooling efficiencies as high as 90%.

Conclusion

The studies presented in this review prove the concept of energy savings through evaporative cooling, however they also reveal the problems related with it. Reducing energy consumption by an air-conditioner comes at a cost whether it's from pre-cooling or using an evaporative condenser. To pre-cool the air a media pad, pump and water distribution system have to be added to the air-cooled condenser. To use an evaporative condenser the water quality has to be strictly maintained. Both processes will consume water because of evaporation.

Pre-cooling may be the most practical way to utilize evaporative cooling for a condenser. The media pad is the only difference between pre-cooling and an evaporative condenser in terms of extra components needed for a system. Pre-cooling will allow the use of regular tap water as apposed to treated or filtered water that has to be used in an evaporative condenser. Evaporative condensers require treated water because the contaminants will lead to scaling which reduces the overall heat transfer of the condenser.

The media pads will also experience water damage [15,17], but they can also be easily replaced. Another crucial parameter of a media pad is the balance between the cooling efficiency and the pressure drop. There will be some point where the disadvantage of reduced airflow through the media pad outweighs the benefit from the reduction in dry-bulb temperature [9]. This can be caused when the relative humidity is high and there is a small temperature depression.

Even though the studies showed the potential of energy savings by increasing the vapor compression cycle efficiency, there are some deficiencies with the analysis. The experiments at ASHRAE standard testing conditions [10-12] only represent the performance enhancement at specified weather conditions. They do not reflect the fluctuations in performance when the weather conditions are varied, such as the relative humidity. Because evaporative cooling performance is dependent on the relative humidity of the air, a high ambient relative humidity will not show much improvement in EER. Mathur and Kaushik [8] used dry-bulb and wet-bulb temperatures for their analysis to account for varying weather conditions throughout the day. The loss of airflow over the coils and additional water pumping power were not included in their overall energy analysis. Goswami et al. [6] performed the most rigorous study with experiments and analysis. Experiments were performed on a condenser during actual use of a building. The data were used in the analysis with the water pumping power and the airflow loss included for the complete system. The energy savings were found using the BIN temperature method. To estimate the energy savings for residential applications, the real-life use of a home has to be replicated in the analysis, which was not the case for these studies [6-8,10-12].

Research Objectives

The goal of this research was to obtain the most realistic estimate of the energy savings for a home using indirect evaporative cooling with an air-conditioner. A combination of different aspects from the previously mentioned studies was incorporated into this research to achieve this goal.

The objectives included running experiments with a used residential air-conditioner and modeling its use on a home. The experiments were run to obtain the energy use from the system at different weather conditions, namely the dry-bulb temperature and relative humidity. They were performed for a baseline case and with the evaporative cooling device installed. A software program was used to create a house and simulate a cooling load on it using weather data and internal loads the residence may experience. An hour-by-hour cooling load was generated along with the corresponding dry and wet-bulb temperatures for the entire cooling season. The experimental data were used with the output from the software to create the energy savings. This process is detailed in a later chapter.

The research presented in this thesis differs from other research because it accounts for all the features involved with evaporative cooling used in conjunction with an air-conditioner. The data with the evaporative cooling device have the effects of increased relative humidity, parasitic power requirements, and pressure drop worked into it to represent a complete system. Also the modeling of the cooling load for a house from actual use has not been done previously. This is very important because of the intermittent use of an air-conditioner. An air-conditioner is turned on when the temperature increases beyond the control setting and turns off when it reduces the

temperature enough. This is all dependent on the internal load and the load created from the weather. These two parameters are simulated from the software.

CHAPTER 3
EXPERIMENTAL APPROACH

This chapter will explain both the experimental setup and the procedure to gather data. The setup includes details of the facility where the experiments were run along with the instrumentation used to collect the data. The evaporative cooling retrofit design is also detailed in this chapter. The procedure will discuss the steps taken to obtain the data and the data points of interest.

Experimental Setup

The laboratory used to conduct the experiments was the University of Florida Air-Conditioning System test facility that was reported by Goswami et al [18]. It is a doublewide mobile home module that consists of three rooms as shown in Figure 3-1. Rooms A and B are the two climate controlled rooms that simulate the outdoor and indoor conditions respectively and Room C is left for the operator and data acquisition system.

The test unit selected for the experiments was a high efficiency split heat pump system. The specifications are found in Table 3-1. It has a SEER of 10 and a total cooling capacity of three tons according to the manufacturer. It was a previously used system before being installed into the test facility.

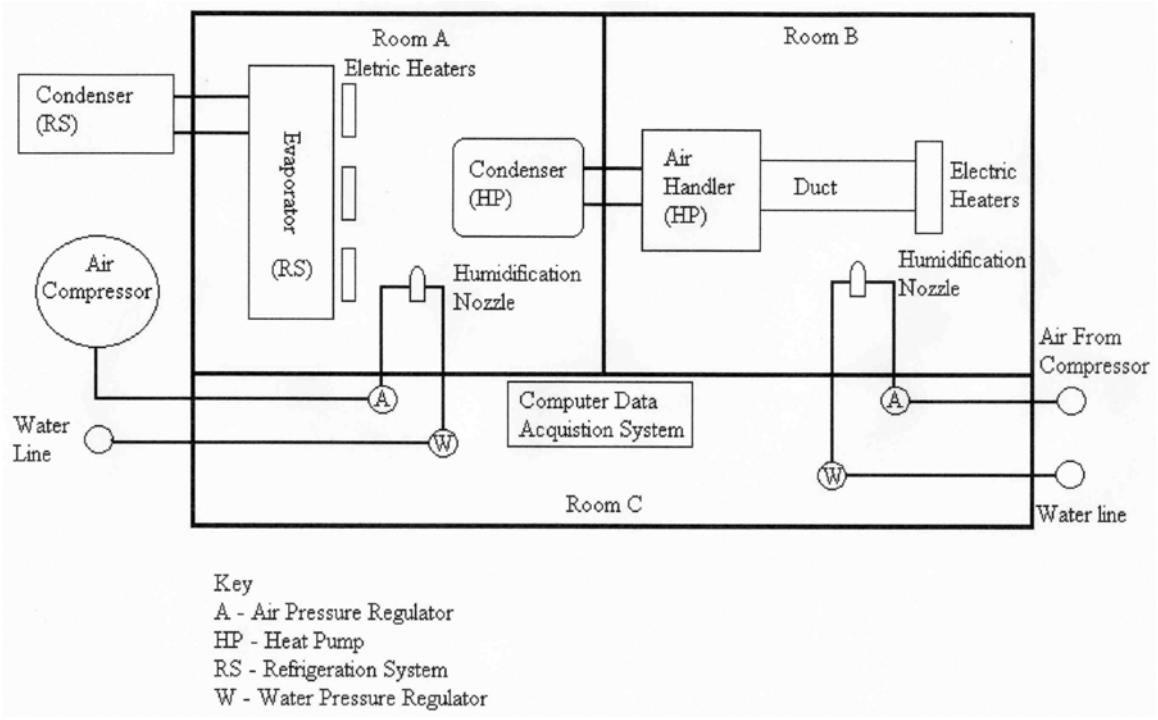

Figure 3-1. The layout of the test facility and the equipment in each room.

Table 3-1. Description of the residential split heat pump used for experiments.

Manufacturer	Goodman Manufacturing Company 1501 Seamist, Houston, Texas 77008
Outdoor section Model	CPE 36-1AB
Indoor air handler	A36
Capacity	35,000 BTUH, 3 tons (nominal)
SEER	10
Serial Number	9502001920

Room A

Room A contains the condenser and compressor configuration because it is used to simulate the outdoor weather conditions. The outdoor conditions are maintained by a refrigeration system described in Table 3-2, three 4.3-kilowatt electric heating elements, and an atomizing humidification nozzle. These can be seen in Figure 3-2.

Table 3-2. Description of the refrigeration system used in Room A.

Bohn: Air Cooled Condensing Unit (Bhonametic): DB9H2 Medium Temperature Evaporator: FL4002G 12 kW heaters for defrosting.

Figure 3-2. Picture of the setup used to control the environment in Room A. A) Evaporator of the refrigeration system. B) Electric heater positioned in front of the evaporator's fan. C) Humidification nozzle.

Figure 3-3. Close up view of an electric heater positioned in front of the evaporator's fan.

The refrigeration system and the heaters are used to maintain the dry-bulb temperature. A close up of the evaporator and one electric heater can be seen in Figure 3-3. One of the heaters is connected to a variac to adjust the heat input while the other two are always turned on to their full heating capacity. The nozzle uses compressed air and water to create a fine mist that supplies humidity to the room that is eliminated by the evaporator. Adjusting the pressures of both the air and water to the nozzle allows the room to reach elevated relative humidities. The room is capable of controlling the temperature in the range of 20-110^{o}F and humidity from 30-100%.

The room was instrumented to measure data of interest that would allow the performance of the test system to be obtained. A list of instrumentation can be found in

Table 3-3. The baseline experiments used three thermocouples that were positioned on each side of the condenser. That configuration allowed for an average dry-bulb temperature to be taken before the air was drawn over the condenser's coils. Two humidity probes were also positioned on two sides of the condenser to measure the relative humidity of the air before entering the coils. The air that exits the condenser was also monitored with a probe that recorded both temperature and relative humidity. An instantaneous power transducer was used to measure the power input to the compressor and the condenser fan. These instruments and their position are shown in Figure 3-4. A pressure transducer and a thermocouple were used to measure the pressure and temperature, respectively, of the refrigerant after exiting the compressor (Figure 3-5). Manual measurements were taken with an anemometer to find the airflow rate of the condenser.

Table 3-3. List of devices and their specifications used in Room A.

Parameter	Device	Range
Relative Humidity	Vaisala HMD20UB Vaisala HMD60Y	0-100 % RH 0-100 % RH
Temperature	Vaisala HMD60Y	-5 - +55 ºC
Temperature	T-type Thermocouple	< 200 ºC
Power	Instantaneous Power Transducer Ohio Semitronics PC5-29F	0-10 kW
High Pressure	Mamac Systems PR-262	0-350 psig
Air Flow Rate	Hot wire anemometer Kay-May KM4107	0-6000 fpm

Figure 3-4. Picture of the test unit's condenser in Room A with its instrumentation. A and B) Thermocouples surrounding the condenser. C and D) The humidity probes surrounding the condenser. E) A combination temperature and humidity probe that measures the air exhausted from the condenser. F) The power transducer that measures the power of the condenser.

Figure 3-5. Picture of the high-pressure line of the condenser. A) Pressure transducer. B) Thermocouple probe.

Room B

Room B maintains the indoor environment as stated earlier. It has the air handler, which includes the evaporator of the test system. The air handler was used to maintain the indoor conditions, while four electric heaters (1, 1.2, 2, 3kW) and a humidifying nozzle were used to simulate the load. Each heater could be turned on separately and the 1-kilowatt heater was connected to a variac. This was done to generate a range of loads and was adjusted to meet the indoor conditions.

The instruments used in Room B are found in Table 3-4. The setup of the room with its equipment and instrumentation are presented in Figures 3-6 to 3-8. The return air to the evaporator was measured with four thermocouples and a humidity probe. A humidity and temperature combination probe was inserted in the duct to record readings of the supply air. The probe was positioned after the blower in the air handler. The anemometer was used to manually measure the airflow in the duct following the method from ASHRAE Handbook of Fundamentals [19]. The suction line or the low-pressure side on the test unit also had a pressure transducer attached to it along with a thermocouple probe to check the temperature. The refrigerant flow rate was monitored with a flowmeter on the high-pressure side. One thermocouple was strategically placed on one of the evaporator tubes. It was attached to the tube with a high thermal conductivity bonding agent and was insulated on the backside. This measurement assisted in the superheat test discussed in a later section.

Table 3-4. List of devices and their specifications used in Room B.

Parameter	Device	Range
Relative Humidity	Vaisala HMD20UB Vaisala HMD60Y	0-100 % RH 0-100 % RH
Temperature	Vaisala HMD60Y	-5 - +55 ºC
Temperature	T-type Thermocouple	< 200 ºC
Air Flow Rate	Hot wire anemometer Kay-May KM4107	0-6000 fpm
Low Pressure	Mamac Systems PR-262	0-250 psig
Refrigerant Flow Rate	Rotameter Brooks 3604	0-2.8 GPM 1.13 SG, 0.18 cp

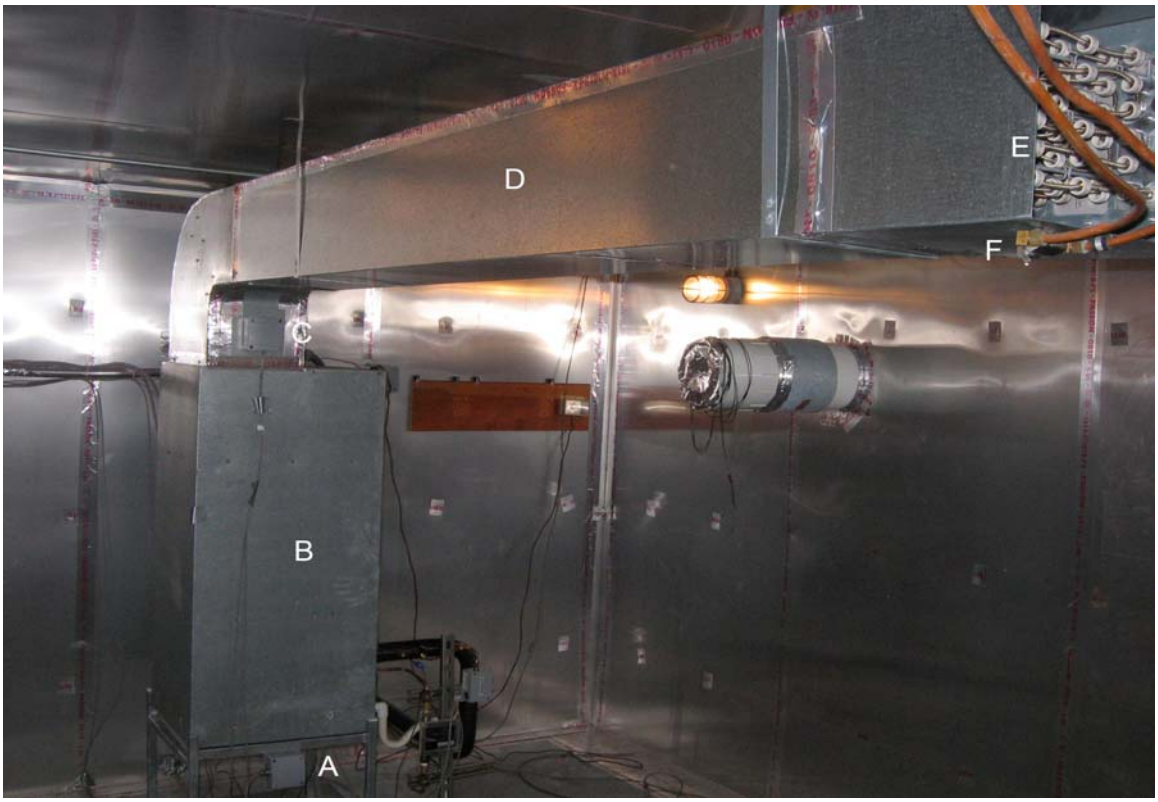

Figure 3-6. Picture of equipment and instruments in Room B. A) Humidity probe that measures the return air. B) The air handler. C) Humidity and temperature combination probe that measures the supply air. D) The supply air duct. E) The four electric heaters inside the duct. F) The humidity nozzle.

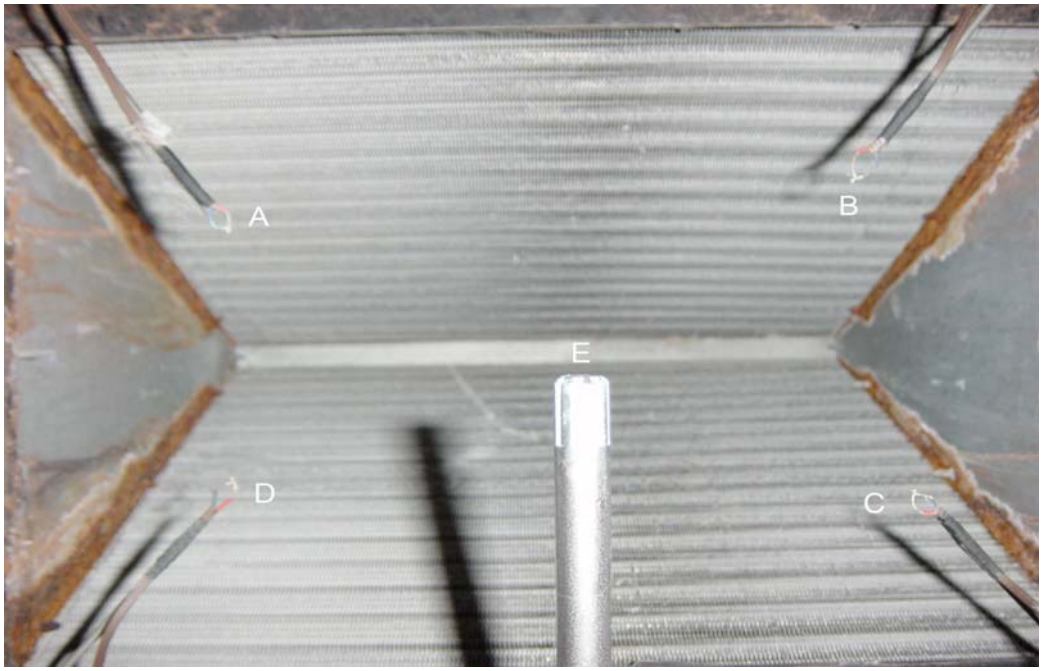

Figure 3-7. View inside the air handler showing the evaporator and the instruments measuring the return air. A, B, C, D) Thermocouples. E) Humidity probe.

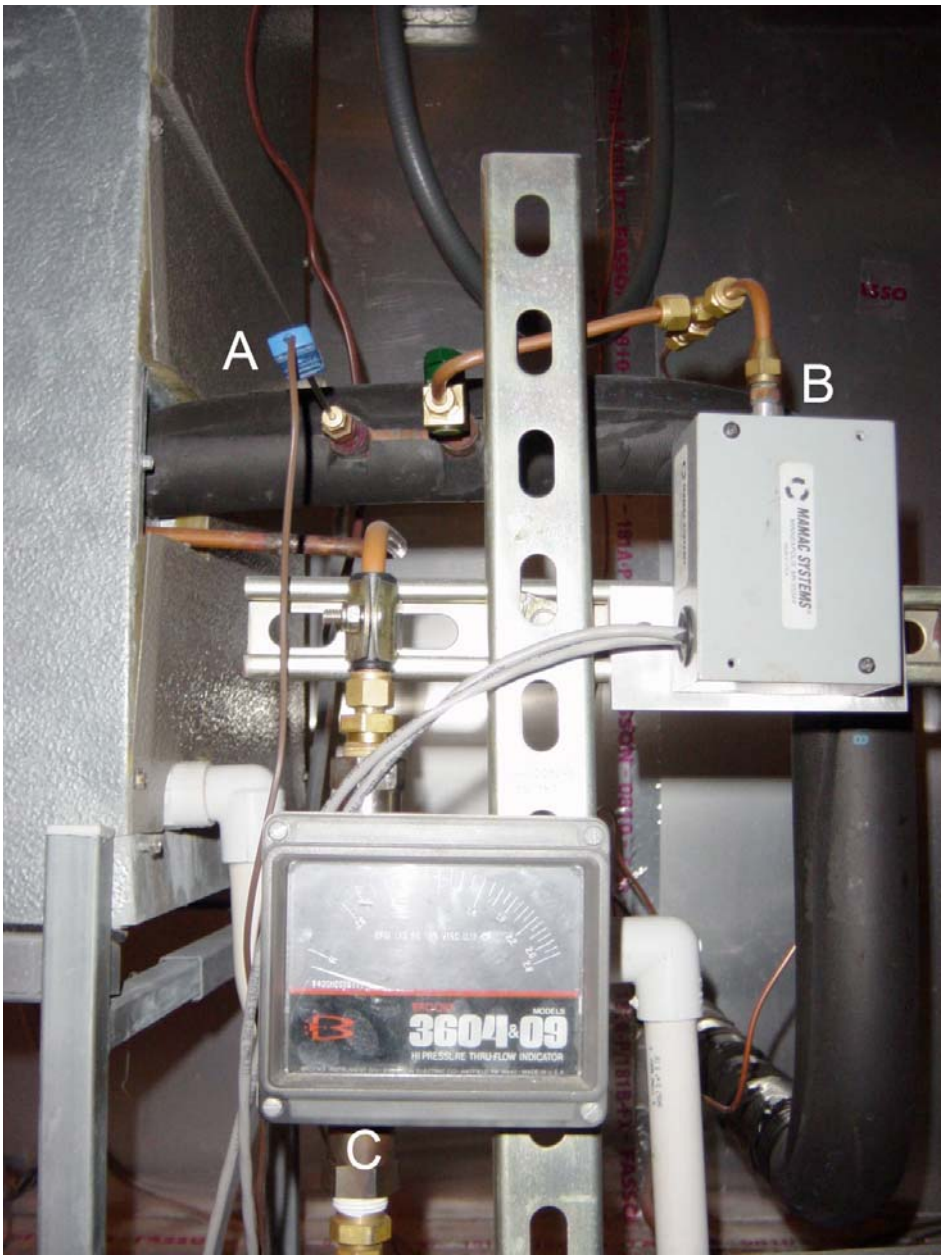

Figure 3-8. Close up view of the suction line and high-pressure line connected to the air handler. A) The thermocouple probe inserted into the suction line. B) The pressure transducer measuring the suction line. C) The flowmeter connected to the high-pressure refrigerant line.

Evaporative Cooling Setup

Room A also contains the evaporative cooling setup for its experiments. The method of evaporative cooling used for the experiments was pre-cooling the inlet air of the condenser. A list of equipment can be found in Table 3-5. The setup was designed

according to Munters [20] and Glacier-Cor [21] specifications and these details are in Appendix A. The sheet metal frame was fabricated to fit around the condenser and house the media pad shown in Figure 3-9. It also served as the collection device for the water that wasn't evaporated and returned it back to the sump. Another important feature of the frame was that it sealed off any gaps between the frame and the condenser to ensure that all the air went through the media pads first before passing over the coils. The sump held the water that was distributed to the media pads via a submersible pump and PVC fittings and pipe. A flowmeter and a ball valve were used to provide the correct flow rate to the media pads. This configuration is also found in Figure 3-9. The water from the header sprayed upward and hit the deflector plates to help distribute the water to the media pads. This can be observed in Figures 3-10 and 3-11. The media pads were the most essential component to the evaporative cooling device. It will be described in a subsequent section.

Table 3-5. List of products used to construct the evaporative cooling device used to pre-cool for the condenser.

Component	Manufacturer
Galvanized Sheet Metal Frame and Sump	N/A
Galvanized Sheet Metal Deflectors	N/A
¾ Inch PVC Pipe	N/A
3, ¾ Inch PVC Elbows	N/A
2, ¾ Inch PVC End Caps	N/A
¾ Inch PVC Tee	N/A
¾ Inch PVC Couplings	N/A
¾ Inch PVC Ball Valve	N/A
Flowmeter	Key Instruments
Small Submersible Sump Pump	Little Giant
Cellulose Evaporative Cooling Pad	Glacier-Cor

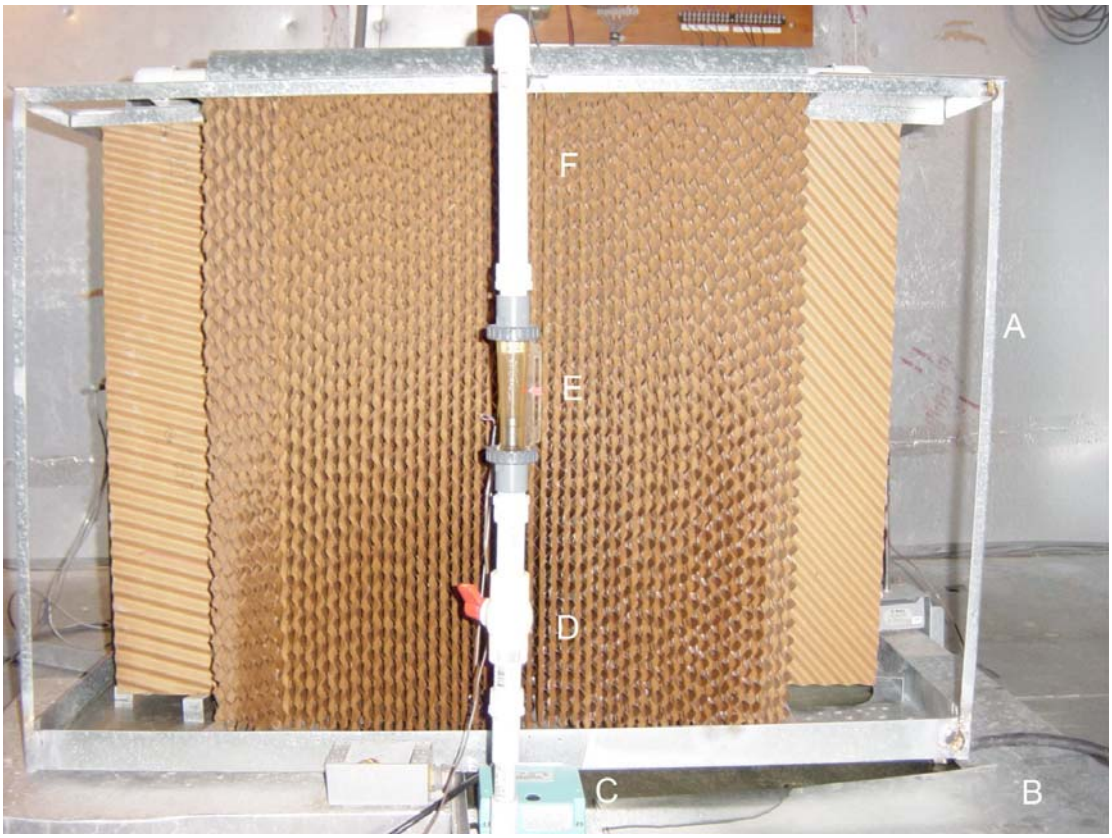

Figure 3-9. View of the evaporative cooling system installed around the condenser. A) A combination frame and gutter system. B) The sump that holds and recollects water. C) Small submersible pump that circulates the water. D) Ball valve used to control the flow rate. E) Flowmeter used to check the flow rate. F) PVC pipe used to transport water.

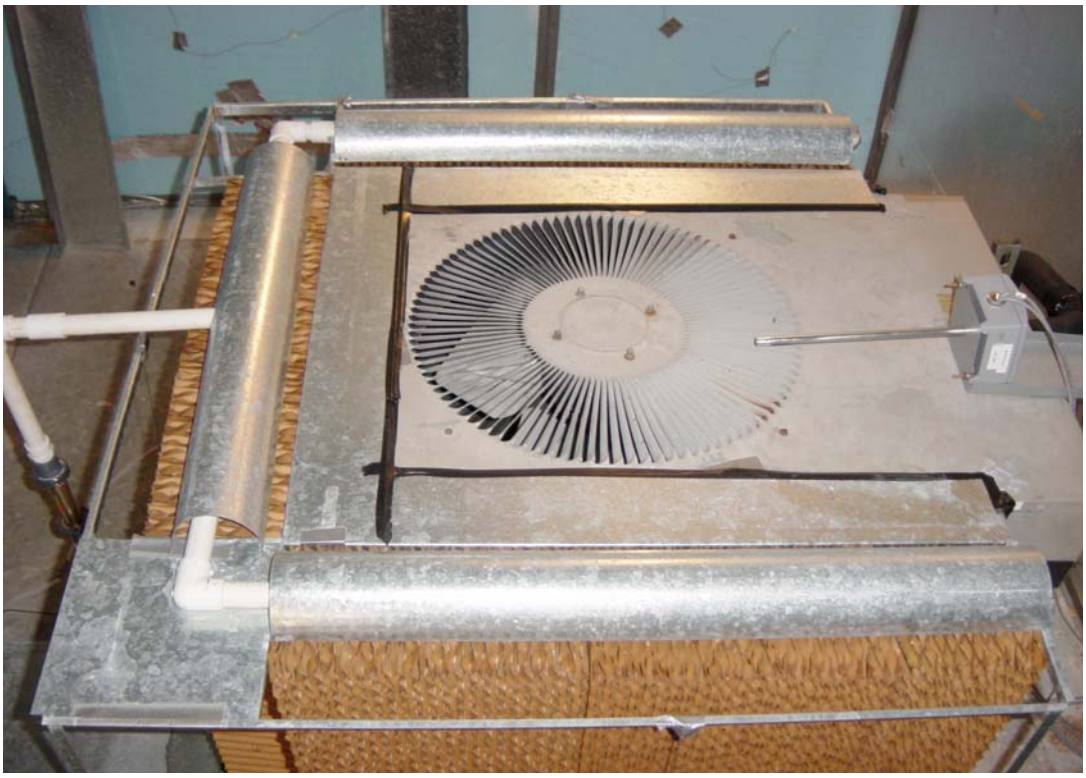

Figure 3-10. The top view of the condenser retrofit showing the header covered by the deflecting plates.

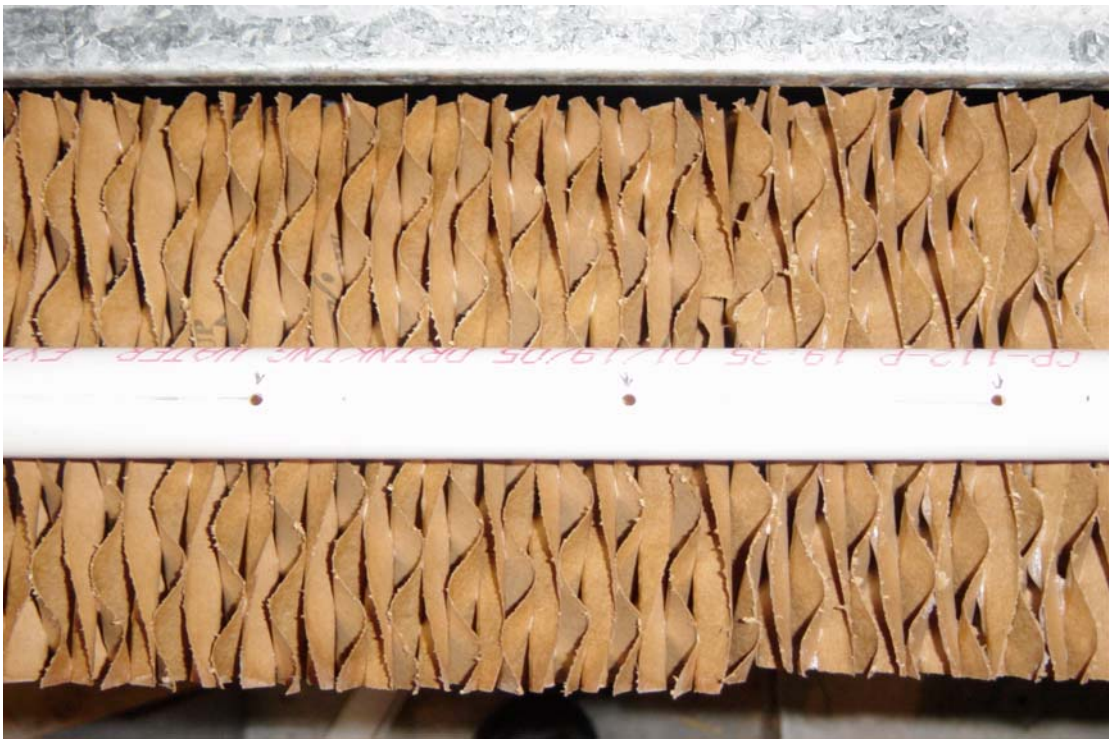

Figure 3-11. Close up view of the header with the deflecting plate removed showing the spray holes.

A slight modification had to be made to the instrumentation in Room A to accompany the evaporative cooling device. Three additional thermocouples were installed around the evaporative cooling pads on each side of the condenser. The two humidity probes were moved to the inlet air side of the evaporative cooling pads. The frame was sized to leave space for the three thermocouples positioned directly in front of the condenser coils. From this setup the dry-bulb temperature and relative humidity of the air entering the retrofitted condenser could be measured, along with the dry-bulb temperature of the air after passing through the pads. Figure 3-12 shows this description. The pump used to distribute the water to the media pad was connected to the compressor and fan's power supply and all three were collectively read by the power transducer.

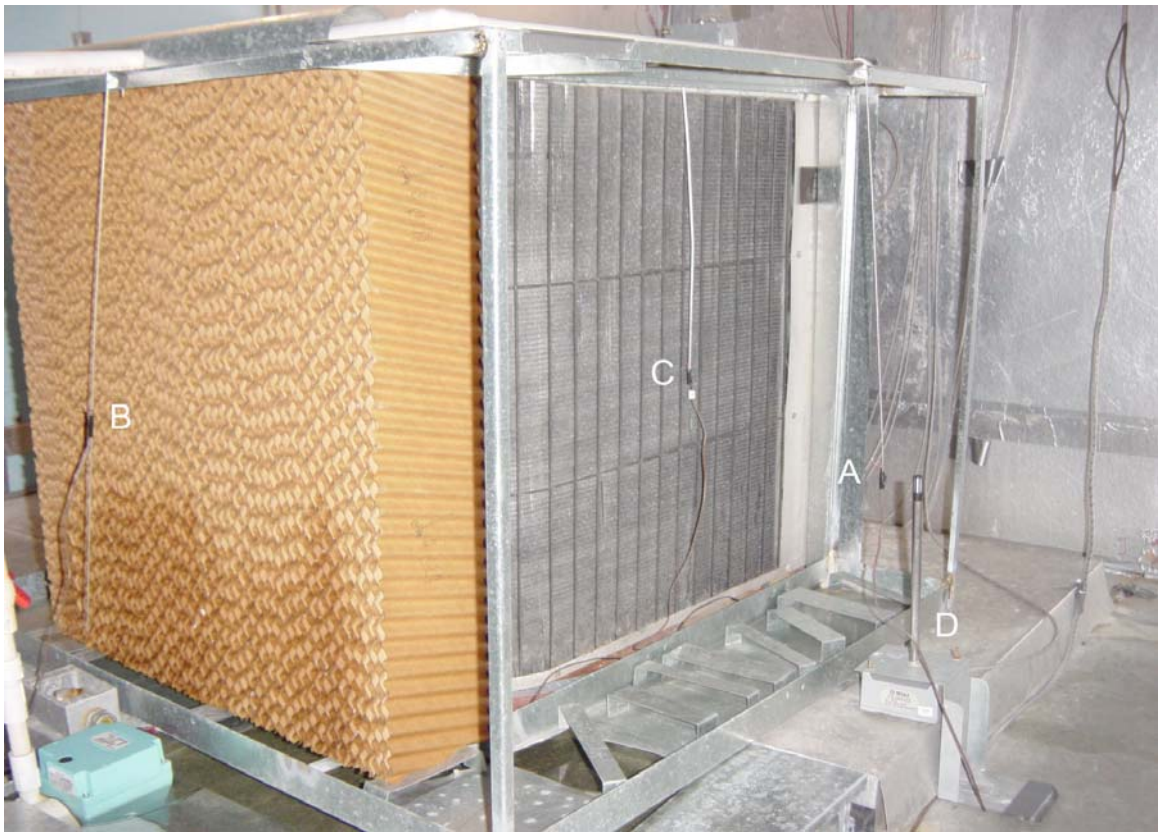

Figure 3-12. Picture of the evaporative cooling pads removed from one side of the condenser. A and B) Additional thermocouples placed on the outside of the media pad. C) Thermocouple in its original position. D) Humidity probe moved to the outside of the media pad.

An important issue came up while running experiments with the evaporative cooling retrofit installed. The lower relative humidities were unattainable because all of the water being introduced into the air in Room A from the media pad's humidification action. Data were still acquired from these points following a different procedure detailed in the experimental procedure section. The dry-bulb temperature that the condenser would experience was calculated and used as a representation of the actual dry-bulb temperature and relative humidity in Room A. These new temperatures are discussed in a later chapter.

Evaporative Cooling Media Pad

The media pad used for these experiments was 45/15 Cellulose Evaporative Cooling Media Pads developed by Munters [17] and Glacier-Cor [21]. The 45/15 in the name refers to the flute angles of the pad. A picture of both flute angles can be seen in Figure 3-13. As water flows from the top of the pad the 45-degree flute angles draw the water toward the front of the pad where the air enters and to flush debris out of it [21]. The 15-degree flute angles serve the same purposes, but at a lesser angle to reduce the pressure drop through the pad [21]. These flute angles create a wavy shape in the pad and increase its surface area as seen in Figure 3-14. The thickness chosen for the pad was six inches. The criteria for choosing the pad thickness are the cooling efficiency and the pressure drop through the pad. Both parameters vary with pad thickness and face velocity of the air. The amount of water used to saturate the pads was a function of the top surface area of the pads. In this case the amount of water used was 5.5 gallons per minute. The material of the pads was a kraft paper that is treated with chemicals to withstand typical water damage such as scaling and mold formation. Proper maintenance of the pads can result in a lifetime of up to five years.

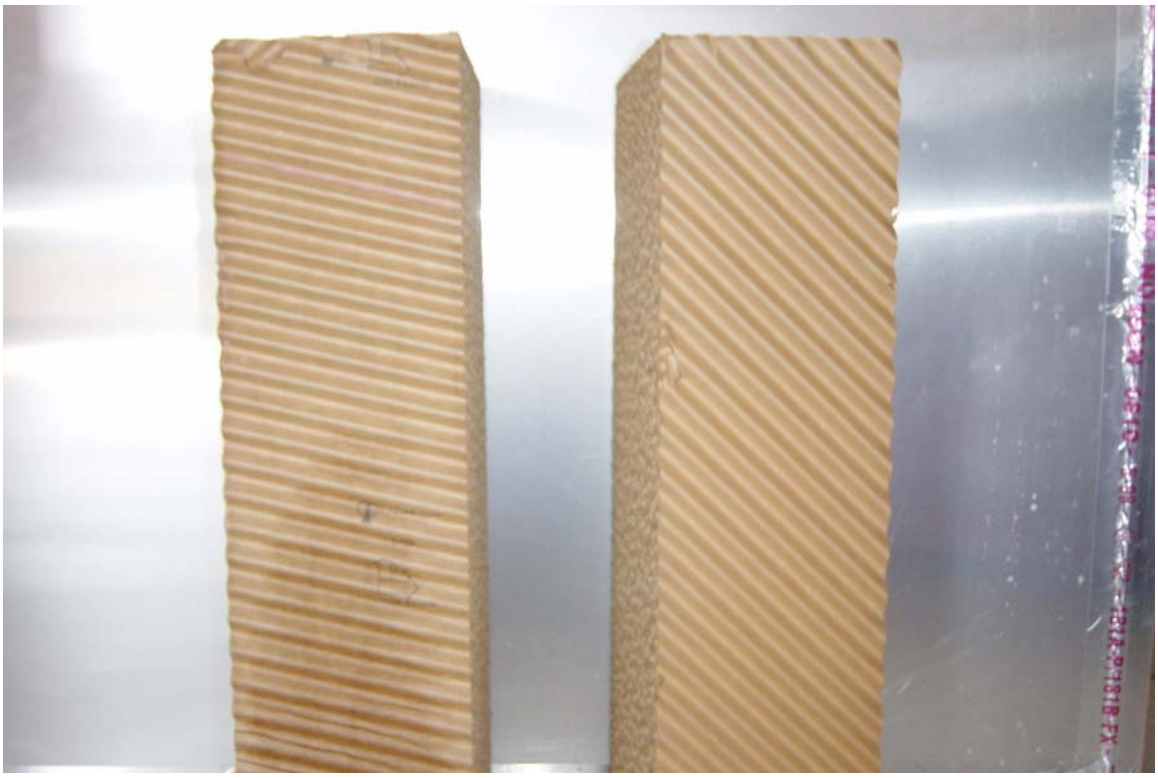

Figure 3-13. Side views of the Glacier-Cor cellulose evaporative cooling pad showing both flute angles. 15-degree flute angle on the left and 45-degree on the right.

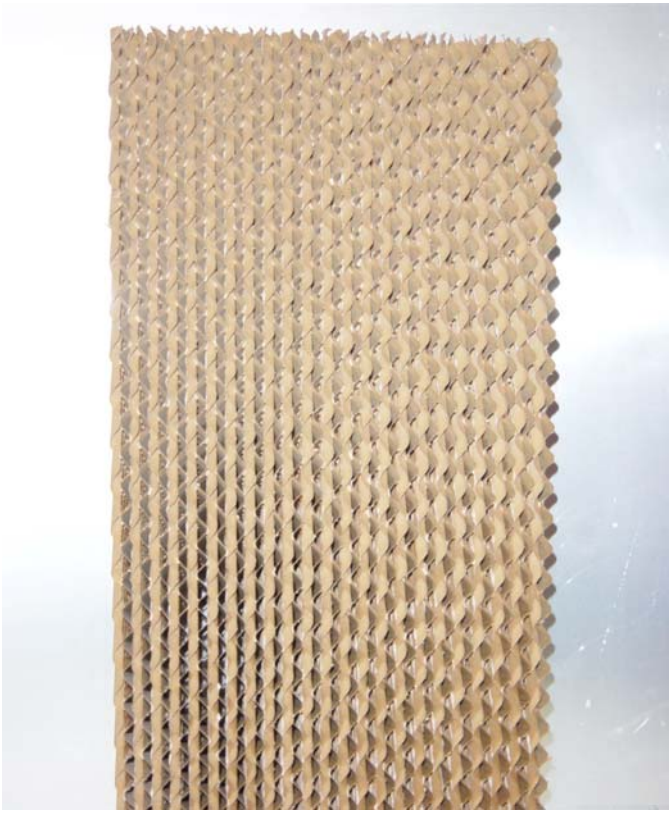

Figure 3-14. Front view of the media pad showing the wavy structure of the pad.

The media pad's purpose was to provide surface area for the humidification process. As water is drained down from the top of the pad, the cellulose material absorbs it. The advantage of this characteristic is the pad will be completely saturated. The air will have a constant source of water to evaporate as it travels through the pad. The air is drawn through the pads by the condenser's fan.

Experimental Procedure

Before any experiments could be run, a superheat test had to be performed. This was done to have the correct amount of refrigerant in the system according to the manufacturer's specifications. While the test unit was turned on the pressure was checked along with the corresponding saturation temperature of the refrigerant. The saturation temperature was subtracted from the refrigerant temperature in the suction line to give the superheat temperature. The thermocouple placed on the evaporator tube was used as a check against the saturation temperature. The superheat temperature varies with different dry-bulb temperatures for outdoors and indoors and with level of refrigerant charge.

The experimental procedure that was followed for each condition is described here. The test system had to be evaluated while the condenser was subjected to different outdoor conditions. The indoor and outdoor conditions are presented in Table 3-6.

Table 3-6. List of data points for indoor and outdoor conditions.

Room	Dry-Bulb Temperature (^{o}F)	Relative Humidity (%)
A (Outdoor Conditions)	60	50, 60,70, 80, 90
	70	40, 50, 60, 70, 80, 90
	80	40, 50, 60, 70, 80, 90
	90	40, 50, 60, 70, 80, 90
	95	40, 50, 60, 70, 80
	100	40, 50, 60, 70, 80
B (Indoor Conditions)	80	50

The outdoor weather conditions are the range of temperatures and relative humidities that cover the cooling season in Florida. The indoor conditions were maintained at the specified temperature in Table 3-6 for all the experiments and follow the standard test procedure for ASHRAE Condition "A" [22]. Each condition was achieved in the test facility and data collected at steady state.

After examining Table 3-6, it can be noticed that the outdoor temperatures are not tested at the same range of relative humidities. At 60^{o}F there is no 40% relative humidity and for 95 and 100^{o}F there is no 90% relative humidity. Room A was incapable of reaching 40% RH at 60^{o}F. At 95 and 100^{o}F, the amount of water required to reach 90% relative humidity caused problems with thermocouples and humidity probes. The first step for the experimental procedure was to turn on the test unit, heaters and spray nozzle inside Room B. The refrigeration system, heaters and spray nozzle in Room A were turned on next. The humidifying nozzles and heaters were adjusted for both rooms until the target conditions were obtained. The output from thermocouples and the humidity probes surrounding the condenser was used to check the prescribed conditions in Room A. The thermocouples and humidity probe for the return air were monitored for Room B. In Room A the lowest relative humidity for each temperature was tested first. For each set of conditions the rooms were maintained for approximately 30 minutes. Data was captured in the beginning of the time frame and towards the end. Over the 30 minutes of steady state, minor adjustments had to be made with the heaters and the humidification nozzle in Room A to sustain the specified conditions. After the data was obtained for the lowest relative humidity, the air and water pressure were increased to provide more humidification into Room A to reach the next relative humidity point. Doing this

required more heat to stay at the same temperature, so the variac was turned up also. This was the standard procedure used to obtain the different data points.

With the evaporative cooling device retrofitted, three additional thermocouples were added and positioned on the air inlet sides of the media pads. These were used to check the dry-bulb temperature in Room A. The rest of the procedure follows the same steps mentioned. Some of the lower relative humidities were not achievable because it was difficult to compensate for the additional humidification introduced by the evaporative cooling pads.

A different procedure was used to record data for lower RH values with the evaporative cooling device installed. The changes were exclusively in Room A where the outdoor conditions had to be met. The humidification nozzle was not used at all. The readings from the thermocouples and humidity probes located on the air inlet side of the media pads were neglected. Dry-bulb temperatures were predicted for each unattainable data point after passing through the media pad. The thermocouples positioned directly outside the condenser were monitored to uphold these predicted temperatures.

In order to simulate the dry-bulb temperatures the condenser coils would be exposed to, the data at higher RH's was used to predict them. For each temperature the dry-bulb temperature exiting the media pad was plotted as a function of relative humidity. A trend line was fit to the available points at high relative humdities and an equation of that line was calculated. Table 3-7 shows the equations formulated for each temperature and the number points used to obtain it. Also the R^2 values shows how well the points fit to the trend lines. Table 3-8 gives the simulated dry-bulb temperatures that would result

after the air passed through the pad from the corresponding dry-bulb temperature and relative humidity.

Table 3-7. Table showing the equations used to predict the dry-bulb temperature after the media pad at lower relative humidities.

Temperature (^{o}F)	Points	Equation	R^2
60	3	0.0963*RH+50.212	0.6605
70	4	0.1592*RH+54.286	0.9776
80	4	0.2327*RH+58.758	0.9960
90	4	0.3056*RH+62.554	0.9966
95	3	0.2881*RH+67.642	0.9915
100	3	0.2992*RH+71.906	1

Table 3-8. List of dry-bulb temperatures used for the experiments at lower relative humdities.

T_{db} (^{o}F)	RH (%)	$T_{db,new}$ (^{o}F)
60	50	55.03
	60	55.99
70	40	60.54
	50	62.25
	60	63.84
80	40	68.07
	50	70.39
90	40	74.78
	50	77.83
95	40	79.17
	50	82.05
100	40	83.87
	50	86.87

A list of directions for the startup and shutdown of the test facility can be found in Appendix B.

Data Acquisition

The data from both environmentally controlled rooms were collected in Room C. The thermocouples, pressure transducers, humidity probes, and dual-purpose humidity and temperature probes were connected to the data acquisition system expansion cards. Through the data acquisition, software, and specific interface cards these measurements were saved on a computer. The airflow rates were taken manually with the anemometer

inside the duct in Room B and around the condenser in Room A as mentioned earlier. The refrigerant flow rate was also checked manually from the flow meter.

CHAPTER 4
RESULTS AND DISCUSSION

The following chapter will present the results from the experiments described in the previous chapter. Data was collected on the performance of the system for a range of outdoor conditions. The experimental results were then applied to simulate the energy consumption of a residential air-conditioner using Typical Meteorological Year (TMY) weather data.

Experimental Results

Cooling Pad Performance

The two parameters used to measure the performance of a media pad are its cooling efficiency as well as the pressure drop. A high cooling efficiency combined with a low pressure drop is desirable for optimum performance. The cooling efficiency of the media pad is defined as:

$$CE = \frac{T_{db,in} - T_{db,out}}{T_{db} - T_{wb}} \tag{4-1}$$

Table 4-1 lists the measured cooling efficiency with the cooling pads fitted around the condenser. The average cooling efficiency was approximately 70%, but if two of the outliers are taken out the average becomes 75%. Table 4-2 gives the measured flow rate of air flowing through the condenser. This translates to a face velocity of 176 and 216 fpm for the evaporative cooling and baseline case respectively. According to the manufacturer's performance data, the media pad has a cooling efficiency of 75% at a face

velocity of 200 fpm (see Figure A-1). The airflow rate was reduced approximately 21% with the media pad surrounding the condenser.

Table 4-1. The cooling efficiency for each temperature and relative humidity.

$T_{db,inlet}$ (^oF)	T_{wb} (^oF)	$T_{db,outlet}$ (^oF)	RH (%)	CE (%)	Uncertainty (%)
60.18	54.63	56.63	70.58	63.92	±11.49
60.36	56.79	58.76	80.73	44.85	±19.17
60.03	58.24	58.48	90.11	86.55	±33.75
70.17	63.64	65.34	70.40	73.99	±9.49
70.20	65.85	66.73	79.84	79.66	±14.07
70.13	68.00	68.76	89.90	64.36	±29.91
80.03	70.55	73.30	63.08	71.00	±6.59
80.40	72.91	75.37	70.35	67.10	±8.44
80.59	75.75	77.34	80.33	67.14	±13.06
80.96	78.58	79.73	90.10	51.63	±28.01
90.10	79.50	81.86	63.27	77.73	±5.80
90.69	82.19	84.18	70.16	76.57	±7.25
90.95	85.48	86.76	80.13	76.66	±11.27
90.55	88.00	90.31	90.40	9.38	±31.73
95.12	83.53	85.66	62.04	81.63	±5.26
95.44	86.75	87.74	70.75	88.60	±6.95
95.65	89.96	90.89	80.24	83.66	±10.68
100.43	88.26	90.49	62.12	81.66	±5.01
100.37	91.25	93.05	70.69	80.25	±6.70
100.09	94.13	95.89	80.15	70.54	±10.49

Table 4-2. The airflow rate for the baseline and media pad cases.

Case	Airflow Rate (SCFM)	Uncertainty (SCFM)
Baseline	2986	± 90
Media Pad	2366	± 71

The appropriate amount of water has to be supplied to the media pad to achieve the highest cooling efficiency (refer to Appendix C). Even when the water is recirculated there is a cost associated with the evaporation. The evaporation rate of the tested media pad is presented in Table 4-3. It includes all the weather conditions other than the simulated points. The lower RH's evaporated more water at each temperature because the

air was drier. This adds to the operation cost and should be considered in an overall economic analysis. It can be a substantial cost depending on location.

Table 4-3. The evaporation rate for the media pad tested.

T_{db} (^{o}F)	RH (%)	Evaporation Rate (gal/hr)
60.18	70.58	1.07
60.36	80.73	0.48
60.03	90.11	0.47
70.17	70.4	1.44
70.2	79.84	1.04
70.13	89.9	0.41
80.03	63.08	1.99
80.4	70.35	1.49
80.59	80.33	0.97
80.96	90.1	0.38
90.1	63.27	2.42
90.65	70.16	1.91
90.95	80.13	1.23
90.55	90.4	0.07
95.12	62.04	2.78
95.44	70.75	2.27
95.65	80.24	1.42
100.43	62.12	2.92
100.37	70.69	2.16
100.09	80.15	1.25

The media pad's characteristics have a profound effect on the performance of the condenser. As the air passes through the media pad the velocity is decreased, but mass is acquired from humidification. The reduced air velocity had a greater influence on the mass flow rate than the additional mass. A 21% decrease in mass flow rate through the condenser was approximated and corresponds the reduction in face velocity. The additional mass increased the difference in enthalpy of the inlet and outlet air. As a result, the condenser rejected more heat than the baseline case. The denser air was able to obtain more energy and outweigh any negative effects of less air entering the condenser, which enhanced the performance of the condenser. Reducing the face velocity approximately 50% yields similar rates of heat rejection between the two cases.

Calculations

The energy efficiency ratio values were calculated based on the airside enthalpies of the tests system's evaporator from the ASHRAE Standard Method of Testing for Rating Unitary Air-Conditioning and Heat Pump Equipment [22]. The enthalpies are calculated for the return and the supply air. The following equations were used to calculate the energy efficiency ratio (EER):

$$p_v = \phi p_g \tag{4-1}$$

$$v_{air} = \frac{R_{air}\left(T_{db} + 460\right)}{p_{atm} - p_v} \tag{4-2}$$

$$w = \frac{0.622\, p_v}{p_{atm} - p_v} \tag{4-3}$$

$$\dot{m}_{air} = \frac{SCFM}{v_{air}} \tag{4-4}$$

$$h_{air} = 0.24T_{db} + w\left(1061 + 0.444T_{db}\right) \tag{4-5}$$

$$\dot{Q}_{air} = 60\dot{m}_{air}\left(h_{air,supply} - h_{air,return}\right) \tag{4-6}$$

$$COP_{air} = \frac{\dot{Q}_{air}}{3.412P_c} \tag{4-7}$$

$$EER_{air} = 3.412COP_{air} \tag{4-8}$$

The water vapor partial pressure (p_v) is a product of the relative humidity (ϕ) and the saturation pressure (p_g) at a specified dry-bulb temperature (Equation 4-1). In Equation 4-2 the specific volume of the air and water vapor mixture (v_{air}) is calculated from the dry-bulb temperature (T_{db}), universal gas constant for air (R_{air}), atmospheric pressure (p_{atm}), and water vapor partial pressure. The humidity ratio (w) is found using the partial

pressure of the water vapor and the atmospheric pressure, Equation 4-3. Equation 4-4 can be used to find the mass flow rate of the air ($\dot{m}_{air}$) from the airflow rate (*SCFM*) and the specific volume of the air and water vapor mixture. The enthalpy of the air (h_{air}) in Equation 4-5 uses the dry-bulb temperature and humidity ratio. Equations 4-1 to 4-5 are all calculated at two points, before (return air) and after (supply air) the evaporator. The rate of heat transfer or cooling capacity ($\dot{Q}_{air}$) in Equation 4-6 is calculated from the mass flow rate and the difference in enthalpies between the return and supply air. The cooling capacity is divided by the compressor power (P_c) to arrive at the coefficient of performance (*COP*) in Equation 4-7. Finally Equation 4-8 provides the energy efficiency ratio (*EER*) by multiplying the coefficient of performance with a constant.

These equations represent the thermodynamic definitions, but the calculations done for this analysis used two modified variables. The variables P_c and $h_{air,supply}$ are the compressor power and enthalpy of the air directly after the evaporator, respectively. In the calculations used throughout this study, the condenser power and the enthalpy of the air after the blower in the air handler were used. The condenser power includes the power of the compressor, the fan and the water pump, when the evaporative cooling device was added. Any change in the fan consumption due to the evaporative cooling device being installed would be included in the measurements.

Measuring air properties after the blower in the air handler lead to two important points. The first being that it accounted for any heat gain from the blower and represented the actual dry-bulb temperature of the air supplied to the conditioned space. Secondly, the blower ensured that the air was well mixed at the point of measurement.

The EER calculated for this research represents a total system EER and should be distinguished from the Seasonal Energy Efficiency Ratio (SEER) that ASHRAE uses.

The following sections break down each temperature providing EER, condenser power, condenser pressure, heat transfer rate, and refrigerant temperature entering the evaporator as a function of relative humidity. Calculations were carried out to find the energy efficiency ratio and rate of heat transfer. The pressure, power, and refrigerant temperature entering the evaporator were measured with their respective instruments. The refrigerant temperature entering the evaporator was measured with the thermocouple bonded to the evaporator tube inside the air handler. It should be pointed out that the simulated points are labeled differently than the points that were found with the actual dry-bulb temperature and relative humidity for each graph.

60^{o}F Ambient Dry-Bulb Temperature

Figure 4-1 presents the results for EER. The baseline case has a higher EER for the entire range of relative humidities experimented at. It can be seen in Figure 4-2 that the total condenser power was greater for the media pad case for all RH's. Each ascending increment in RH showed a more substantial difference between the two cases. Figure 4-3 shows that the condenser pressure was lower at all tested RH's for the media pad case. It was a result of cooler ambient air entering the condenser. Also the compressor power was reduced because of lower condenser pressures. As the relative humidity rose, the condenser pressure for the media pad case approached the baseline case. The lower condenser pressure also led to a lower refrigerant temperature as it entered the evaporator shown in Figure 4-3. Again, as the RH is increased the media pad case approaches the baseline case. It can be seen in Figure 4-5 that the rates of heat transfer through the evaporator for both cases were practically the same. The difference in refrigerant

temperature entering the evaporator was inadequate for additional heat transfer with the maximum of only 2°F at 50% RH. Even with a reduction of the ambient air temperature produced by the media pad, it was not able to overcome the additional water pumping power to enhance the performance.

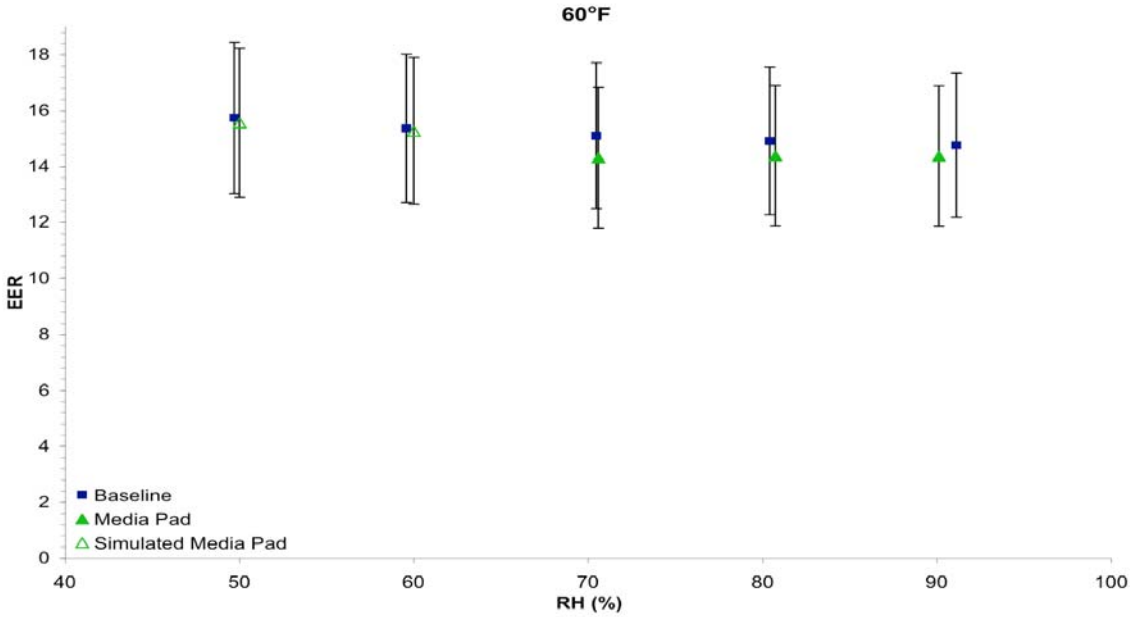

Figure 4-1. EER vs. RH graph for 60°F ambient temperature.

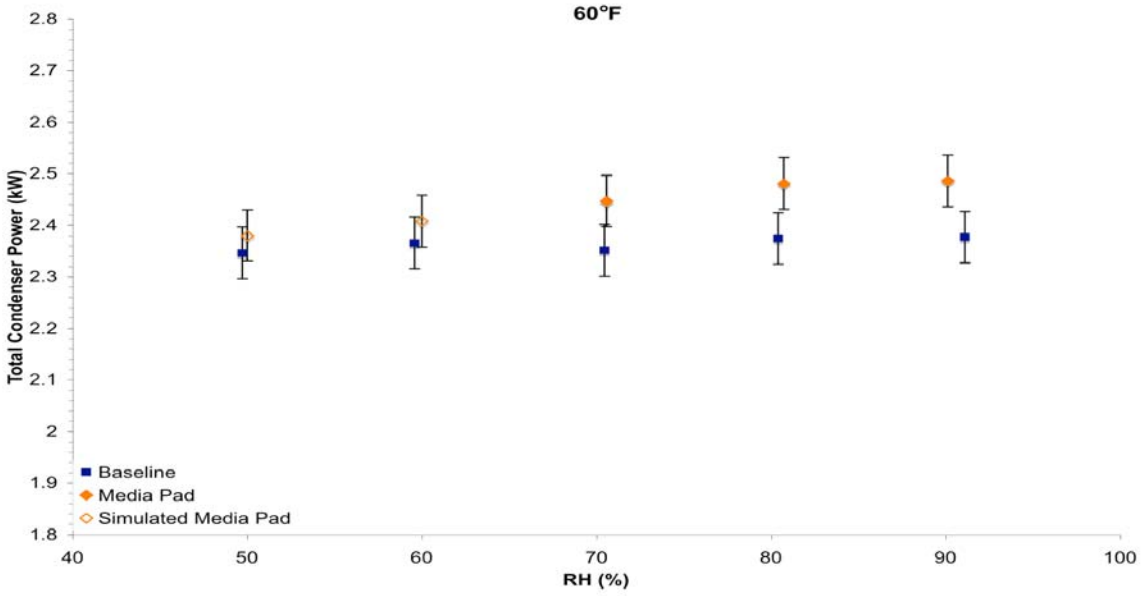

Figure 4-2. Total condenser power vs. RH graph for 60°F ambient temperature.

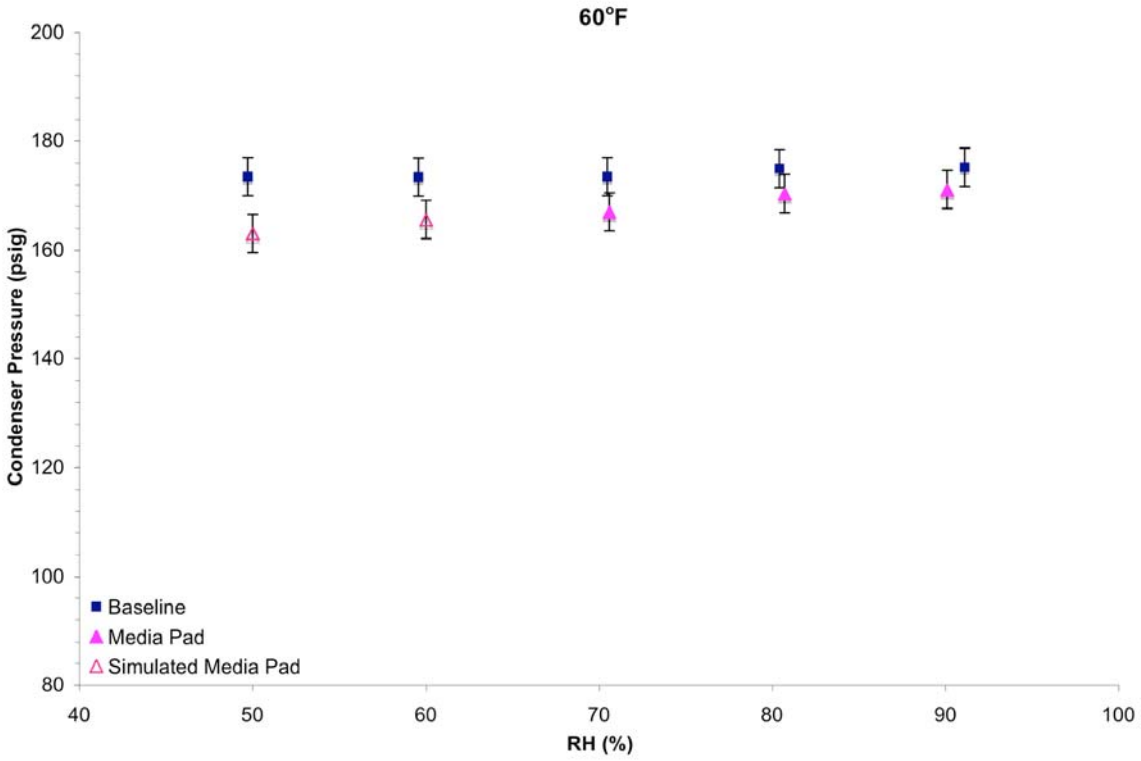

Figure 4-3. Condenser Pressure vs. RH graph for 60°F ambient temperature.

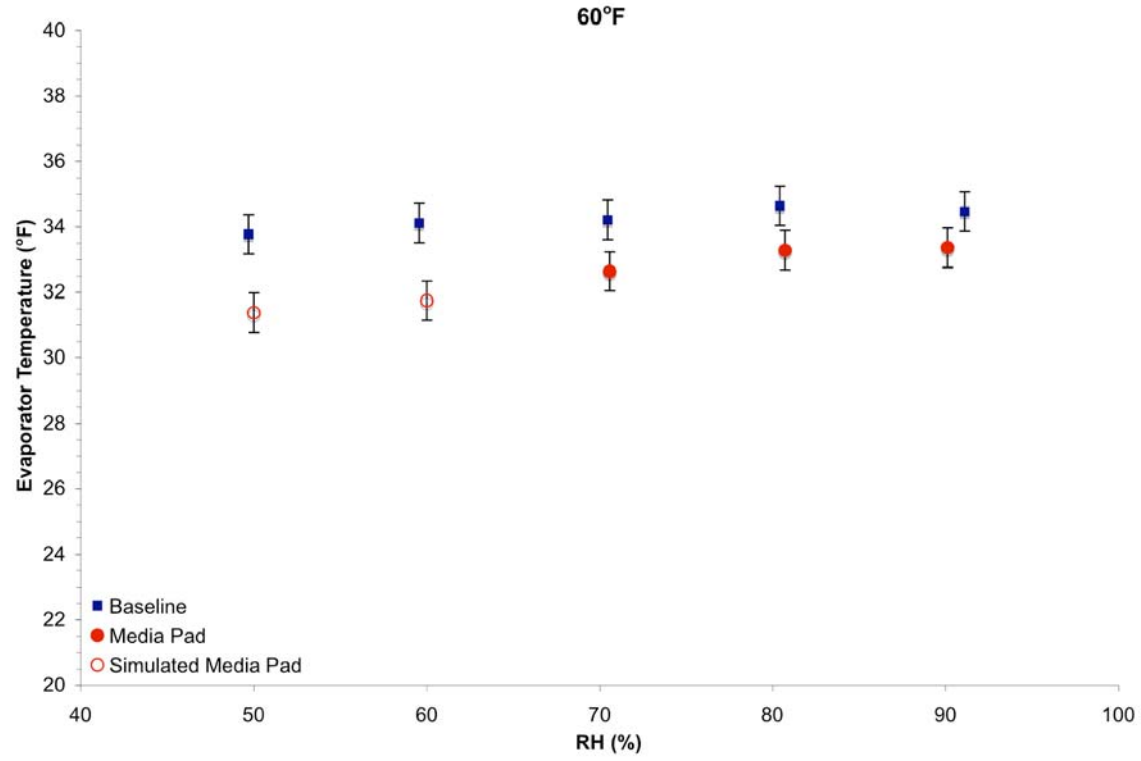

Figure 4-4. Refrigerant temperature entering the evaporator vs. RH graph for 60°F ambient temperature.

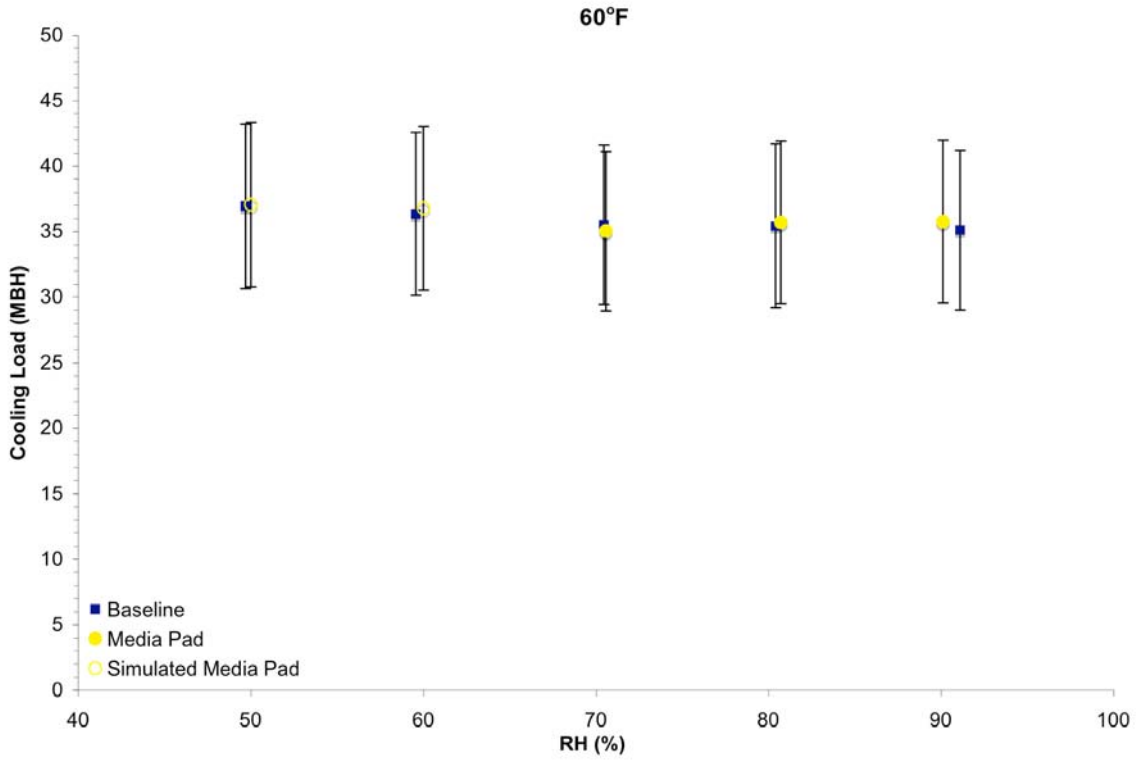

Figure 4-5. Cooling load vs. RH graph for 60°F ambient temperature.

70°F Ambient Dry-Bulb Temperature

At 70°F the increase in performance can be seen in Figure 4-6. The EER was improved at all tested RH's with the evaporative cooling device installed. At 40 and 50% RH the total condenser power was reduced below the baseline case (Figure 4-7). However, at 60% RH the condenser power rises above the baseline case. The difference between the two cases increases at 80 and 90% RH. Figure 4-8 presents a significant decrease in condenser pressure at low RH's. When the RH was increased the media pad case approached the baseline case. Figure 4-9 shows the difference in refrigerant temperature between the two cases is growing at lower relative humidities. It stayed lower for the media pad case up to 80%. The cooling capacities in Figure 4-10 are similar, but show a slight advantage at 80 and 90% RH for the media pad case. At low RH's (40 and 50%) the EER improvement was accounted for by the reduction in

condenser power. At the high RH's (80 and 90%) the efficiency improvement was a result of more heat transfer.

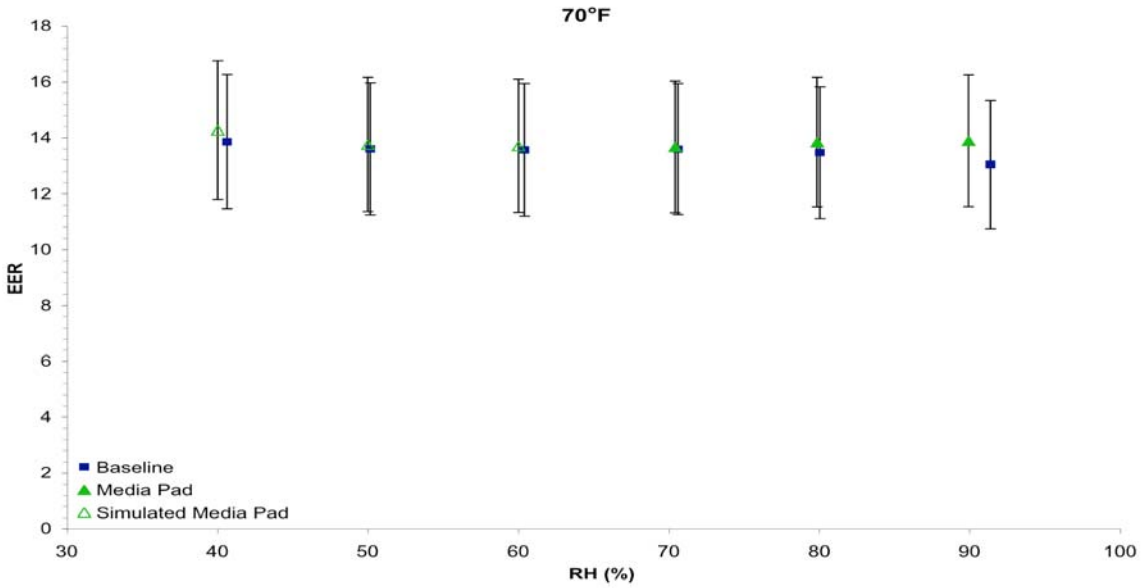

Figure 4-6. EER vs. RH graph for 70°F ambient temperature.

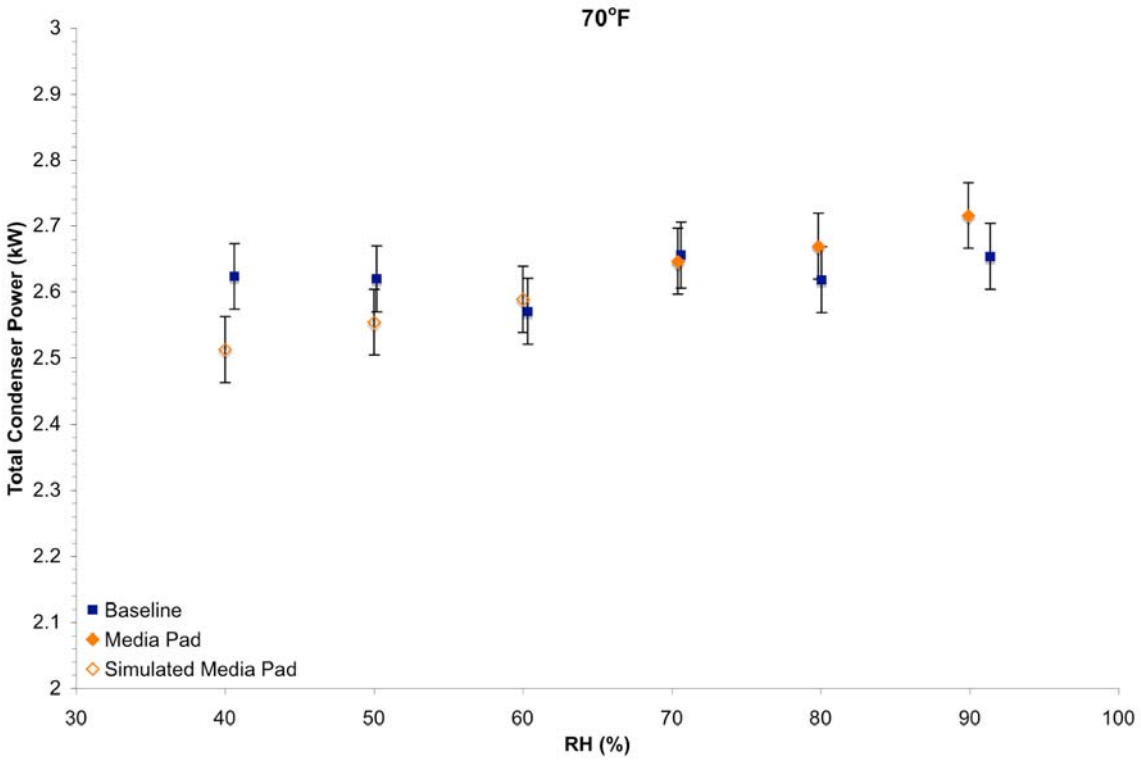

Figure 4-7. Total condenser power vs. RH graph for 70°F ambient temperature.

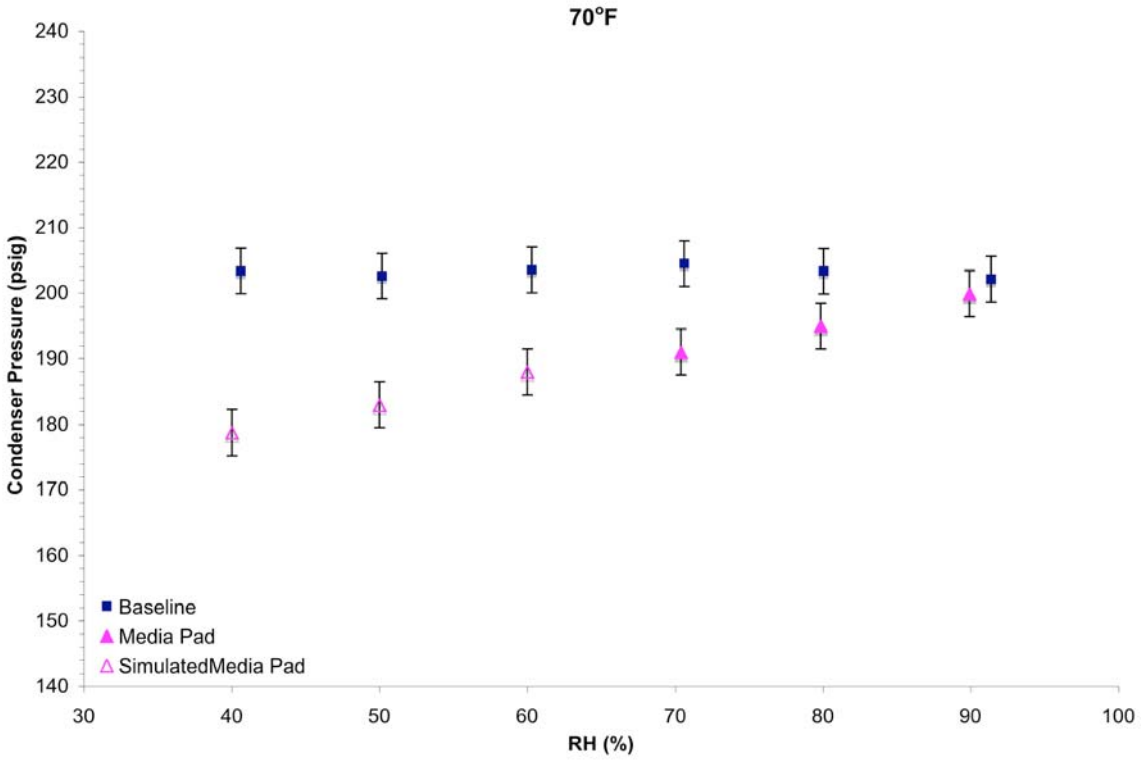

Figure 4-8. Condenser Pressure vs. RH graph for 70°F ambient temperature.

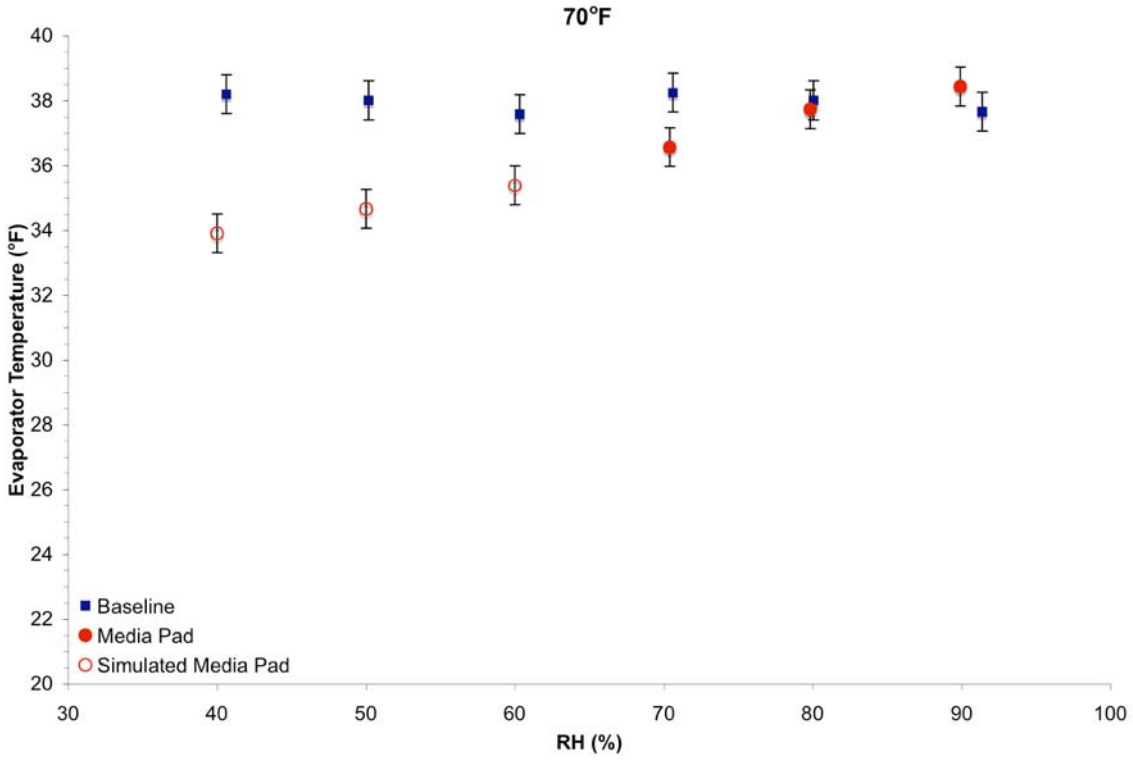

Figure 4-9. Refrigerant temperature entering the evaporator vs. RH graph for 70°F ambient temperature.

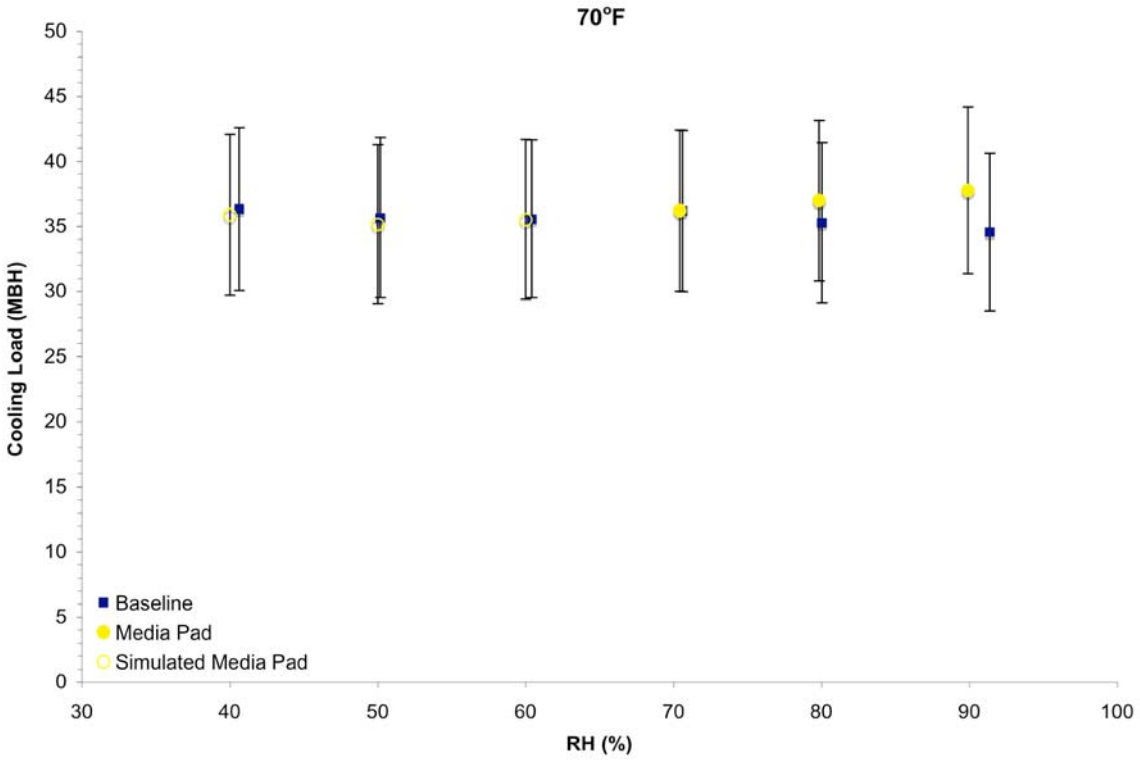

Figure 4-10. Cooling load vs. RH graph for 70°F ambient temperature.

80°F Ambient Dry-Bulb Temperature

Figures 4-11 displays a more definitive increase in EER for all the data points compared to 70°F. The condenser power in Figure 4-12 is lower for the media pad case at low RH's and greater at high RH's. The media pad case crosses over between 70 and 80% RH. Figure 4-13 shows a 13% decrease in condenser pressure at 40% RH for the media pad case and gradually declines until the pressures are equal for both cases at 90% RH. The refrigerant temperature for the media pad case intersects the baseline between 80 and 90% RH shown in Figure 4-14. The cooling capacity in Figure 4-15 is higher for the media pad case above 60% RH. The EER was improved by the decrease in condenser power at low RH and an increase in cooling capacity at high RH.

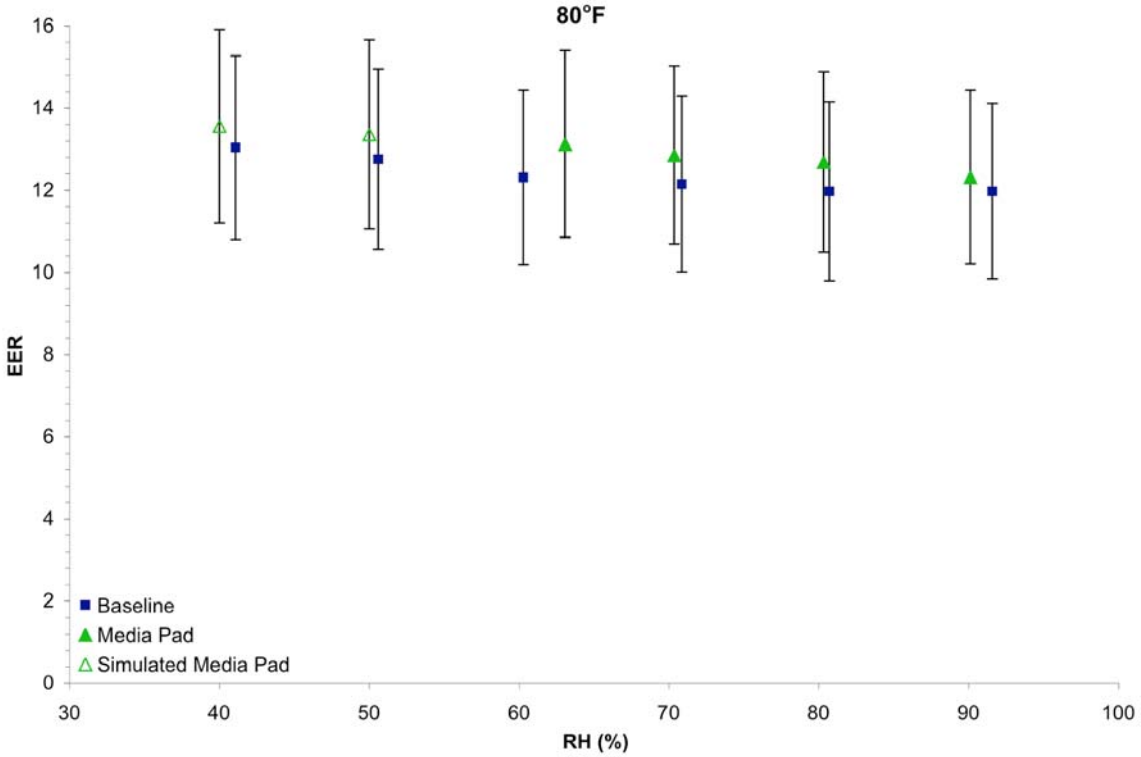

Figure 4-11. EER vs. RH graph for 80°F ambient temperature.

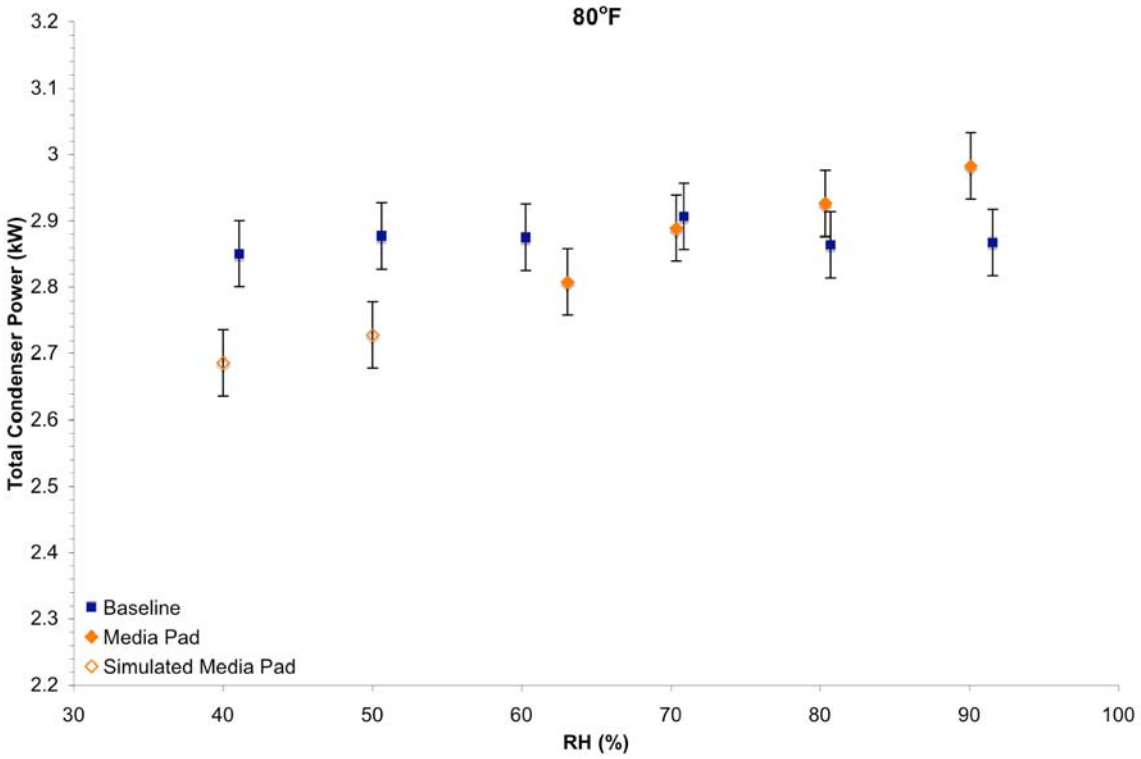

Figure 4-12. Total condenser power vs. RH graph for 80°F ambient temperature.

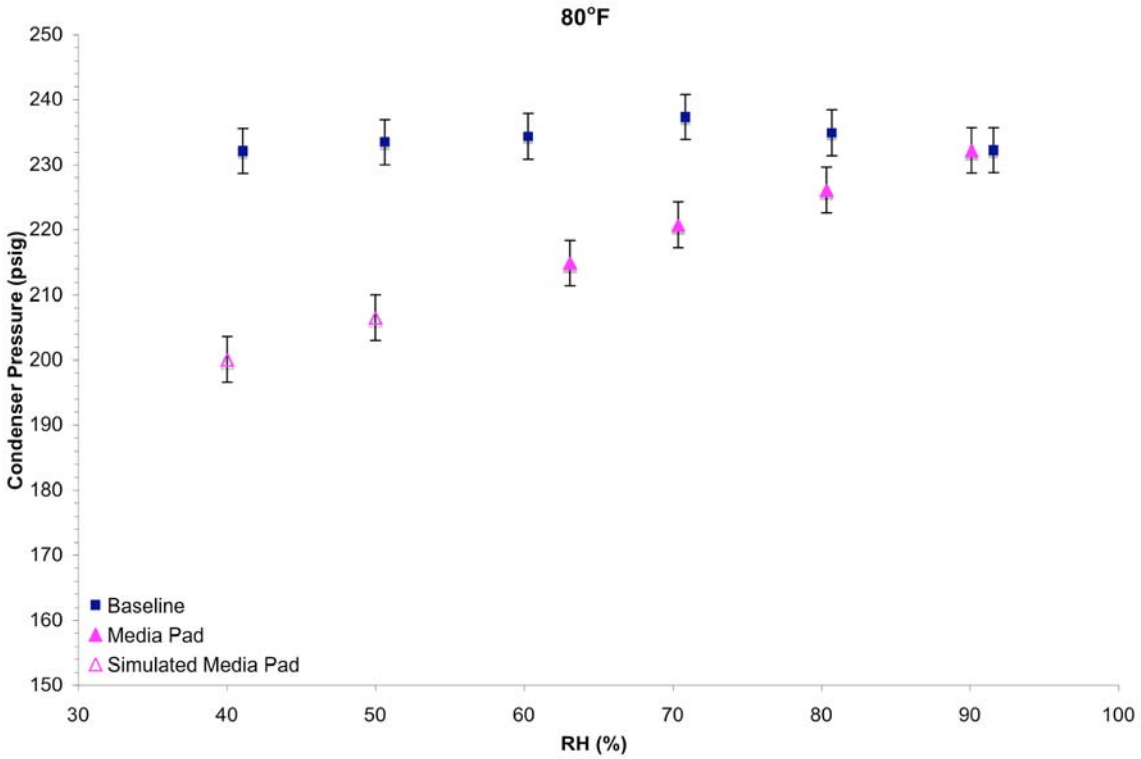

Figure 4-13. Condenser Pressure vs. RH graph for 80°F ambient temperature.

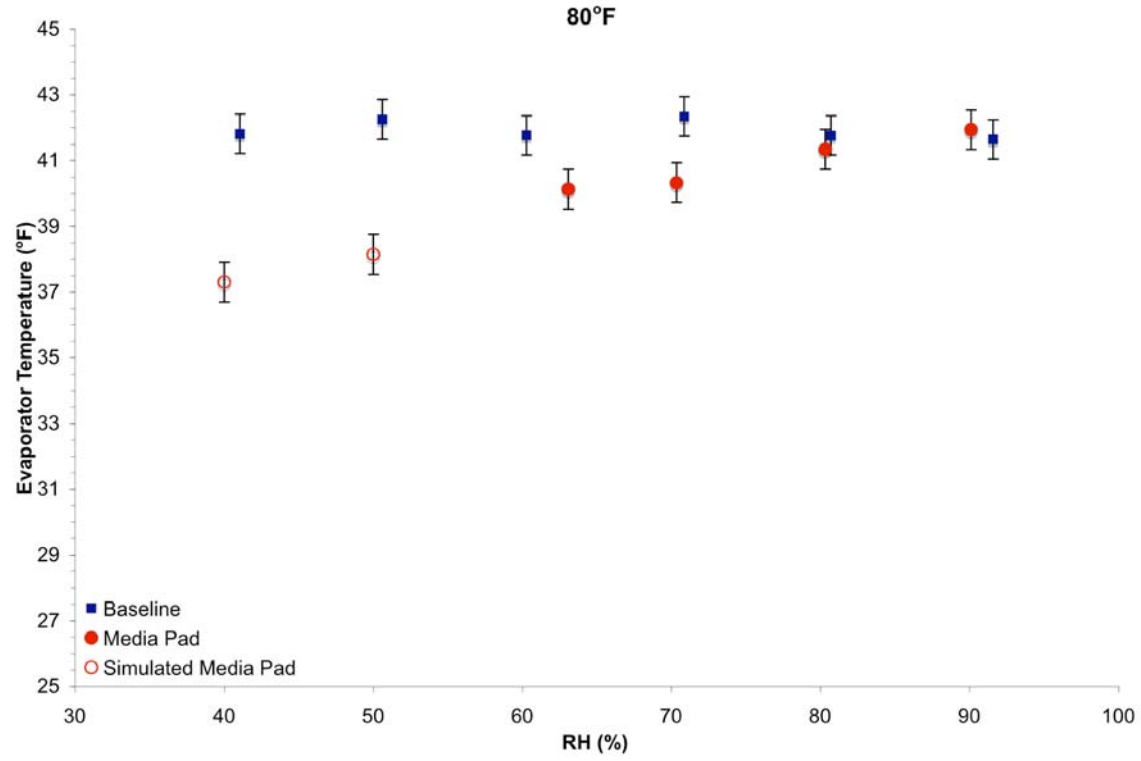

Figure 4-14. Refrigerant temperature entering the evaporator vs. RH graph for 80°F ambient temperature.

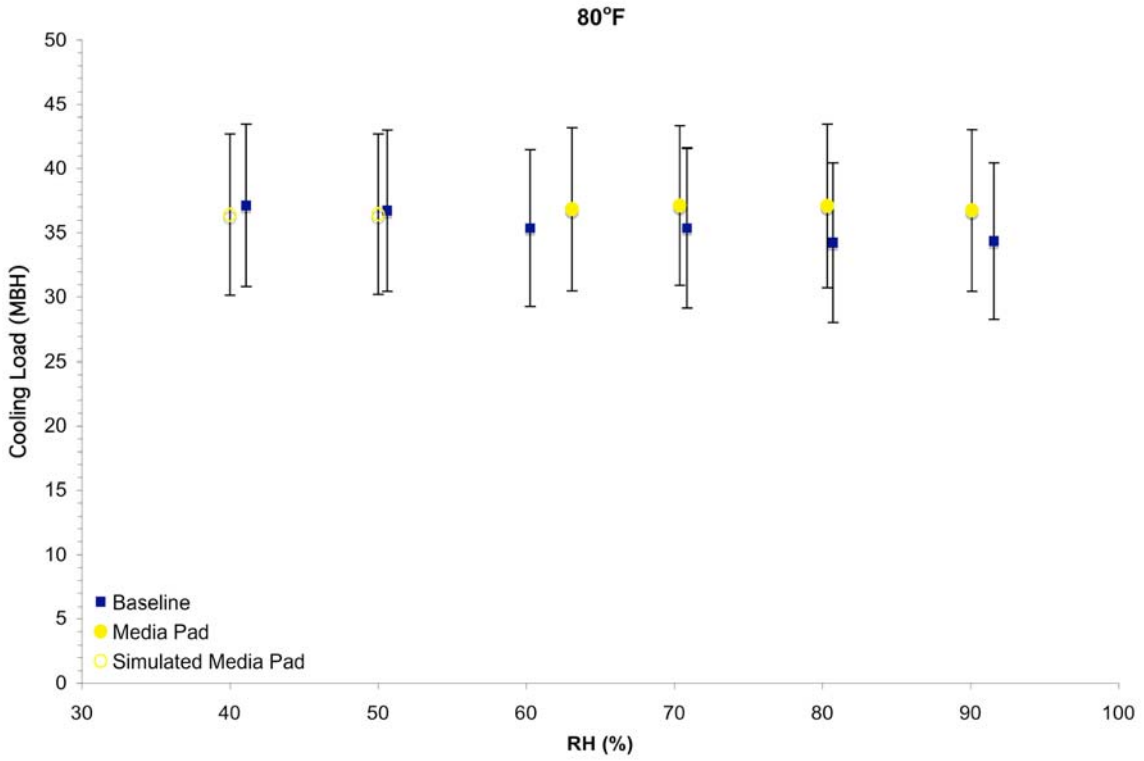

Figure 4-15. Cooling load vs. RH graph for 80°F ambient temperature.

90°F Ambient Dry-Bulb Temperature

Figure 4-16 shows the trend that is expected for EER. The improvement in EER is highest for 40% RH and declines as it reaches 90% RH. Each elevation in RH shows less improvement than the previous data point. The intersection between the condenser power is between 70 and 80% RH, Figure 4-17. The same trend is found in Figure 4-18 as the previous temperatures, but shows more reduction for each RH. The refrigerant temperature in Figure 4-19 shows the intersection of the two cases occurring between 80 and 90% RH. The cooling capacity at 90°F is higher at all RH values for the media pad case. The combination of more heat transfer in the evaporator and lower condenser power resulted in greater improvement in EER from 40 to 70% RH. The increase in EER at higher RH values is attributed to an increase in cooling capacity.

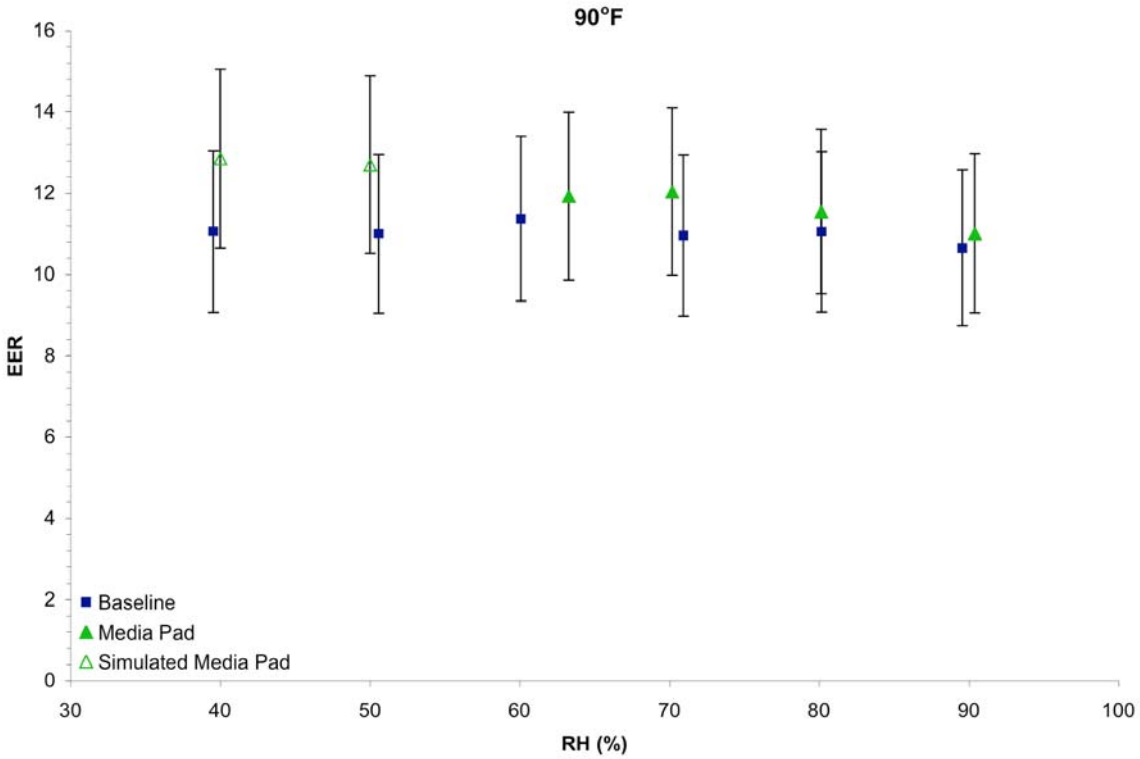

Figure 4-16. EER vs. RH graph for 90°F ambient temperature.

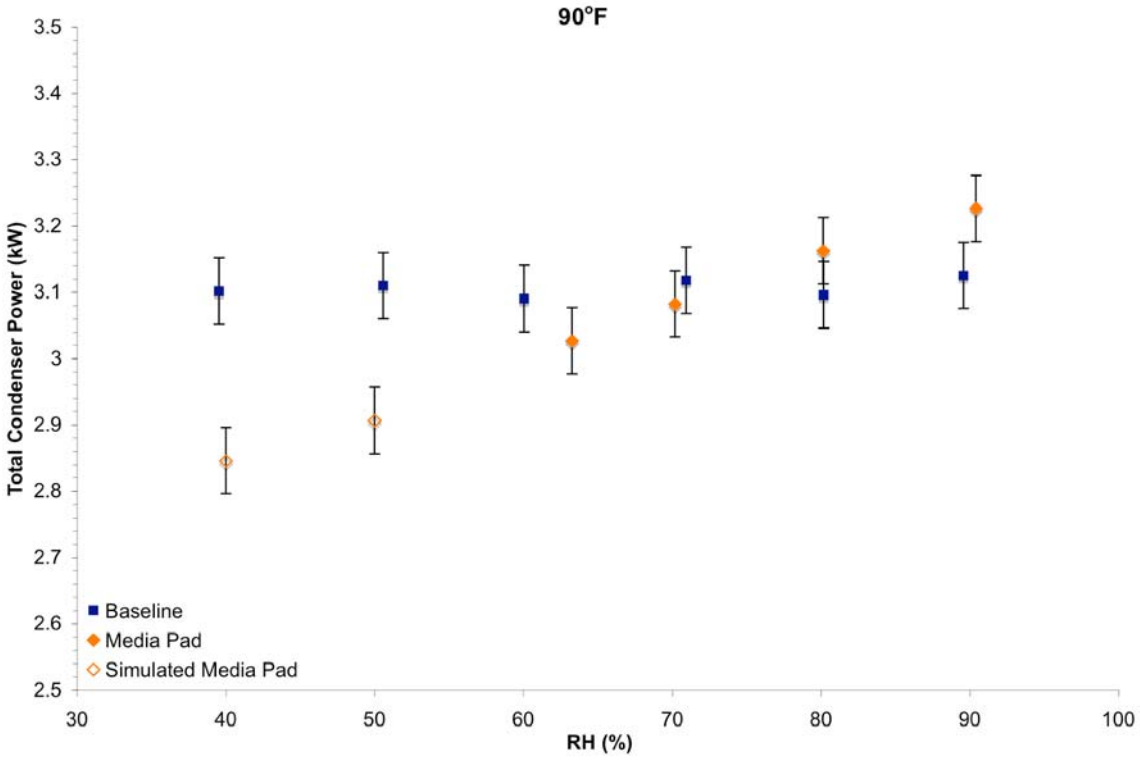

Figure 4-17. Total condenser power vs. RH graph for 90°F ambient temperature.

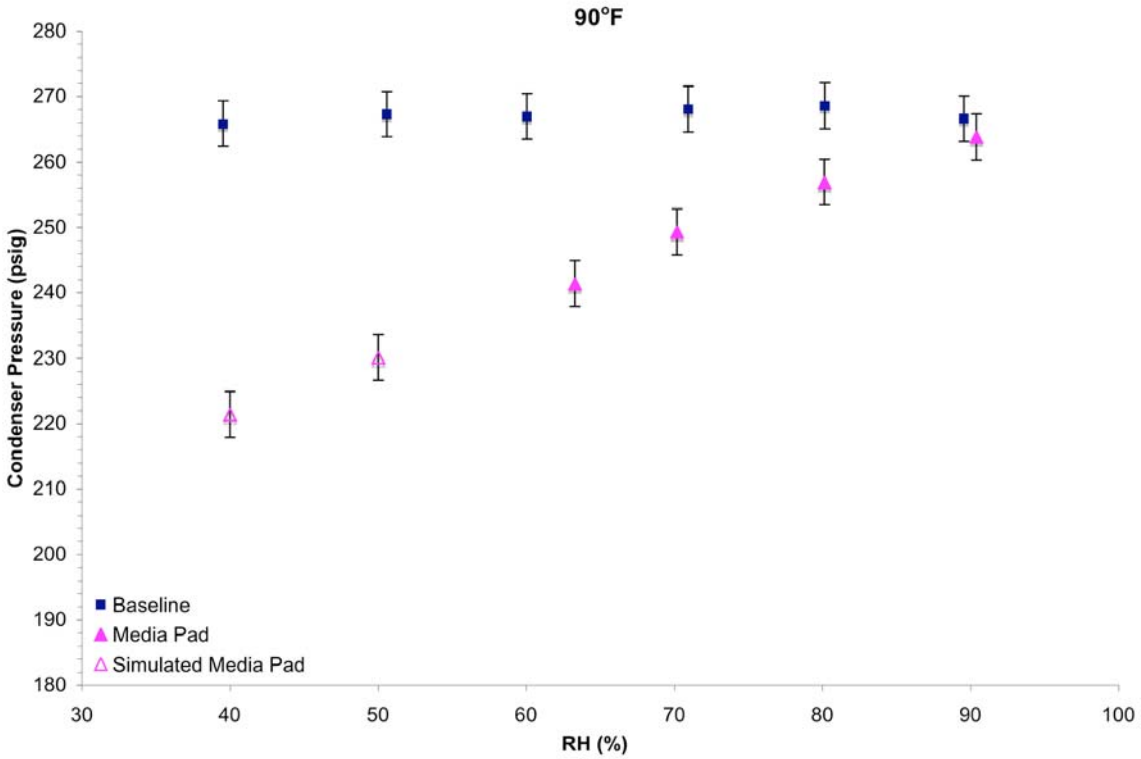

Figure 4-18. Condenser Pressure vs. RH graph for 90°F ambient temperature.

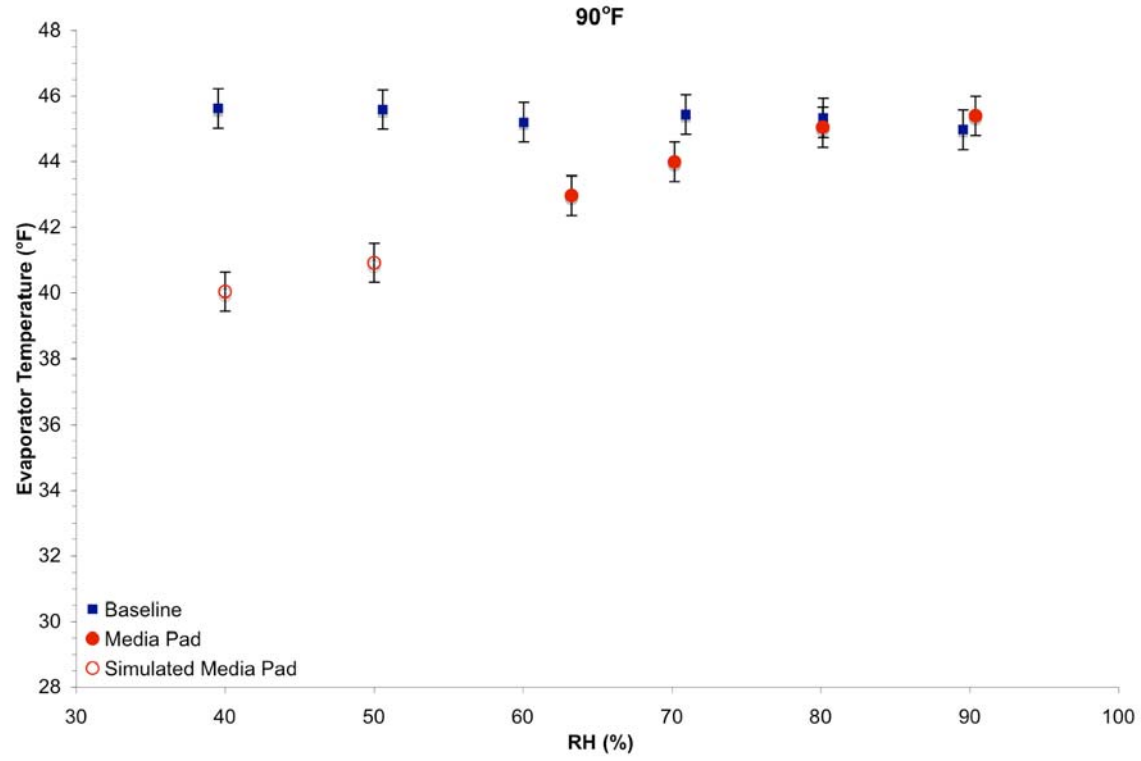

Figure 4-19. Refrigerant temperature entering the evaporator vs. RH graph for 90°F ambient temperature.

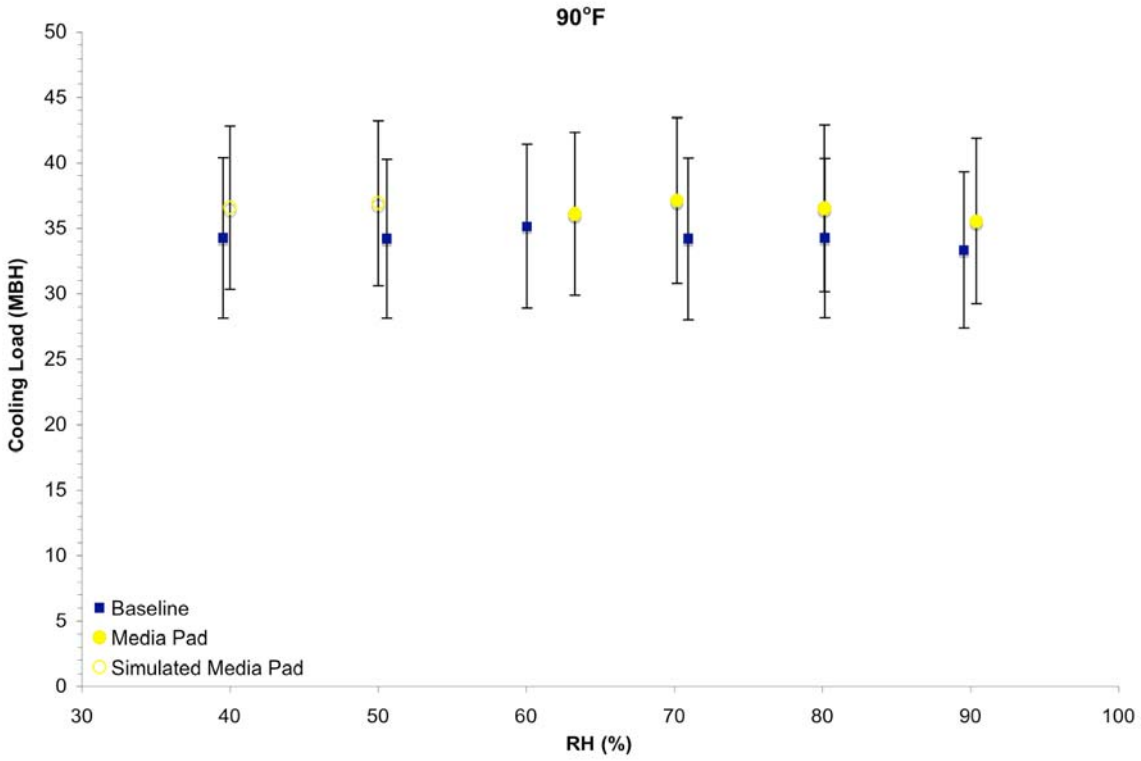

Figure 4-20. Cooling load vs. RH graph for 90°F ambient temperature.

95°F Ambient Dry-Bulb Temperature

The graphs for 95°F are shown in Figures 4-21 to 4-25. The significance of the graphs for 95°F is that it has the point at which Air-Conditioning and Refrigeration Institute (ARI) [23] and American Society of Heating, Refrigerating and Air-Conditioning Engineers (ASHRAE) [22] conduct testing for rating air-conditioners. The indoor conditions were maintained at their standards for all the tests and outdoor conditions were 95°F and 40% relative humidity. The trends were much the same as for the 90°F case. The most notable difference is in the power graph in Figure 4-22. It shows that the cross over had not occurred up to 80% relative humidity. Focusing specifically on the standard testing conditions there was 22% increase in EER for the media pad case. Indirect evaporative cooling also resulted in 11% gain in cooling capacity and 28% reduction of compressor power.

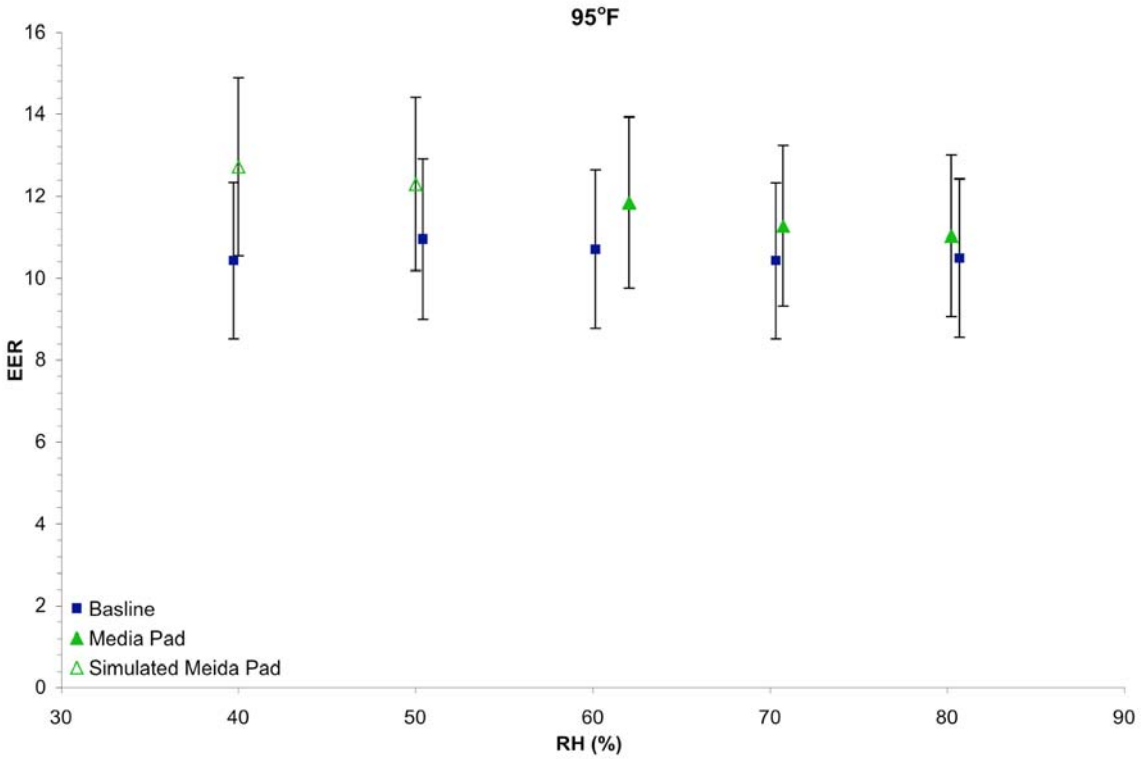

Figure 4-21. EER vs. RH graph for 95°F ambient temperature.

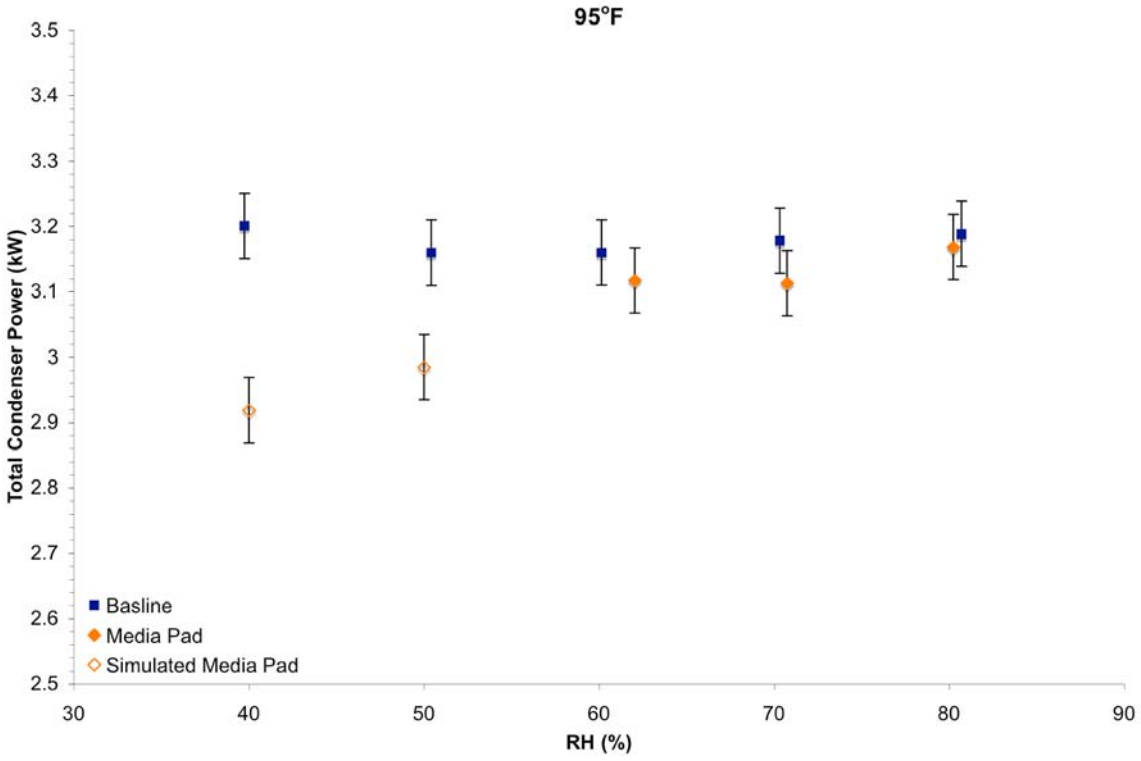

Figure 4-22. Total condenser power vs. RH graph for 95°F ambient temperature.

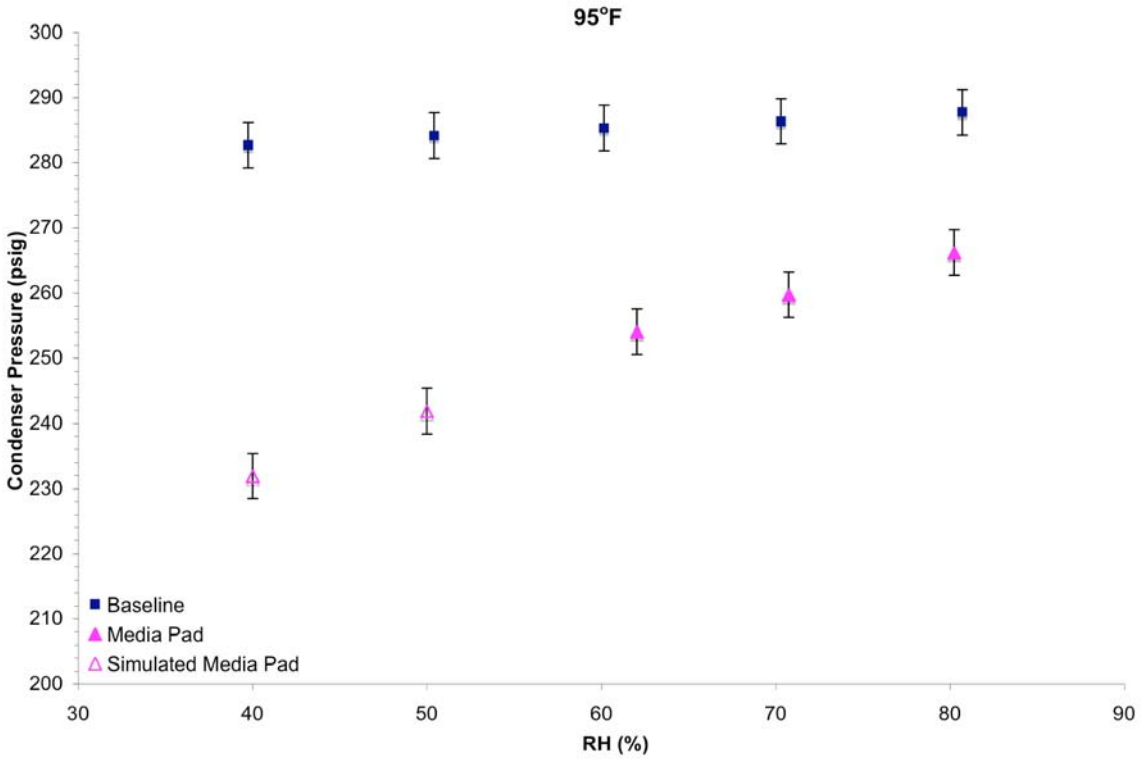

Figure 4-23. Condenser Pressure vs. RH graph for 95°F ambient temperature.

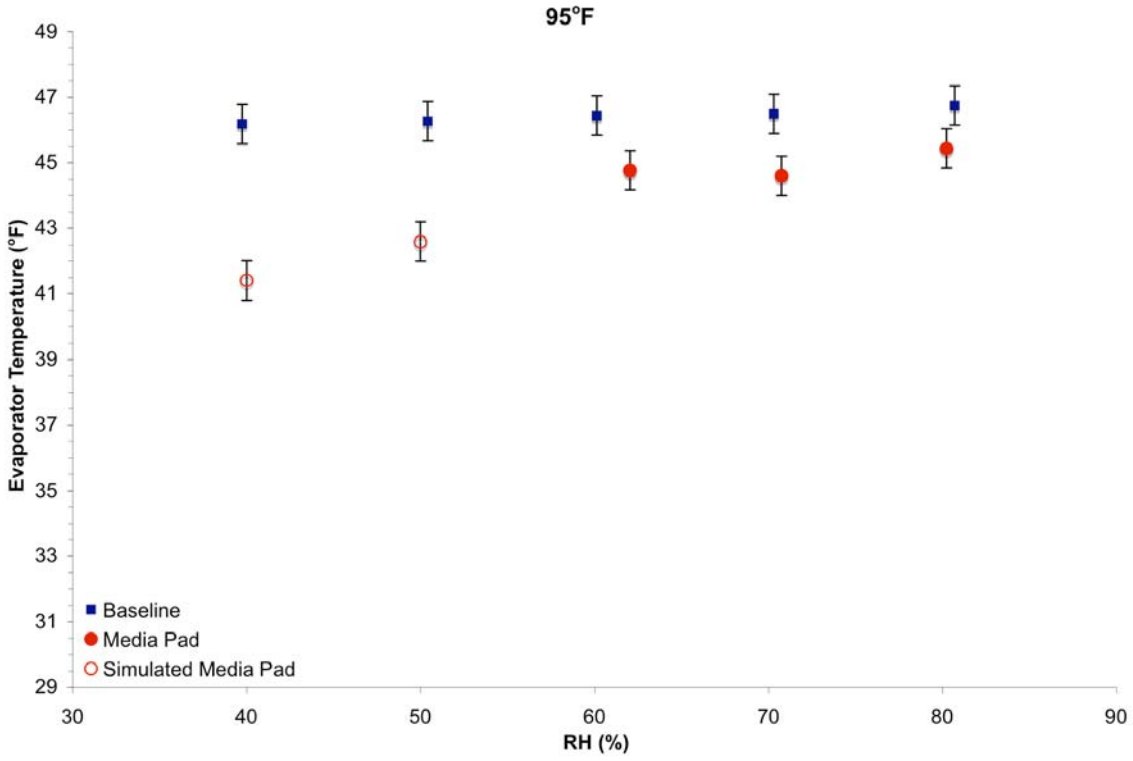

Figure 4-24. Refrigerant temperature entering the evaporator vs. RH graph for 95°F ambient temperature.

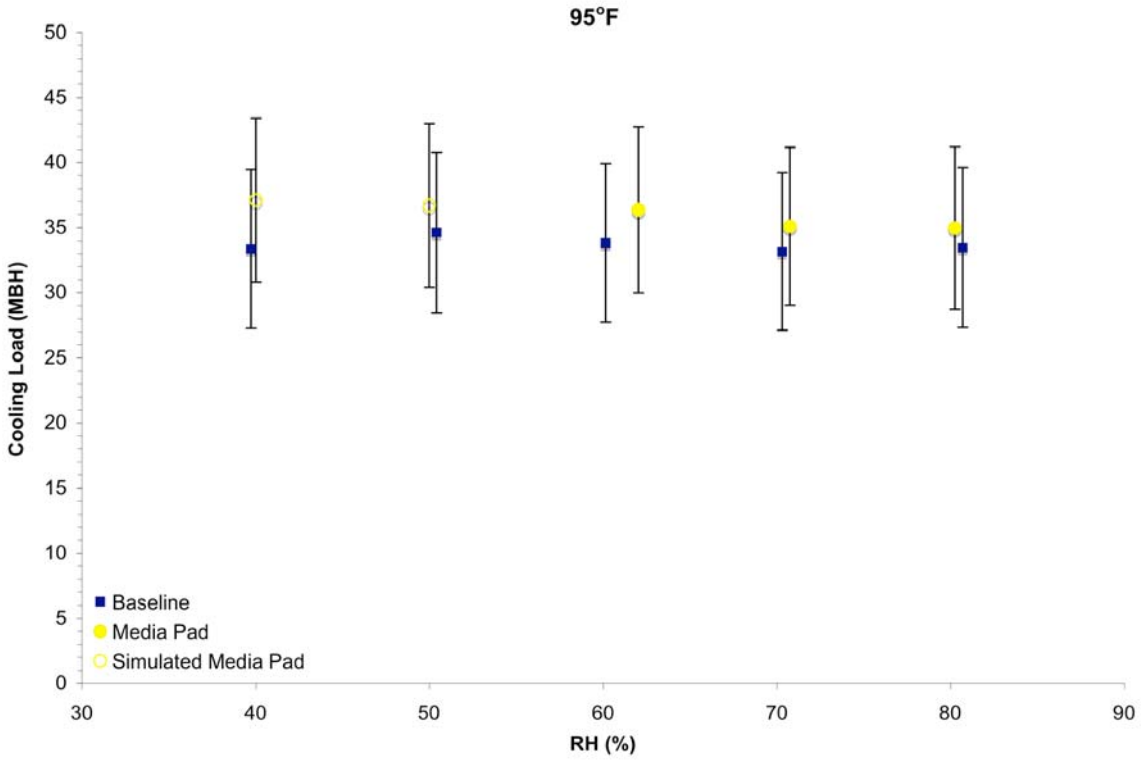

Figure 4-25. Cooling load vs. RH graph for 95°F ambient temperature.

100°F Ambient Dry-Bulb Temperature

The graphs for 100°F are shown in Figures 4-26 to 4-30. The experimental results for 100°F followed the same trends as the previous two temperatures. Figure 4-27 shows the intersection of condenser power between 70 and 80% RH, which differs from 95°F that doesn't show an intersection up to 80% RH. The same can be said for the refrigerant temperature. The intersection occurs between 70 and 80% RH in Figure 4-29, but Figure 4-24 does not show an intersection for 95°F. This may be a result of the uncertainty because the error bars overlap each other at 80% RH in both Figures 4-27 and 4-29. Figure 4-30 shows an increase in cooling capacity for the media pad case at all tested RH values. From 40 to 70% RH the combination of enhanced cooling capacity and reduced condenser power improved the EER. At 80% the increased cooling capacity led to the improved EER.

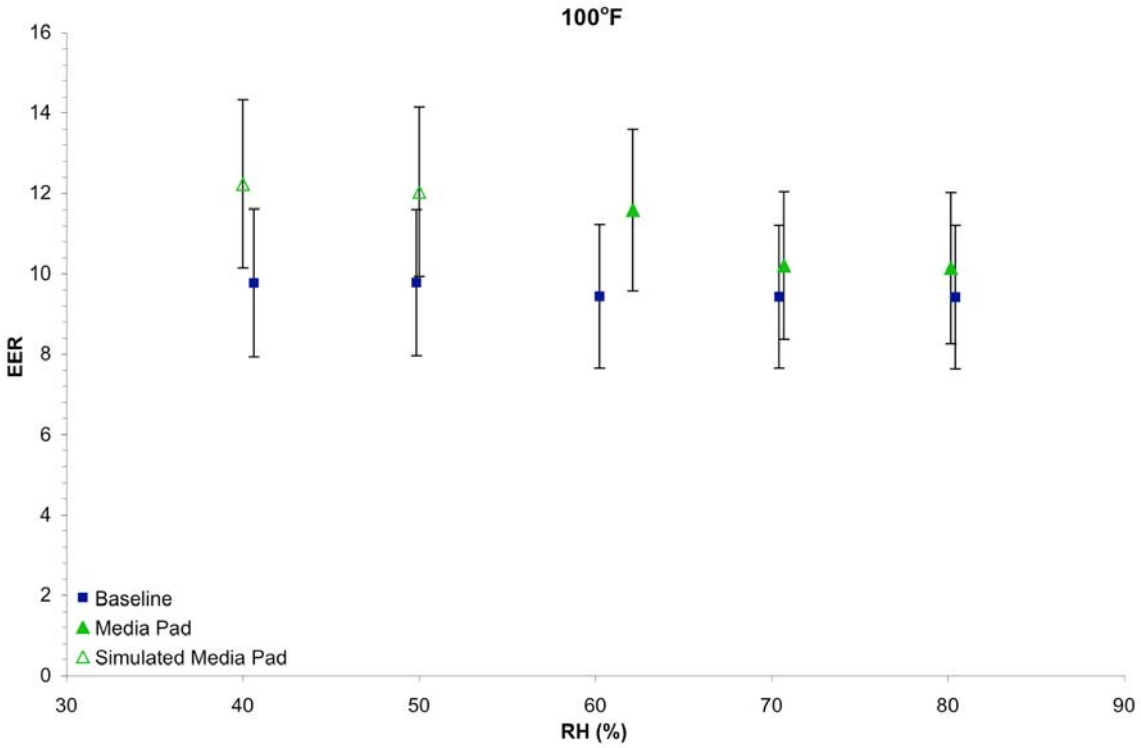

Figure 4-26. EER vs. RH graph for 100°F ambient temperature.

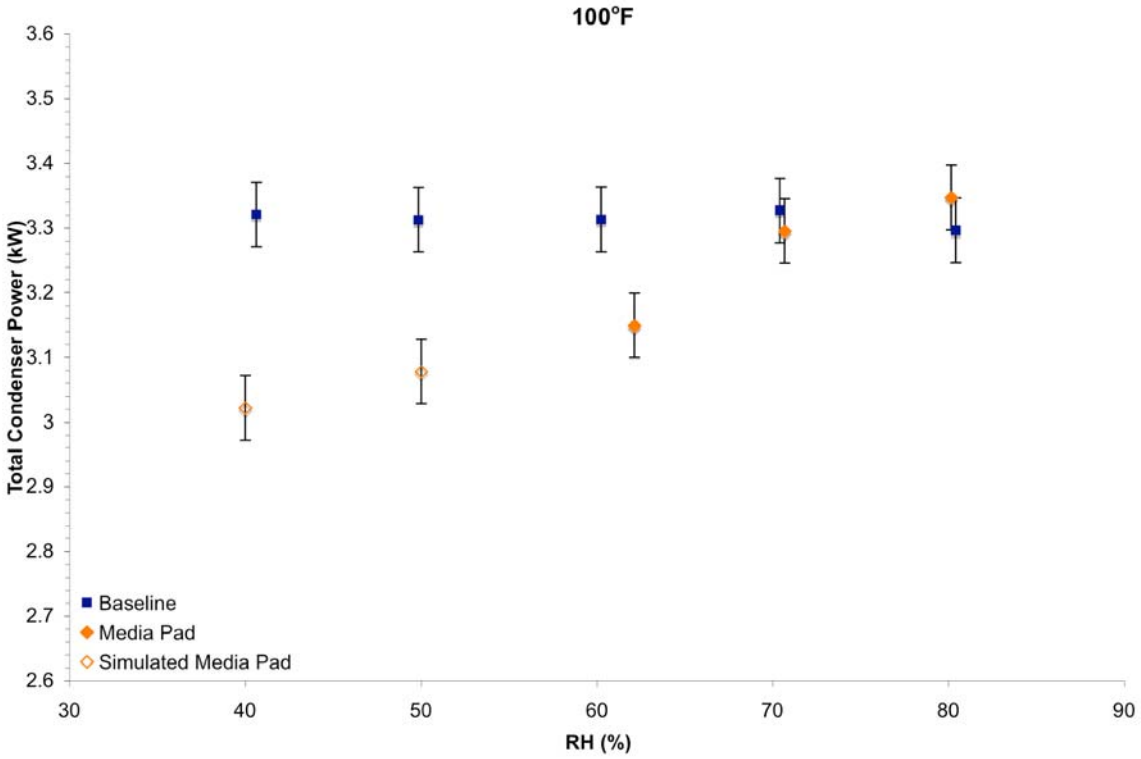

Figure 4-27. Total condenser power vs. RH graph for 100°F ambient temperature.

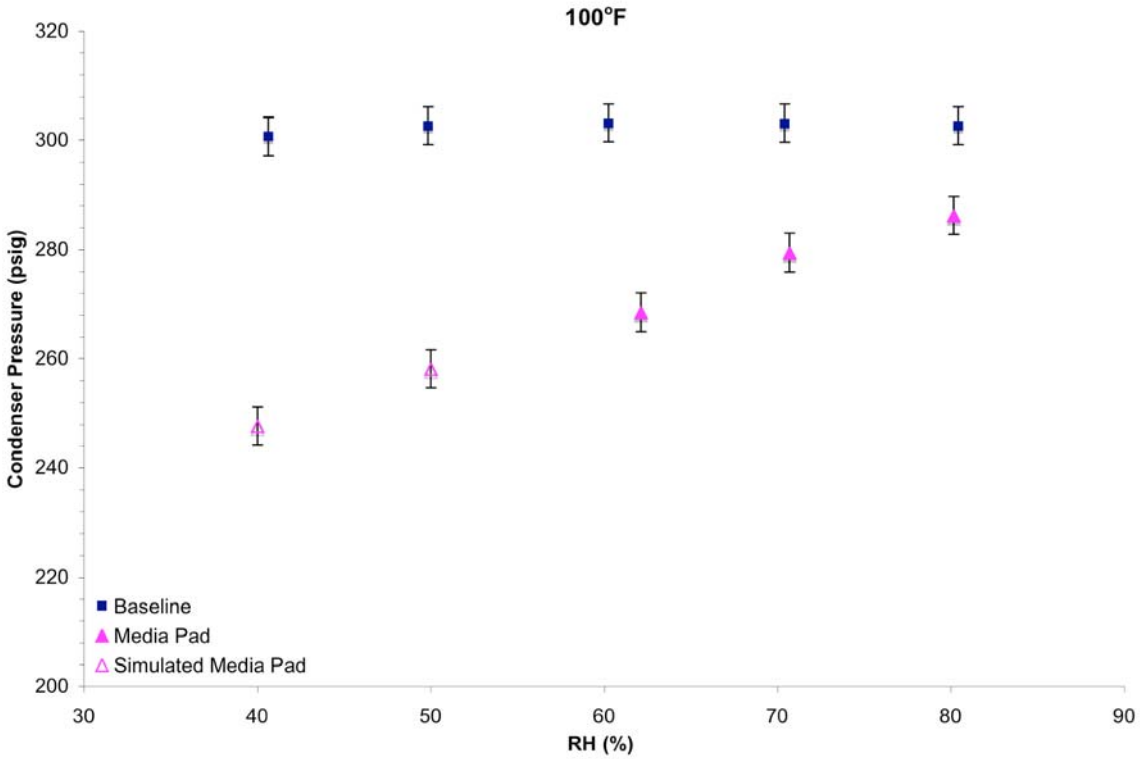

Figure 4-28. Condenser Pressure vs. RH graph for 100°F ambient temperature.

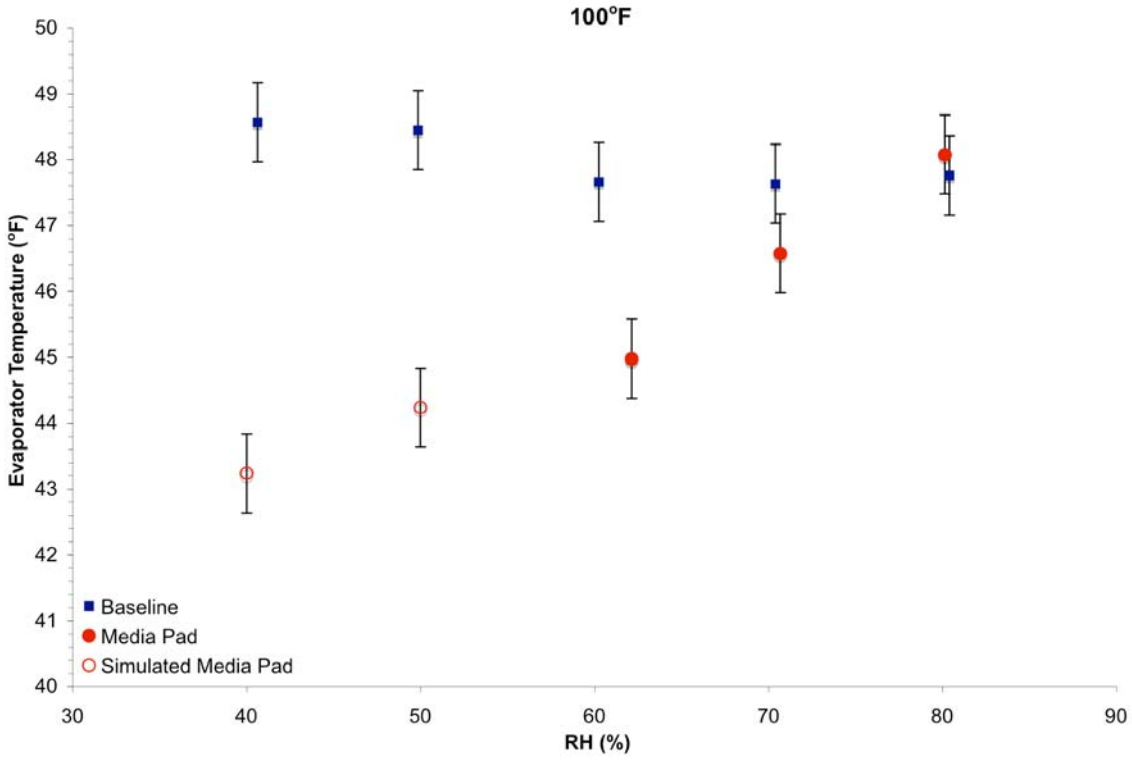

Figure 4-29. Refrigerant temperature entering the evaporator vs. RH graph for 100°F ambient temperature.

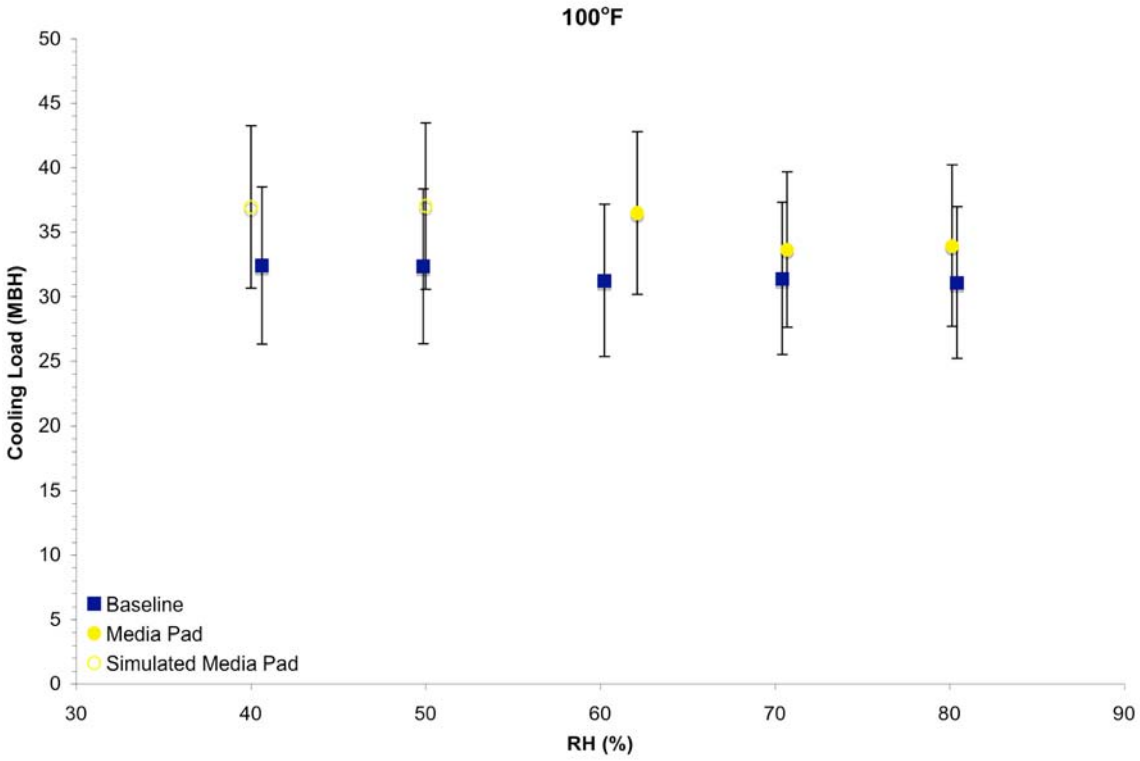

Figure 4-30. Cooling load vs. RH graph for 100°F ambient temperature.

Conclusion

The experimental data provided insight into what happens to the air-conditioning system as a whole when indirect evaporative cooling was implemented. Pre-cooling the condenser's inlet air not only reduced the power consumption, but also increased the cooling capacity of the evaporator. The total power consumption by the condenser and evaporative cooling arrangement was higher than the baseline case under elevated RH values, but the EER was still higher for the media pad case because of the increase in cooling capacity. An increase in cooling capacity suggested that the refrigerant temperature in the evaporator was lower with the media pad as it entered the evaporator (see Figures 4-4, 4-9, 4-14, 4-19, 4-24, 4-29). The drop in inlet temperature did generate lower pressures for all cases and they drew near the baseline case as the relative humidity rose. At 70 and 80°F the improvement in EER was a result of the reduction in condenser

power at low RH values. The higher RH values showed an increase in cooling capacity, which led to the increase in EER. The temperatures tested at from 90^{o}F and above showed more improvement in EER compared to 70 and 80^{o}F at low relative humidities. This was because the combination of lower condenser power and increased cooling capacity. The high RH values again improved the cooling capacity to enhance the EER. Overall the evaporative cooling device required additional power and reduced the airflow over the coils, but it lowered the dry-bulb temperature of the ambient air and increased the cooling capacity, which were the overriding characteristics that enhanced the EER.

Simulation

A simulation was performed with the Carrier HAP software. The program allowed a space to be created and a load profile to be produced from it taking into account a number of parameters. A detailed list of these parameters is in Appendix C. This chapter will cover the main attributes of the house that were simulated for this study.

The simulation was run for five cities in Florida, namely Jacksonville, Miami, Orlando, Tallahassee, and Tampa. One house was created to satisfy all the minimum residential building requirements according to the Florida Building Code [24]. Figure 4-25 shows the floor plan of the house and how it is oriented. The number of windows, doors, and rooms can also be observed along with the square footage. Table 4-4 provides the particulars of the building envelope. The internal loads are listed in Table 4-5. The internal loads were set on schedules for each day of the week through out the year. The schedules determined the percentage of a particular load that is on during a certain time of day. The loads and there schedules were taken from data for residential use from ASHRAE Handbook of Fundamentals [19], the Energy Information Administration [25], and Hendron et al. [26], to follow the theme of actual home use.

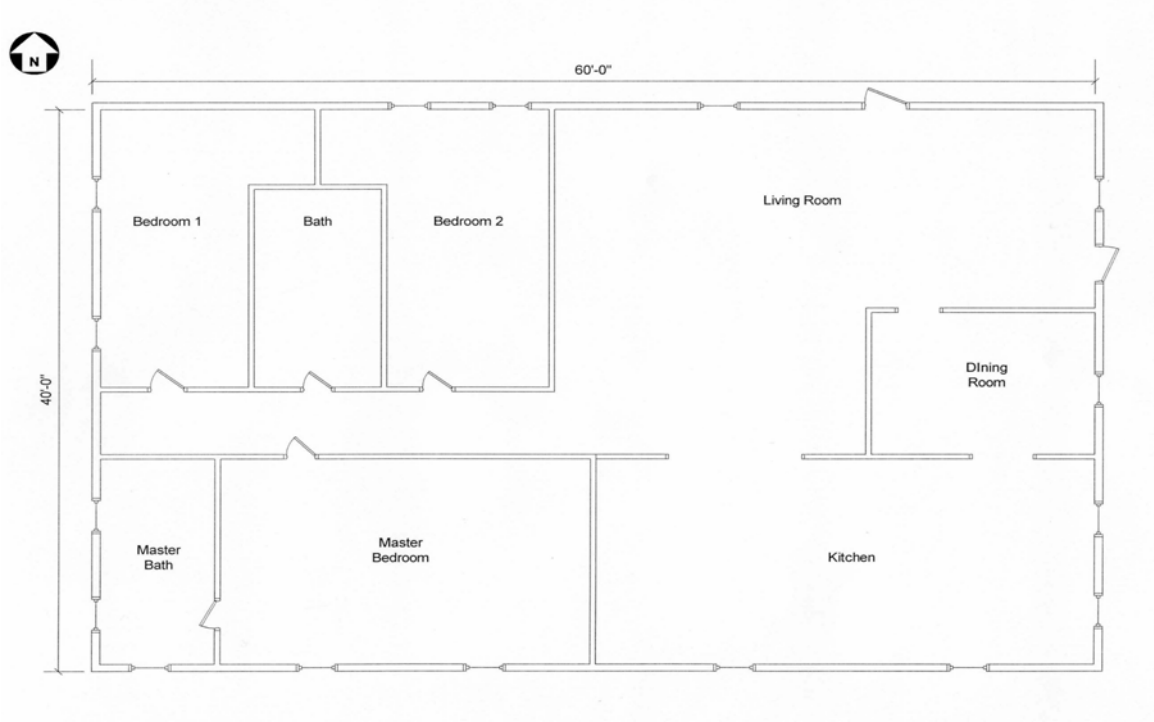

Figure 4-31. Floor plan of the house that was used for the simulation.

Table 4-4. Building envelope components and their overall U-value.

House Component	Overall U-value (Btu/ft^2hr^oF)
Walls	0.068
Floor	0.100
Roof	0.031
Windows	0.608
Doors	0.300

Table 4-5. A list of internal loads for the house.

Internals	Load
Overhead lighting	3400[a] W
Electrical Equipment	17344[b] W
People, Occupancy = 4[c]	
Sensible	230[c] Btu/hr/person
Latent	190[c] Btu/hr/person
a- Hendron et al. [26] b- Energy Information Administration [25] c- ASHRAE Handbook of Fundamentals [19]	

The simulation does have its shortcomings. The disadvantage of the simulation was attempting to account for the human element. The schedules were put in to resolve this issue, but are only averages across the U.S. One assumption made with the

simulation was that the air-conditioner would be on at all times, meeting any load the house would experience. That included small cooling loads that were generated at temperatures of 70°F and lower. A homeowner may open windows or run a fan to lower the indoor temperature instead of using the air-conditioner. It is up to the individual user to decide when the temperature in their home becomes uncomfortable and needs to use the air-conditioner, which cannot be simulated for. What is understood from the simulation is the less the air-conditioner is used with the indirect evaporative cooling device the less energy savings are achieved.

Energy Savings

The energy savings for each city were found using the experimental data and the data provided by the simulation for the house. The experimental data was used to create a curve fit that related the dry-bulb and wet-bulb temperature to an EER using SigmaPlot. The inputs for both cases are found in Table 4-6.

Table 4-6. Inputs to create a curve fit.

Media Pad			Baseline		
T_{db}	T_{wb}	EER_{air}	T_{db}	T_{wb}	EER_{air}
60	50.22	15.570	60.14	50.27	15.741
60	52.33	15.275	59.97	52.21	15.365
60.18	54.63	14.317	59.99	54.44	15.104
60.36	56.79	14.390	60.05	56.43	14.917
60.03	58.24	14.381	60.26	58.64	14.765
70	55.77	14.277	70.47	56.3	13.861
70	58.44	13.764	69.92	58.42	13.607
70	60.98	13.718	70	61.08	13.570
70.17	63.64	13.678	70.32	63.83	13.594
70.2	65.85	13.848	70.43	66.11	13.464
70.13	68	13.902	70.37	68.55	13.042
80	63.48	13.558	80.19	63.98	13.035
80	66.66	13.355	80.22	67.02	12.755
80.03	70.55	13.120	80.21	69.9	12.307
80.4	72.91	12.854	80.49	73.13	12.152
80.59	75.75	12.683	80.18	75.46	11.970
80.96	78.58	12.318	80.26	78.25	11.974

90	71.2	12.851	90.25	71.21	11.055
90	74.91	12.701	90.38	75.43	10.999
90.1	79.5	11.923	90.33	78.65	11.370
90.65	82.19	12.040	90.29	82.1	10.959
90.95	85.48	11.552	90.25	84.83	11.049
90.55	88	11.013	92.25	89.42	10.645
95	75.07	12.711	95.09	75.03	10.423
95	79.05	12.295	95.21	79.38	10.950
95.12	83.53	11.843	95.39	83.1	10.701
95.44	86.75	11.269	95.28	86.47	10.423
95.65	89.96	11.032	95.47	89.93	10.488
100	78.97	12.235	100.08	79.31	9.767
100	83.21	12.037	100.43	83.51	9.779
100.43	88.26	11.585	100.25	87.41	9.441
100.37	91.25	10.210	100.16	90.97	9.429
100.09	94.13	10.144	100.07	94.2	9.416

SigmaPlot produced an equation from the data that followed the form of:

$$EER = EER_o + aT_{db} + bT_{wb} \tag{4-9}$$

The coefficients for both cases are found in Table 4-7.

Table 4-7. Table of coefficients used in the curve fit for both cases.

Case	EER_o	A	B
Baseline	23.2072	-0.1026	-0.03664
Media Pad	20.4653	-0.001896	-0.1030

These equations show that the baseline case was more dependent upon the dry-bulb temperature while the media pad case had a greater dependency on the wet-bulb temperature. Both EER's were used to calculate the energy used for each case from the load. It was done for each hour of the day for the entire cooling season. A sample of the simulation output and the calculation of the energy for both cases in Miami are in Table 4-8. Table 4-9 presents the energy savings for each city. The cooling season is based on the best estimate of when a home would use its air-conditioner. The cooling season is longer for Miami, Orlando, and Tampa because of their geographic location. An average of approximately 5% energy savings resulted from using evaporative cooling, with

Orlando saving the most energy with 304 kilo-watt-hours. The peak for each city showed a significant improvement and averaged 15% for the five cities with Tallahassee gaining the highest peak savings at 16.6%.

Table 4-8. Sample output of the simulation for Miami.

Month	Day	Hour	Dry-Bulb Temp (°F)	Wet-Bulb Temp (°F)	Cooling Coil Load (MBH)	Baseline EER	Media Pad EER	Energy Savings (kWh)
Jul	29	8	80.5	76.7	23.4	12.136	12.409	0.042
Jul	29	9	81.5	77	26.2	12.022	12.376	0.062
Jul	29	10	83.5	77.5	21.7	11.799	12.321	0.078
Jul	29	11	82	76.1	18	12.004	12.468	0.056
Jul	29	12	78.5	74.5	16.2	12.422	12.640	0.022
Jul	29	13	79.5	76.1	23.2	12.261	12.473	0.032
Jul	29	14	81.5	76.7	22.3	12.033	12.407	0.056

Table 4-9. Table of the energy savings for the cooling season for the five Florida cities.

City	Cooling Season	Energy Savings (kWh)	%	Peak (kWh)	%
Jacksonville	May 1 - Sep. 30	220	5.0	0.534	16.3
Miami	April 1 - Oct. 31	296	4.5	0.376	12.9
Orlando	April 1 - Oct. 31	304	5.2	0.427	15.3
Tallahassee	May 1 - Sep. 30	207	4.9	0.350	16.6
Tampa	April 1 - Oct. 31	299	5.1	0.343	14.6

The most important aspect that a homeowner has interest in is the monetary savings. A list of parts used to construct the evaporative cooling device is in Table 4-10. These are the specific parts used for this particular prototype used in this study's experiments. Most of the cost comes from two parts being the pump and media pad. The cost of labor is not figured into the total and that could add a substantial amount. The flowmeter may not be needed in a practical application, which would reduce the cost. One part that is needed for a practical application is a float valve with a water line directly connected to it to maintain the water level in the sump. It was not used in this situation because the operator could monitor the water level. The monetary savings and

simple payback are shown in Table 4-11. A savings of less than thirty dollars per cooling season was found for all cities and lead to extremely uneconomical paybacks of up to twenty years for Tallahassee. Assuming a best-case scenario the media pads can have a life span of five years, so this would increase the payback time. It would take more than four years for Tampa to be reimbursed the cost of the media pads, which showed the most monetary savings. The cost of water wasn't factored in and would just add to the cost of operation, furthering the time to experience a payback. The monetary savings from evaporative cooling are not substantial enough to make up the cost to build a device and achieve a reasonable payback.

Table 4-10. Price list used for the indirect evaporative cooling device used in this research.

Parts	Qty.	Price ($)
Cellulose Evaporative Cooling Pad	8	126.00
Small Submersible Sump Pump	1	133.40
Flowmeter	1	57.63
Galvanized Sheet Metal	2	90.00
¾ inch PVC Pipe	2	3.38
¾ inch PVC Elbows	3	0.56
¾ inch PVC End Caps	2	0.54
¾ inch PVC Tee	1	0.22
¾ inch PVC Couplings	1	0.11
¾ inch PVC Ball Valve	1	1.50
Total		413.34

Table 4-11. The monetary savings and simple payback for each city.

City	Price of Electricity[a] ($/1000kWh)	Savings ($)	Simple Payback (years)
Jacksonville	100.34	22.07	18.7
Miami	92.81	27.47	15.0
Orlando	89.61	27.24	15.2
Tallahassee	99.97	20.69	20.0
Tampa	97.95	29.28	14
a- JEA [27]			

The simulation also provided insight into the performance of the heat pump with the indirect evaporative cooling at relative humidities above 90%. This is where

experimentation was unable to attain data. Table 4-12 shows the energy savings for relative humidity above 90%. It shows that the baseline case uses less energy than the media pad case, which is expected because the temperature depression is small. There would not be a significant enough reduction in the ambient air temperature to reduce the compressor power. This occurred mostly in the morning hours when the sun has not been able heat up the ambient air. From an economic standpoint this is not desirable, but infrequency of its occurrence makes it negligible when considering the whole cooling season.

Table 4-12. Sample of the output from the simulation showing relative humidity above 90%.

Dry-Bulb Temp (°F)	Wet-Bulb Temp (°F)	RH (%)	Cooling Coil Load (MBH)	Baseline EER	Media Pad EER	Energy Savings (kWh)
72.5	71	93.05	4.9	13.166	13.012	-0.004
72	70.9	94.85	4	13.221	13.023	-0.005
71.1	70.3	96.2	3.1	13.335	13.087	-0.004
71.1	70.3	96.2	9.6	13.335	13.087	-0.014
73	71.2	91.74	16.6	13.107	12.990	-0.011

Conclusion

The simulation provided a look into the potential energy savings from indirect evaporative cooling. It created a load profile on a house based on a number of parameters for the cooling season. Five cities were used to predict the energy savings for different parts of Florida. Each city experienced energy savings of approximately 5% for the cooling season. There was a substantial gain during peak weather conditions of up to 17%. From an economic standpoint the evaporative cooling device didn't show promise because of the nonsensical payback. Only one city was found to payback the price of the

media pad before it needs to be replaced. The evaporative cooling device will undoubtedly save energy, but is not expected to provide any financial gain.

CHAPTER 5
CONCLUSIONS AND RECOMMENDATIONS

Conclusions

The conclusions of this research from experimentation and the simulation are summarized below:

- There is restriction to airflow and additional power requirements associated with utilizing indirect evaporative cooling with an air-cooled condenser. Also the water requirement is an additional cost of operation.

- The reduced airflow shows no negative impact on performance of the condenser. The additional mass accumulated as the air passes through the media pad allows the condenser to reject more heat even with the less air. A smaller condenser with an indirect evaporative cooling device can replace an air-conditioner's typical condenser and provide the same performance.

- The maintenance becomes a high priority to make the media pad last as long as possible. Air-cooled condensers dominate the market for residential air-conditioners because of their low maintenance requirements.

- While testing it was noticed that when the evaporative cooling device was started it took several minutes for the media pad to become completely saturated and in some cases there were dry spots. It resulted from the random way in which the water flowed off the deflecting plate onto the media pad. This was not an issue during testing because the operator could monitor the situation and make any corrections. In a practical application this problem would not allow the evaporative cooling device work to its full capability and could even degrade the performance of the condenser. This could be countered by adding more holes to the header.

- Indirect evaporative cooling was proven to enhance the EER experimentally with the inclusion of the water pumping power.

- Between 60^{o}F and 70^{o}F outdoor dry-bulb temperature the evaporative cooling device degrades the performance of the heat pump because the lower dry-bulb temperature does not compensate for the additional water pumping power.

- For 70^{o}F and above outdoor DBT the EER was higher with the media pad at all tested relative humidities.

- At 70 and 80°F outdoor DBT the reduction in condenser power led to higher EER at lower RH values. The EER was improved at higher RH values because the cooling capacity was increased.

- At 90°F outdoor DBT and above the EER was improved because of the combination of the reduction in condenser power and the increase in cooling capacity at low RH values. Only the improved cooling capacity resulted in higher EER values at elevated relative humidities.

- The higher outdoor temperatures showed more improvement in EER at similar relative humidities because the temperature depression is greater, which allows more pre-cooling.

- The lower condenser power was a result of a reduction in condenser pressure due to lowering the dry-bulb temperature of the outdoor air. The compressor used less power to arrive at its reduced exit pressures.

- At higher relative humdities the total condenser power was higher for the media pad case because of the additional water pumping power. However the cooler inlet air to the condenser still led to lower condenser and evaporator refrigerant pressures. That made the refrigerant temperature entering the evaporator lower and increased the cooling capacity.

- At ASHRAE Condition 'A' the EER was improved by 22%, cooling capacity by 11%, and showed a decrease in compressor power consumption by 28%.

- The energy savings were found for five Florida cities, Figure 5-1, with an average seasonal savings of approximately 5% and peak of 15%.

Table 5-1. Table of the energy savings for the cooling season for the five Florida cities.

City	Cooling Season	Energy Savings (kWh)	%	Peak (kWh)	%
Jacksonville	May 1 - Sep. 30	220	5.0	0.534	16.3
Miami	April 1 - Oct. 31	296	4.5	0.376	12.9
Orlando	April 1 - Oct. 31	304	5.2	0.427	15.3
Tallahassee	May 1 - Sep. 30	207	4.9	0.350	16.6
Tampa	April 1 - Oct. 31	299	5.1	0.343	14.6

- Using the cost of electricity, the money saved for the cooling season was less than thirty dollars for each city. A simple payback was calculated and found to be up to twenty years for this particular indirect evaporative cooling setup.

- The simulation provides insight to relative humidities above 90% and showed the baseline case was more effective. This was expected because as the wet-bulb approaches the dry-bulb temperature there is not a significant enough drop in temperature to overcome the pumping power and reduced airflow to the condenser.

- Indirect evaporative cooling was shown to save energy when using an air-cooled heat pump in the cooling season, but in order to be an economically viable product the cost of parts has to be reduced.

Recommendations

There are two recommendations made for any further experimentation using the same indirect evaporative cooling device. The first is to use more accurate relative humidity probes. They were the main contributor to the high uncertainty of the EER. The second recommendation is to run experiments at a lower dry-bulb temperature in Room B to represent the indoor conditions. The 80^{o}F used in this research is probably higher than the typical thermostat setting in the average home. A range of temperatures from 72 to 76^{o}F should be used in the experiments.

Based on the results and conclusion formed from this research an alternative indirect evaporative cooling device is proposed for investigation. For an evaporative cooling device of this design to become a viable product, the cost has to be drastically reduced. The recommendations made are ones that may be able to make a product of this kind advantageous to use.

The sheet metal, pump, and media pad make up the majority of the cost of the parts. The frame could be made of plastic or some other inexpensive material that can withstand water exposure. The pad is the most crucial component. There is not much of a selection in the market beyond the product tested in this study and Aspen-wood excelsior. Instead of using the media pads a humidification chamber can be created using the same frame. An air permeable material can be wrapped around the perimeter of it making a humidification chamber. This will create an open cavity inside the frame where the evaporation will happen. Nozzles would be positioned inside the cavity spraying a mist of water in the opposite direction to the inlet air. This configuration can be found in

Figure 5-1. The type of nozzle is critical because the cooling efficiency depends on the water droplet size and its trajectory since it is in a confined space [28]. The larger droplets may not fully evaporate and will catch in the air permeable material and drain down to the sump. The droplets that are caught by the material can still be evaporated as they travel down the material. The air would enter the cavity and evaporate the water droplets reducing the dry-bulb temperature before entering the condenser. The material wrapped around the frame would serve two purposes. It would catch any water droplets not evaporated before contacting the coils and keep debris out of the humidification chamber. The pump and spray nozzles would be similar to the type used for a small greenhouse or terrarium. There are many types of these systems available and are considerably cheaper than the pump and media pad system used.

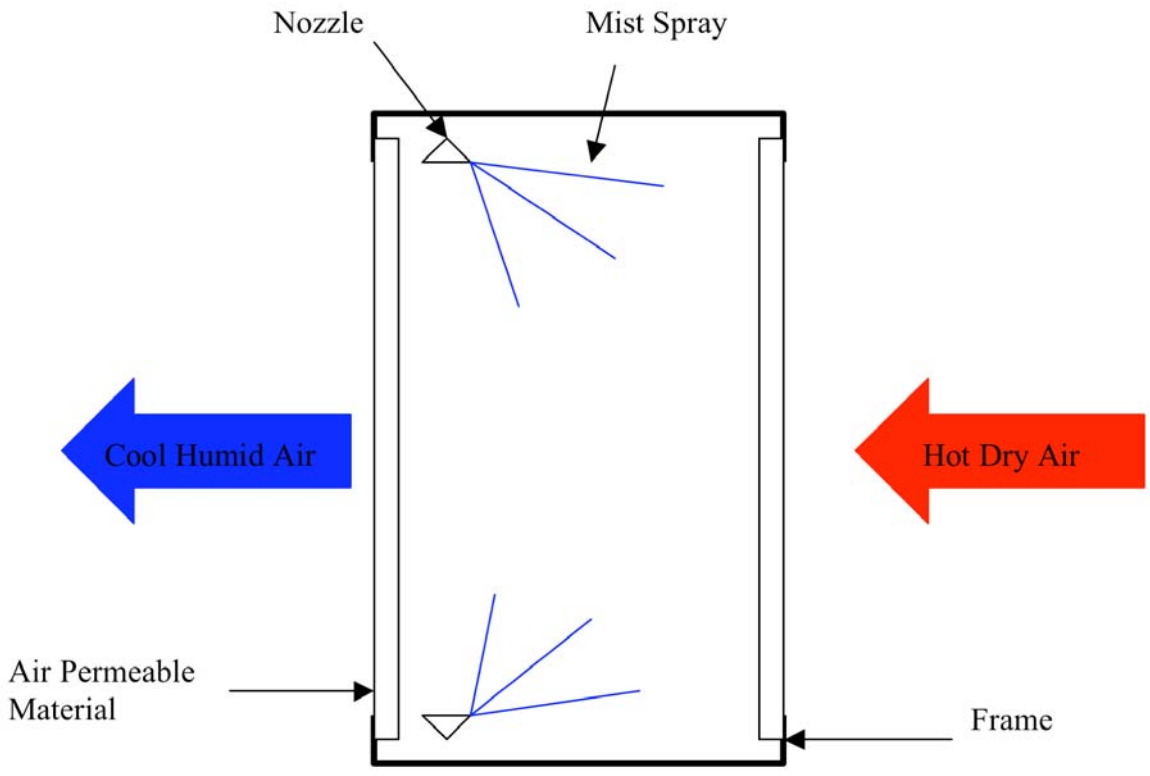

Figure 5-1. View inside the proposed indirect evaporative cooling device.

The performance of this system is based on some speculation, but may be worth some investigation. The maintenance of this proposed system would not be as tedious as the one with the media pad, which a consumer would find attractive. When the system is turned on the mist would immediately fill the humidification chamber and be readily available for the air. The media pad had a problem with not becoming fully saturated until after a few minutes passed. The airflow rate should not be reduced as much depending on how permeable the material is. The cooling efficiency would be greater than the media pad because the amount of water surface area created by the spray nozzles. Compared to the media pad case this proposed one would improve airflow and produce a cooler temperature. For these reasons the air-conditioner would experience an even greater improvement in its performance. The only disadvantage of this system is there will be more water consumed, which adds to the operating cost. This can be a significant cost depending on location and should be factored into an overall economic evaluation.

APPENDIX A
DESIGN OF THE EVAPORATIVE COOLING DEVICE

The evaporative cooling device followed the design specifications of Munters [20] and Glacier-Cor [21]. Munters developed the evaporative cooling pad and Glacier-Cor is a subsidiary selling the same basic product.

The first design choice was the thickness of the pad and all other design aspects followed as a result. Choosing the pad thickness could only be done after knowing the face velocity of the air going into the condenser. This was measured manually with the anemometer using 85 points around the condenser coils. The average of all the points taken was 217 fpm. The graph from Glacier-Cor in Figure A-1 was used to estimate the pressure drop and cooling efficiency for the given face velocity. A six inch pad was selected because it provided a high cooling efficiency and a low pressure drop. The low pressure drop was desirable because the condenser fan is not designed to handle a high pressure drop. After knowing the thickness and the length of pad needed to surround the perimeter of the condenser coils, the table from Figure A-2 was used to select the diameter of the distribution pipe, the spacing of the holes and their diameter on the header, and the water flow rate. Table A-1 shows the selections made for the evaporative cooling device.

Table A-1. Table of design specifications used for the evaporative cooling device.

Water Flow Rate (GPM)	Pipe Diameter (Inches)	Hole Spacing (Inches)	Hole Diameter (Inches)
5.5	¾	3	1/8

The water flow rate was calculated by using the perimeter length and providing 1.5 gpm for every lineal foot. Next a rough estimate of the pressure drop through the distribution system had to be determined in order to choose a pump. The pressure drop was estimated to be 6 feet of head. A submersible pump was selected to sit inside the sump. The pump chosen was the Little Giant small submersible pump, model 3E-12R, Figure A-3.

The pump and the frame of the device were designed to accommodate a pad of up to eight inches thick. Those are the two components of the design that would have to be modified if the pad thickness was changed. It was done in case further investigation was to be done with different thicknesses.

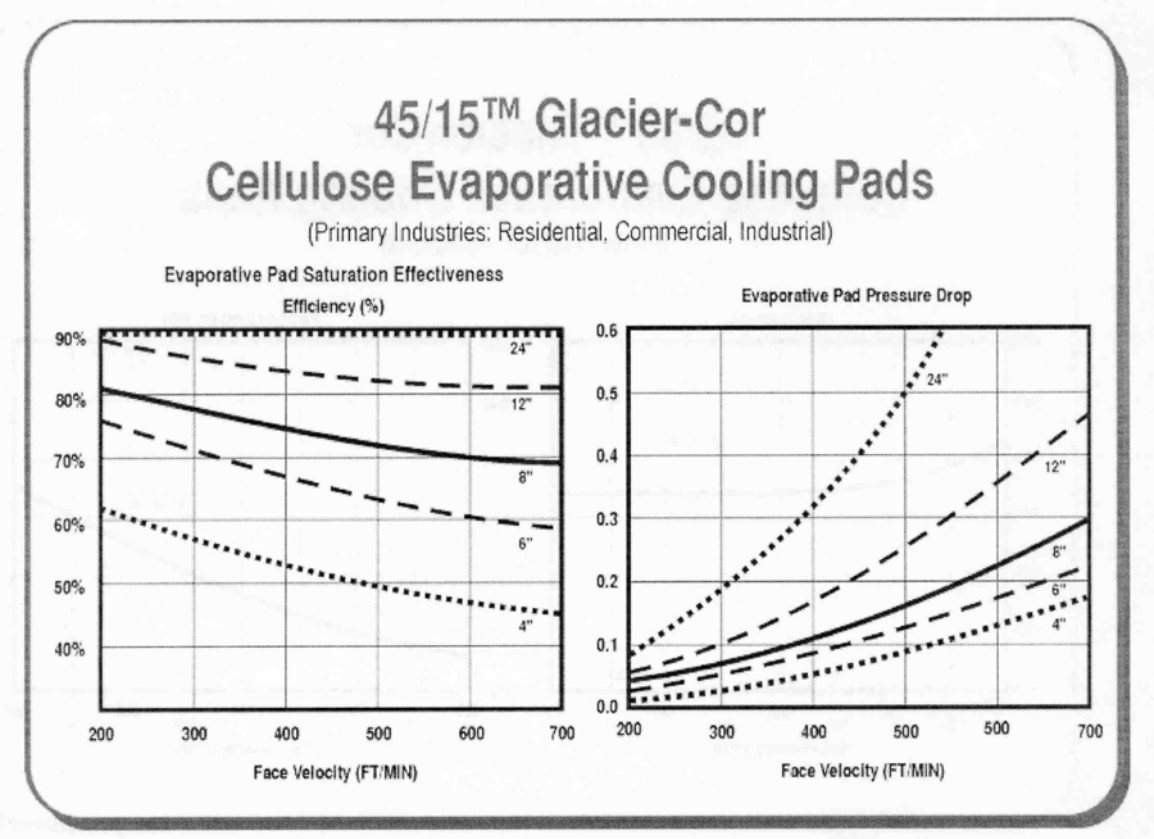

Figure A-1. Chart of performance specification for the 45/15 Glacier-Cor Cellulose Evaporative Cooling Pads [21].

RECOMMENDED DISTRIBUTION PIPE DESIGN FOR FULL FACE COVERAGE

MEDIA DEPTH (inches)	PIPE LENGTH** (Feet)	DESIGN FLOW (GPM / linear ft of pipe)	PIPE DIAMETER (Inches)	HOLE DIAMETER (Inches)	HOLE SPACING (inches)
4	2-16	.25-.67	1/2, 3/4	1/8	6
4	2-16	.25-.87	1/2, 3/4, 1	1/8	4
4, 6	4-16	.35-1.0	3/4	1/8	4
4, 6	4-16	.35-1.0	1	1/8	4
6, 8	6-12	.5-1.25	1/2	1/8	3
6	10-12	.67-1.0	1/2	1/8	3
6, 8	4-16	.5-1.25	1, 1 1/4, 1 1/2	1/8	3
6, 8	6-16	.67-1.25	3/4, 1	1/8	3
6	16	.67-1.0	3/4	1/8	3
6, 8	4-8	.5-1.25	1 1/4	3/32	2
6	10-16	.5-1.1	1 1/4	3/32	2
12	6-10	1.0-1.75	3/4	1/8	2
8	12-16	.75-1.5	3/4	1/8	2
8, 12	4-16	.75-1.75	1, 1 1/4, 1 1/2	1/8	2
8, 12	10-16	.75-1.75	1 1/2	1/8	2
12	8-10	1.0-1.75	3/4	5/32	3
8, 12	12-16	.75-1.75	3/4	5/32	3
8, 12	8-16	.75-1.75	1	5/32	3
12	8-16	1.25-2.0	3/4	5/32	3
12	8-16	1.0-1.75	1	5/32	3

** If center fed, this is the distance from the "T" to the end of the pipe. If fed from one side, this is the length of the distribution pipe.

Figure A-2. Table for selecting the distribution pipe diameter, the spacing of the holes and their diameter on the header and flow rate requirements [20].

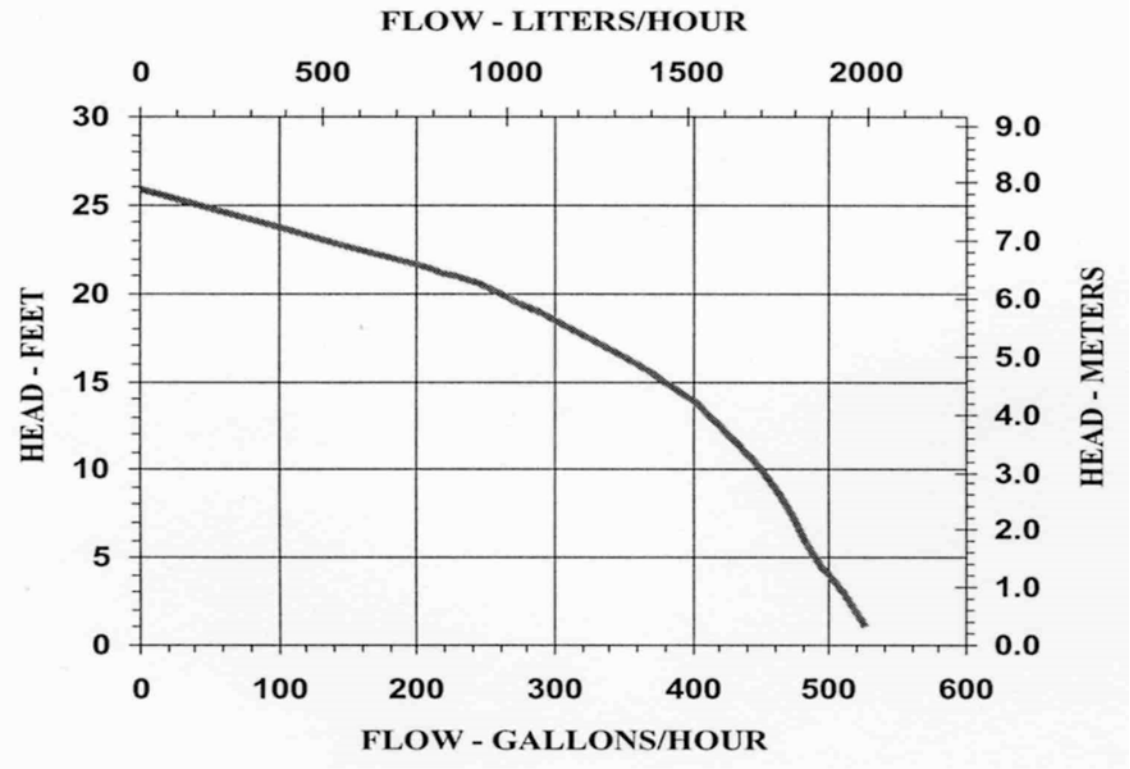

Figure A-3. Graph of the performance specifications for the submersible pump, Little Giant Pump Company [29].

APPENDIX B
STARTUP AND SHUTDOWN PROCEDURE OF SEECL HEAT PUMP TEST FACILITY

This appendix provides directions for the startup and shutdown of the test facility for both climate-controlled rooms, Figure B-1. Each room has its own set of manual controls. Either room can be turned on first, but knowing which temperature will be tested can save some time. If testing at a high outdoor temperature, it is beneficial to turn Room B's equipment on first in order to heat up Room A.

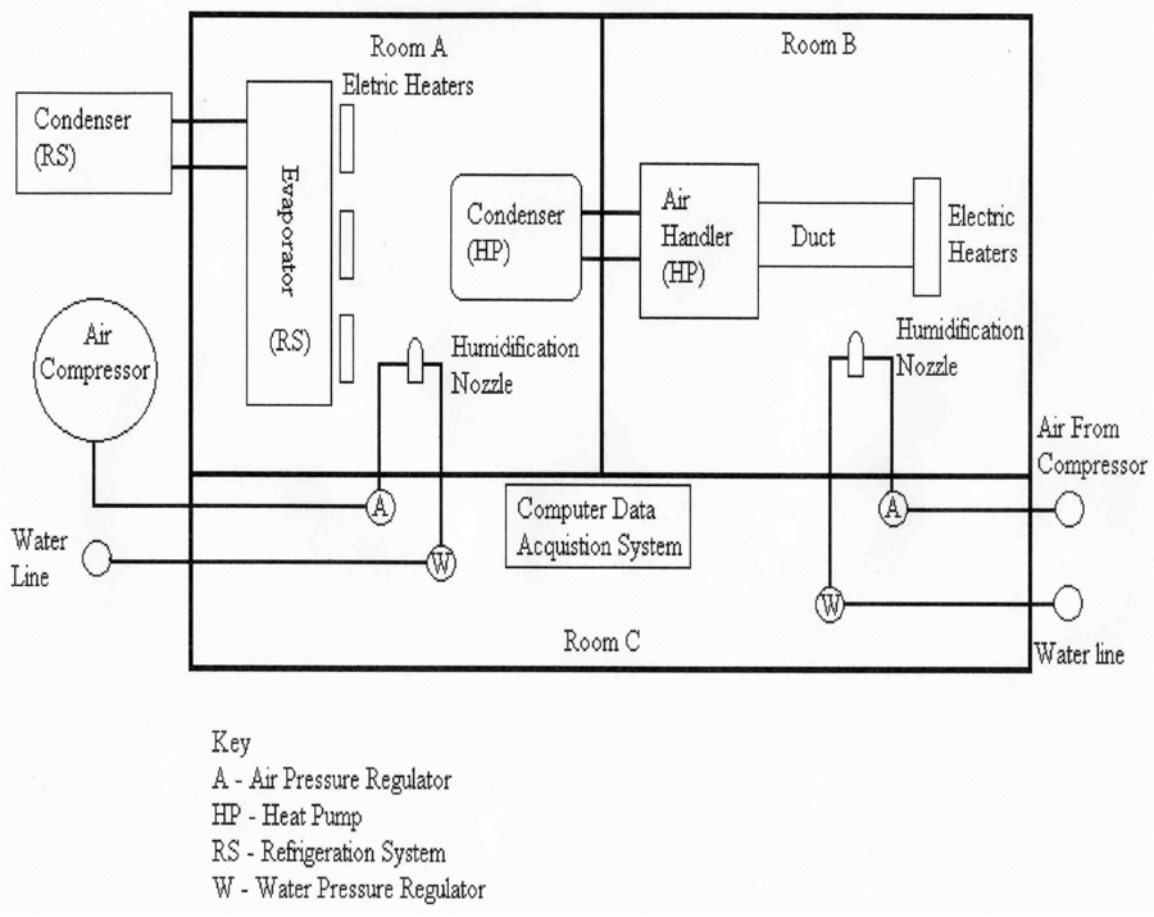

Figure B-1. The layout of the test facility.

Startup

The compressed air and the water were supplied to both rooms. The compressor and the water valve are turned on before starting up the other equipment for the rooms. Both rooms have pressure regulators for the air and water.

Room A (Outdoor Conditions)

1. Turn condenser on.
2. Turn evaporator on.
3. Turn heaters on.
4. Open regulator for compressed air to the humidification nozzle (if on).
5. Open regulator for the water to the humidification nozzle (if on).

Room B (Indoor Conditions)

1. Turn test unit evaporator on.
2. Turn test unit condenser on.
3. Turn heaters on.
4. Open regulator for compressed air to the humidification nozzle.
5. Open regulator for the waster to the humidification nozzle.

When the evaporative cooling device is installed the pump is turned on when the test system condenser is turned on. The pump is directly connected to the condenser's power source. The sump water level should be checked before the pump is turned on. This will prevent a low water level and running the pump dry, which will damage it.

Shutdown

Room A (Outdoor Conditions)

6. Close regulator for the water to the humidification nozzle (if on).
7. Close regulator for compressed air to the humidification nozzle (if on).
8. Turn heaters off.

9. Turn condenser off.

10. Five minutes after the condenser has been off, turn the evaporator off.

Room B (Indoor Conditions)

11. Close regulator for the water to the humidification nozzle.

12. Close regulator for compressed air to the humidification nozzle.

13. Turn heaters off.

14. Turn test unit condenser off.

15. Five minutes after the condenser has been off, turn test unit evaporator off.

After these directions are completed the compressor and the water valve can be turned off.

APPENDIX C
INPUTS FOR THE SOFTWARE USED FOR THE SIMULATION

The Carrier HAP software is used primarily to size air-conditioning equipment based on a number of parameters. It follows the heat balance method to calculate the cooling load on a space. A space is defined as a room with its own internal loads. A zone is one space or series of spaces controlled by one thermostat. In this case the entire house was considered a zone.

The layout of the house is found in Figure C-1. Table C-1 provides the general data of the house. The area of the walls and their direction are found in Table C-2. It also specifies the amount of windows and doors in each wall. This can also be observed in Figure C-1. Table C-3 show the wall assembly and gives the overall U-value calculated from its materials. The Florida Building Code [24] requires insulation with a minimum of R-11 value. The details of the windows and their overhang shading device are found in Tables C-4 and C-5 respectively. The Florida Building Code [24] requires double pane windows with at least a two-foot overhang above them. This setup can be found in Figure C-2. Also, the maximum amount of window area cannot exceed 20% of the floor area. The window area for the simulated house is within this limit. The roof assembly is in Table C-6 and is required to have insulation with at least an R-30 value [24]. Table C-7 provides the floor details. A slab floor on grade is not obligated to have edge insulation [24].

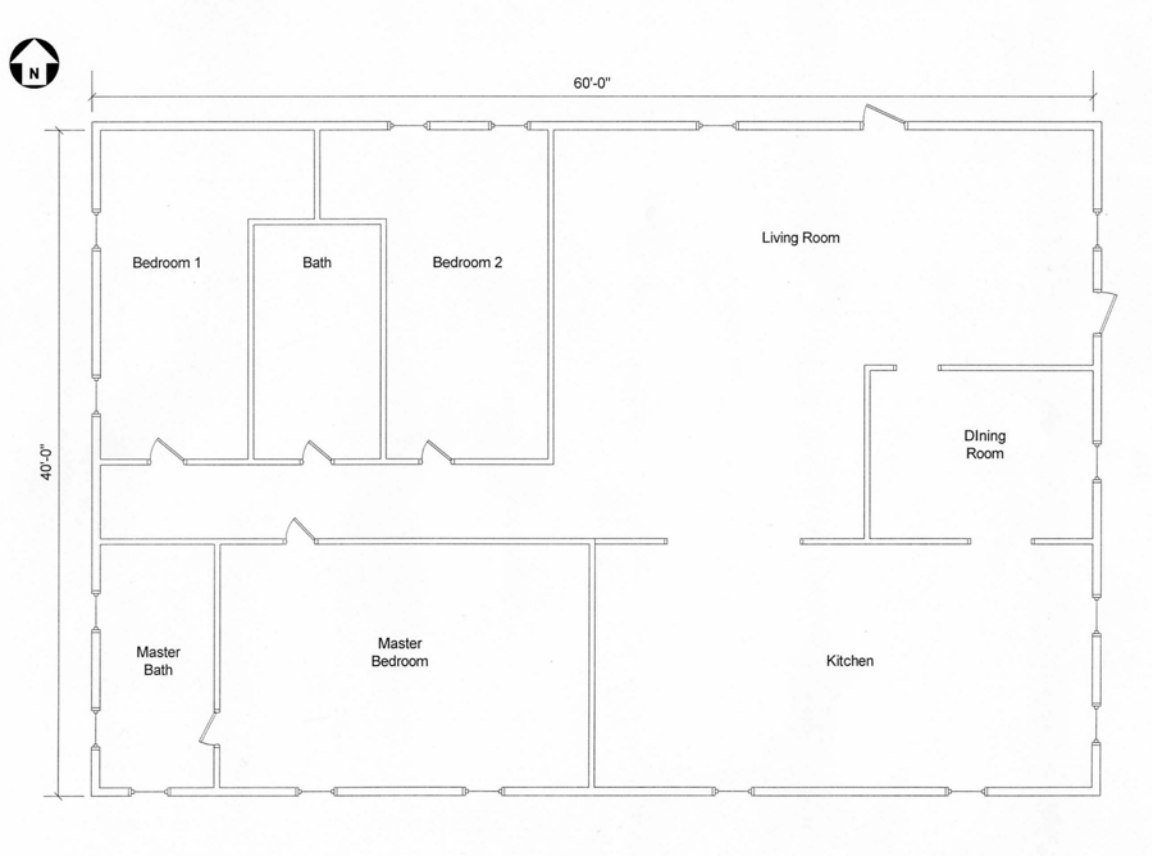

Figure C-1. The floor plan of the house that was used in the simulation.

Table C-1. General inputs for the house.

Floor Area	2400 ft^2
Avg. Ceiling Height	8 ft
Building Weight	30 lb/ft^2

Table C-2. Inputs for the walls.

Wall Direction	Gross Wall Area (ft^2)	Window Qty.	Door Qty.
East	320	4	1
West	320	4	0
North	480	3	1
South	480	5	0

Table C-3. Inputs for all the walls.

Wall Assembly					
Layers: Inside to Outside	Thickness Inches	Density Lb/ft^3	Specific Ht. Btu/lb/F	R-Value $hr\text{-}ft^{2}\text{-}F/Btu$	Weight Lb/ft^2
Inside Surface Resistance				.680	
½ in. Gypsum Board	.5	50	.26	.448	2.1
R-13 Batt Insulation[d]	4	.5	.20	12.82	0.2
Face Brick	4	125	.22	.433	41.7
Outside Surface Resistance				.25	
Totals	8.5			14.63	43.9
Outside Surface Color	Light				
Absorptivity	0.450				
Overall U-value	0.068 $Btu/hr/ft^2/F$				
d- Florida Building Code [24]					

Table C-4. Inputs for all of the windows.

Window Detail				
Area	25 ft^2			
Frame Type	Aluminum w/o Thermal Breaks			
Internal Shade Type	Roller Shades-Dark-Opaque			
Overall U-value	0.608 $Btu/hr/ft^2/F$			
Overall Shade Coefficient	0.714			
Glazing	Glass Type	Transmissivity	Reflectivity	Absorptivity
Outer glazing	1/8 in clear	0.841	0.078	0.081

Table C-4. Continued.

Glazing #2	1/8 in clear	0.841	0.078	0.081
Gap Type	¼ in Argon			

Table C-5. Inputs for the window shade.

Shade	
Overhang	
Projection From Surface	24[d] inches
Height Above Window	6 inches
d- Florida Building Code [24]	

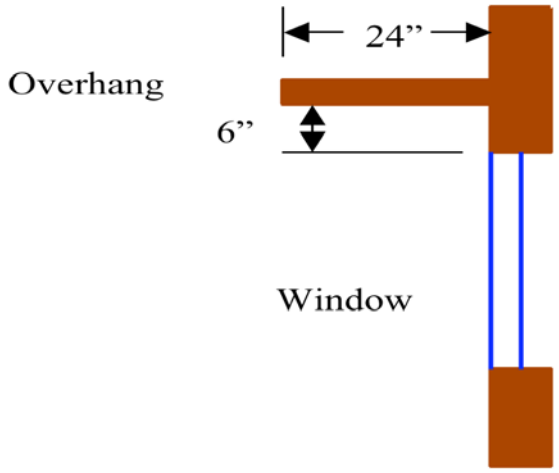

Figure C-2. The window and overhang setup.

Table C-6. Inputs for the roof.

Roof Assembly					
Horizontal					
Layers: Inside to Outside	Thickness Inches	Density Lb/ft^3	Specific Ht. Btu/lb/F	R-Value hr-ft^2-F/Btu	Weight Lb/ft^2
Inside Surface Resistance				.920	
½ in. Gypsum Board	.5	50	.26	.448	2.1
R-30 Batt Insulation[d]	9.5	.5	.20	30.449	0.2
Built-up Roofing	.376	70	.22	.332	2.2
Outside Surface Resistance				.333	
Totals	10.376			32.48	4.7
Overall U-value	0.031 Btu/hr/ft^2/F				

Table C-6. Continued.

Outside Surface	Dark
Absorptivity	0.900
d- Florida Building Code [24]	

Table C-7. Inputs for the floor.

Floor	
Floor type	Slab floor on grade
Total U-value	0.1 Btu/hr/ft^2/F
No edge insulation[d]	
d- Florida Building Code [24]	

The internal loads are listed in Table C-8. The amount of lighting was found from Hendron et al. [26] for a 2400 square foot house. This number was reduced from the annual to the hourly amount. The amount of electricity used by equipment comes from the U.S. Energy Information Administration [25], again for a 2400 square foot home. The amount of annual electricity was reduced down to the daily consumption, which represents the value listed. The number of people was calculated using the number of bedrooms in the home [19]. There were two people counted for the first bedroom and one person for each additional bedroom. The latent and sensible loads for each person were also found from ASHRAE Handbook of Fundamentals [19]. These values represent the loads for residential use. The infiltration also contributes to the internal load as the outside air leaks into the house. The value listed was taken from the Florida Building Code [24].

Table C-8. Inputs for the internals.

Internals	Load
Overhead lighting- free hanging (Ballast Multiplier)	3400[a] W (1.00)
Electrical Equipment	17344[b] W
People, Occupancy = 4[c]	
Sensible	230[c] Btu/hr/person
Latent	190[c] Btu/hr/person
a- Hendron et al. [26] b- Energy Information Administration [25] c- ASHRAE Handbook of Fundamentals [19]	

Table C-9. Inputs for the infiltration.

Infiltration	
ACH	.5[d]
Occurs	All Hours
d- Florida Building Code [24]	

For a realistic approach the internal loads are all put on schedules throughout the day. The schedules were used to determine what fraction of the load was present for each hour of the day. Multiple schedules can be created and assigned to different days of the week and times of year. The schedules for the lighting, electrical equipment, and people are found in Figures C-3 to C-5 respectively. All the schedules were taken from Hendron et al. [26].

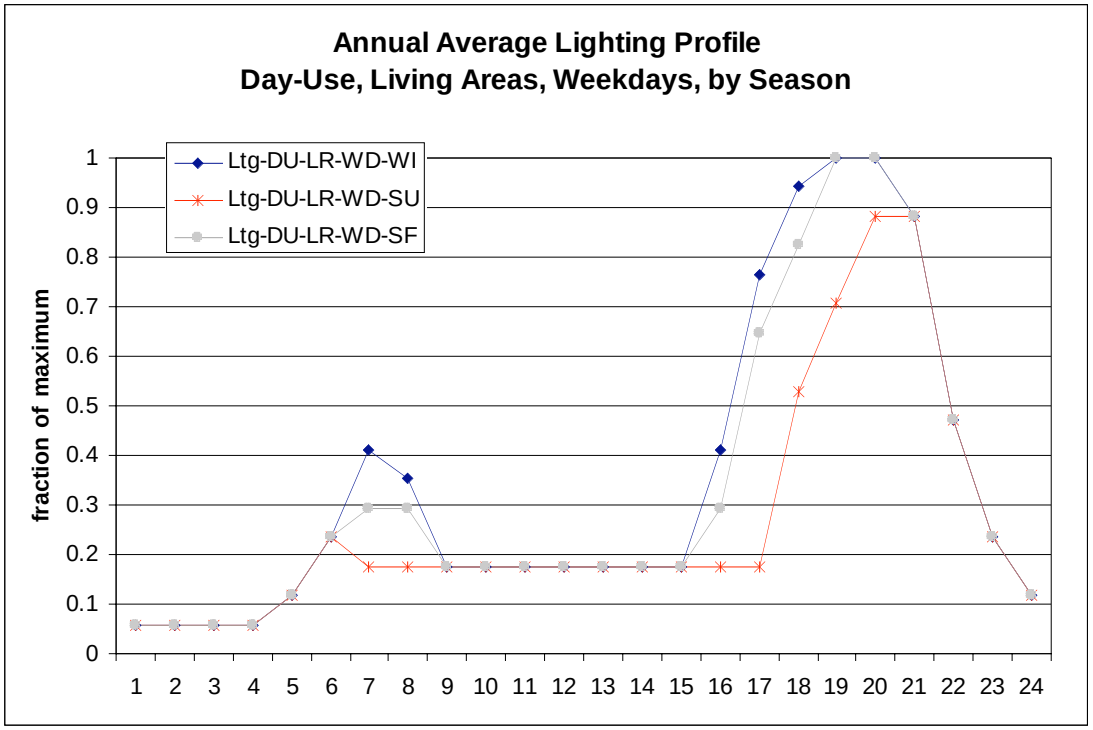

Figure C-3. The schedule used for lighting. (WI) winter, (SU) summer, (SF) spring and fall, Hendron et al. [26].

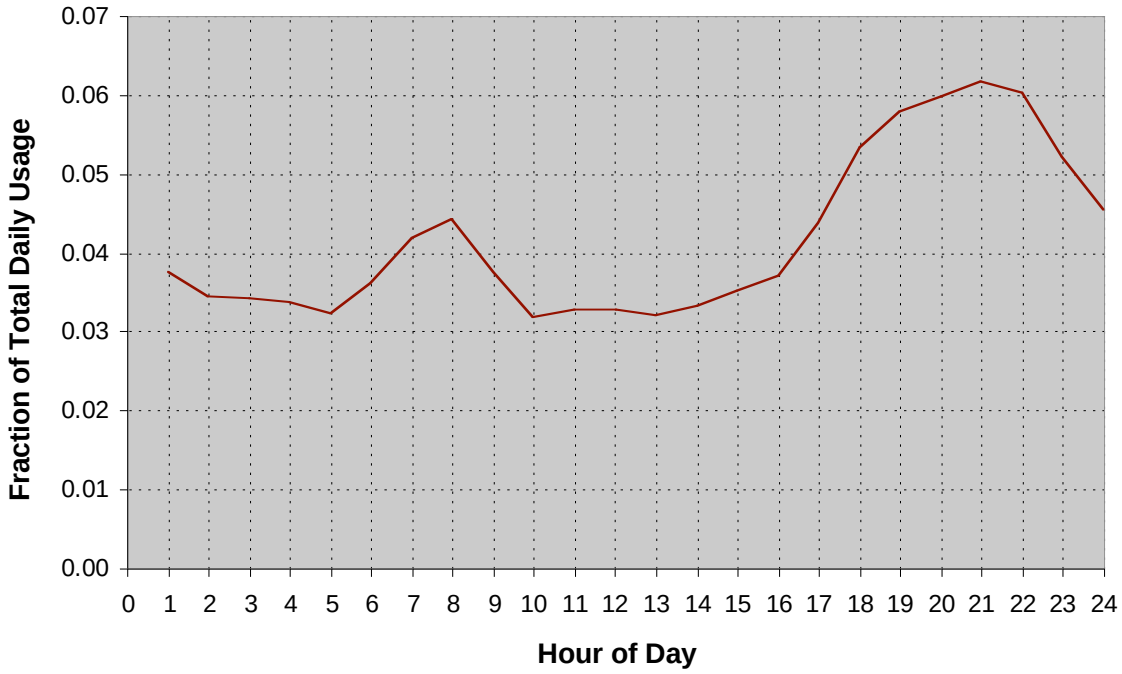

Figure C-4. The schedule used for electrical equipment, Hendron et al. [26].

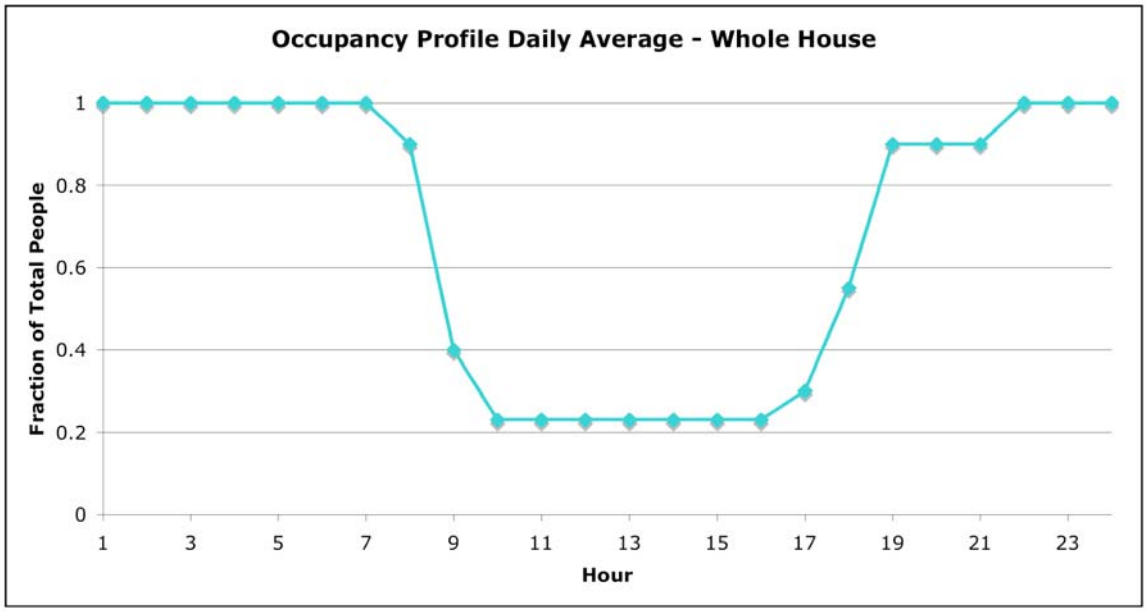

Figure C-5. The schedule used for people occupancy, Hendron et al. [26].

One of the most critical inputs was the thermostat setting, Table C-10. It was set at 79^{o}F and can be throttled up to 81^{o}F. This corresponds with the temperature used in Room B (indoor conditions) for the experiments. Cooling would be required from the

system only when the room temperature rose above 81^{o}F. The cooling load per hour calculated by the simulation was how much cooling had to be done to bring the room temperature with in the specified range. The cooling load was a result of the internal load, the weather conditions, insolation, infiltration as well as the heat transfer to the outside.

Table C-10. Inputs for the thermostat setting.

Thermostat	
Cooling T-Stat Setpoint	79^{o}F
T-Stat Throttling Range	2^{o}F

APPENDIX D
EXPERIMENTAL DETAILS

This appendix provides further details to the experimental approach not included in Chapter 3. Details of the instrumentation and how they were used with the data acquisition system are provided along with the propagation of uncertainty from direct to derived measurements.

Data Acquisition and Instrumentation

A list of all equipment used for the experiments is detailed in Table D-1. Their respective locations are described in Chapter 3. The Daqbook200 was used to collect all the measurements from the thermocouples and transducers. It is the medium between the measuring devices and the computer. Each device sent its output to its respective expansion card where the DaqBook200 converted the data to the output read on the computer as temperature, pressure, etc.. The DBK82 and DBK19 expansion cards were used for the thermocouples and the DBK15 was used for the transducers. The software used at the computer interface was DaqView. It allowed the thermocouples and transducers to be assigned a channel where the calibration was set. The thermocouples connected to the DBK 82 expansion card were set to the 'T' type. Additional thermocouples and transducers connected to the DBK 19 and DBK 15 respectively, were set by entering the slope and intercept. The methods used to find the slope and intercept are discussed later in this appendix. The DaqView was also used to set the sampling rate of 300 scans per minute and converted the data to an ASCII format so it could be saved.

Table D-1. List of equipment used for the experiments.

Device	Manufacturer	Model
Data Acquisition	Iotech	Daqbook200
Thermocouple Cards	Iotech	DBK 82 DBK 19
Voltage Card	Iotech	DBK 15
Relative Humidity Probe	Vaisala Vaisala	HMD20UB HMD60Y
Temperature	Vaisala	HMD60Y
Temperature T-Type Thermocouple Probe	Omega	TMQSS-125U-6
Instantaneous Power Transducer	Ohio Semitronics	PC5-29F
Pressure Transducers	Mamac Systems	PR-262
Flowmeter	Rotameter Brooks	3604
Hot Wire Anemometer	Kay-May	KM4107

Uncertainty of Direct Measurements

The direct measurements of temperature, relative humidity, power, and airflow rate are the basis of the derived results. This section will go over how the devices were calibrated and the uncertainty in the measurements. All the calibrations were conducted prior to the experiments.

Temperature

The temperature was measured with two devices, namely T-type thermocouples and temperature and relative humidity combination probes. The T-type thermocouples connected to the DBK 82 expansion card were calibrated using a two point linear calibration at 0^{o}C and 38^{o}C in a constant temperature bath that covered the range of temperatures from the experiments. They had a very high accuracy and needed no further calibration. The 'T' option was selected in DaqView. The three thermocouples connected to the DBK 19 expansion card were also calibrated with a two point linear calibration. They were checked at 0^{o}C and 100^{o}C with a high accuracy thermometer. The three thermocouple's accuracies were improved by setting the calibration constants

shown in Table D-2. These three thermocouples were placed on each side of the evaporative cooling device. The uncertainty associated with these measurements was ±0.6°C.

Table D-2. Calibration constants for the thermocouples connected to the DBK 19 card.

Location	Slope	Y-Intercept (°F)
Right	1.8155	29.00499
Front	1.8293	29.00799
Left	1.8358	21.62777

The manufacturer calibrated the temperature probes with NIST traceability. The uncertainty of these temperature measurements was ±.2°C. The calibration constants used for this device to measure temperature were the same and were inputted to DaqView shown in Table D-3.

Table D-3. Calibration constants for the temperature probes.

Device	Slope (°C/mV)	Y-Intercept (°C)
Temperature Probe	25	-45

Relative Humidity

The relative humidity probes were calibrated by exposing them to three saturated salt solution environments. The salt solutions differed by the accuracy of relative humidity range. For example, one was more accurate at high relative humidity and another at low relative humidity. The salt solution temperature corresponded with a relative humidity and the output of the probe was checked against this value. The accuracy of the probes were improved by adjusting the offset and gain potentiometers. The manufacturer reported the uncertainty of these measurements as ±2% of the reading. The same calibration constants were set in DaqView for all the relative humidity probes shown in Table D-4.

Table D-4. Calibration constants for the relative humidity probes.

Device	Slope (RH/mV)	Y-Intercept (RH)
Relative Humidity Probe	25	-25

Pressure

Dead weights were used for the pressure in the calibrator. The pressure transducers were connected to the calibrator. The output was measured and converted to a pressure. Both the offset and gain could be adjusted using potentiometers. The manufacturer provided the uncertainty of the low and high-pressure transducers as ±2.5 psig and ±3.5 psig, respectively. The calibration constants used for both pressure transducers are found in Table D-5.

Table D-5. Calibration constants for the pressure transducers.

Pressure Transducer	Slope	Y-Intercept (psig)
High Pressure	87.5 (psig/VDC)	-87.5
Low Pressure	25 (psig/VAC)	0

Power

The power transducer was calibrated at the manufacturer Ohio Semitronics. The uncertainty of its readings was ±50 Watts. Its calibration constant is presented in Table D-6.

Table D-6. Calibration constants for the pressure transducers.

Device	Slope (kW/mV)	Y-Intercept (kW)
Power Transducer	406.5	0

Airflow Rate

The manufacturer Kay-May calibrated the hot wire anemometer used to measure the airflow in the duct. The uncertainty of its measurements was ±3% of the reading.

Uncertainty of Derived Measurements

The uncertainty of the derived measurements is a function of all the uncertainties associated with the direct measurements. Equation D-1 provides the general form where the calculated quantity, r, is a function of j measured variables X_i.

$$r = r\left(X_1, X_2, ..., X_j\right) \tag{D-1}$$

The uncertainty can be calculated from Equation D-2:

$$\xi_r = \left[\left(\frac{\partial r}{\partial X_1}\xi_{X_1}\right)^2 + \left(\frac{\partial r}{\partial X_2}\xi_{X_2}\right)^2 + \cdots + \left(\frac{\partial r}{\partial X_j}\xi_{X_j}\right)^2\right]^{\frac{1}{2}} \tag{D-2}$$

The following sections detail the method for finding the uncertainty of the derived quantities.

Cooling Capacity

The cooling capacity was determined from a series of calculations using measured data. The calculations included the humidity ratio, enthalpy of the return and supply air, mass flow rate of the air, specific volume of the air, and partial pressure of the water vapor. The direct measurements used for the calculations were the temperature and relative humidity of the return and supply air and the airflow rate. The calculation could not be made without thermodynamic properties from the direct measurements such as saturation pressure, universal gas constant for air, and atmospheric pressure.

Cooling Capacity = *f* (temperature of return air, relative humidity of return air, temperature of supply air, relative humidity of supply air, saturation pressure, partial pressure of water vapor, humidity ratio, enthalpy of return air, enthalpy of supply air, airflow rate, mass flow rate of air, specific volume of air)

(D-3)

EER

The energy efficiency ratings were dependent on the cooling capacity and the power of the condenser. The cooling capacity and its dependencies were discussed earlier and the power was dependent on its direct measurement.

The uncertainty of EER was on the order of ±19%. The relative humidity uncertainty was the greatest contributor to this.

$$\text{EER} = f(\text{cooling capacity, condenser power}) \quad \text{(D-4)}$$

Cooling Efficiency

The cooling efficiency of the media pad was determined from the direct measurements of the dry-bulb temperature and relative humidity of the inlet air and the dry-bulb temperature of the outlet air. Also the wet-bulb temperature was used for the calculation. An assumption was made that it remained constant because it is an adiabatic process.

$$\text{Cooling Efficiency} = f(\text{dry-bulb temperature of inlet air, relative humidity of inlet air, dry-bulb temperature of outlet air, wet-bulb temperature}) \quad \text{(D-5)}$$

LIST OF REFERENCES

1. United States Energy Information Administration, 2005, “Electric Air-Conditioning Energy Consumption in U.S. Households by Climate Zone, 2001,” http://www.eia.doe.gov/emeu/recs/recs2001/ce_pdf/aircondition/ce3-c_climate2001.pdf, last accessed July 16, 2005.

2. United States Energy Information Administration, 2005, “ Electricity Consumption by End Use in U.S. Households, 2001,” http://www.eia.doe.gov/emeu/reps/enduse/er01_us_figs.html#2, last accessed July 18, 2005.

3. Cengel Y., R. Turner, 2001, *Fundamentals of Thermal-Fluid Sciences*, McGraw-Hill, New York, pp. 376-382.

4. American Society of Heating, Refrigerating, and Air-Conditioning Engineers, Inc. (ASHRAE), ASHRAE Handbook of HVAC Systems and Equipment, 1996, Inc., Atlanta.

5. American Society of Heating, Refrigerating, and Air-Conditioning Engineers, Inc. (ASHRAE), ASHRAE Handbook of HVAC Applications, 1995, Atlanta.

6. Goswami, D.Y., G. D. Mathur, and S. M. Kulkarni, 1993, “Experimental Investigation of Performance of a Residential Air-Conditioning System with an Evaporatively Cooled Condenser,” *Journal of Solar Energy Engineering*, **115** (4), pp. 206-211.

7. Grant, Matthew, F. Wicks, R. Wilks, 2001, “Identification and Analysis of Psychometric Methods for Enhancing Air Conditioner Efficiency and Capacity,” *Proceedings of the Intersociety Energy Conversion Engineering Conference*, Savannah, **2**, pp. 715-719.

8. Mathur, A.C., and S.C. Kaushik, 1994, “Energy Savings Through Evaporatively Cooled Condenser Air in Conventional Air-Conditioning Units,” *International Journal of Ambient Energy*, **15**, pp. 78-86.

9. Kutscher, C., and D. Costenaro, 2002, “Assessment of Evaporative Cooling Methods for Air-Cooled Geothermal Power Plants,” *Transactions – Geothermal Resources Council*, **27**, pp. 775-779.

10. Hwang, Y., R. Radermacher, W. Kopko, 2000, "An Experimental Evaluation of a Residential-Sized Evaporatively Cooled Condenser," *Journal of Enhanced Heat Transfer*, **7**, pp. 273-287.

11. Ettouney, H. M., H. El-Dessouky, W. Bouhamra, B. Al-Azmi, 2001, "Performance of Evaporative Condensers," *Heat Transfer Engineering*, **22**, pp. 41-55.

12. Goswami, D. Y., S. A. Sherif, C. Jotshi, C. Ejimofor, N. Vashishta, 1996, "Evaluation of the Effect of a Compact Indirect Evaporative Cooling Unit on the Performance of a Three-Ton Heat Pump," Report No. UFME/SEECL-9601 Submitted to Florida Power and Light Company, University of Florida.

13. Hosoz, M., and A. Kilicarslan, 2004, "Performance Evaluations of Refrigeration Systems with Air-Cooled, Water-Cooled and Evaporative Condensers," *International Journal of Energy Research*, **28**, pp. 683-696.

14. Hasan A., and K. Siren, 2003, "Performance Investigation of Plain and Finned Tube Evaporatively Cooled Heat Exchangers," *Applied Thermal Engineering*, **23**, pp. 325-340.

15. Al-Sulaiman, F., 2002, "Evaluation of the Performance of Local Fibers in Evaporative Cooling," *Energy Conversion and Management*, **43**, pp. 2267-2273.

16. Liao Chung-Min, and K. H. Chiu, 2002, "Wind Tunnel Modeling the System Performance of Alternative Evaporative Cooling Pads in Taiwan Region," *Building and Environment*, **37**, pp. 177-187.

17. Munters, *Specifications for CELdek EB-CS-0204*, 2002, Amesbury.

18. Goswami, D.Y., G. D. Mathur, S. M. Kulkarni, and J. R. Windham, 1992, "Improved Efficiency Air Conditioning Unit for Agricultural and Residential Applications," Report No. UFME/SEECL-9204 Submitted to the Florida Energy Extension Service, University of Florida.

19. American Society of Heating, Refrigerating, and Air-Conditioning Engineers, Inc., (ASHRAE), ASHRAE Handbook of Fundamentals, 2001, Atlanta.

20. Munters, *Installation Details for Industrial Evaporative Coolers and Humidifiers Equipped with CELdek® and GLASdek® Media,*2001, Amesbury.

21. Glacier-Cor, *Technical Brochure Commercial and Industrial*, 2002, Fort Myers.

22. American Society of Heating, Refrigerating, and Air-Conditioning Engineers, Inc., (ASHRAE), ASHRAE Standard Method of Testing for Rating Unitary Air-Conditioning and Heat Pump Equipment, ANSI/ASHRAE 37-1988, Atlanta.

23. Air-Conditioning and Refrigeration Institute (ARI), ARI Standard 210/240 – 2003 for Unitary Air-Conditioning and Air-Source Heat Pump Equipment, Arlington.

24. The Florida Department of Community Affairs-Building Code Information System, 2004, Florida Building Code 2004 Residential, http://www2.iccsafe.org/2004_florida_codes, last accessed July 20, 2005.

25. Energy Information Administration, 2005, "Appliances Energy Consumption and Expenditures by Square Feet and Household Demographics, 2001," http://www.eia.doe.gov/emeu/recs/recs2001/ce_pdf/appliances/ce5-52u_sqft_demo2001.pdf, last accessed July 18, 2005.

26. Hendron R., R. Anderson, C. Christensen, and M. Eastment, 2004, "Development of an Energy Savings Benchmark for all Residential End-Uses," NREL/CP-550-35917, National Renewable Energy Laboratory, Boulder.

27. JEA, 2005, "JEA Variable Fuel Rate Charge Increase Reflects Soaring Fuel Costs," http://www.jea.com/services/electric/rates_quarterly.asp, last accessed September 10, 2005.

28. Welander, P., and T. Vincent, 2001, "Selecting the Right Spray Nozzle," *Chemical Engineering Progress*, **97**, pp. 75-79.

29. Little Giant Pump Company, 2005, "Little Giant Pump Company 3E-12R Series," http://www.lgpc.com/Product/ItemDetail.aspx?ProductID=785, last accessed May 12, 2005.

BIOGRAPHICAL SKETCH

Christopher Cheng was born on September 30, 1981, in Schenectady in upstate New York. He spent almost his entire life in the Capital Region. Christopher attended nearby Rensselaer Polytechnic Institute where he received his bachelor's degree in mechanical engineering. While attaining his degree he gained an interest in renewable energy. He decided to further his education and attended the University of Florida where he received his Master of Science in mechanical engineering while being part of the Solar Energy and Energy Conversion Laboratory.